

A WEATHER-AWARE TRAFFIC MODEL USING DEEP LEARNING APPROACHES

A Thesis
Presented to
the Faculty of the College of Computer Studies
De La Salle University

In Partial Fulfillment
of the Requirements for the Degree of
Bachelor of Science in Computer Science

by

MAGPALE, Nicolle G.
NIEVA, Dyan Raisa L.
REAMON, David Angelo H.
RECCION, Maria Victoria B.

Rafael A. CABREDO, Ph.D.
Adviser

August 30, 2018

Abstract

Several traffic models were already developed to alleviate traffic congestion, while also considering the effect of weather. However, they were not designed and tested in countries with poor road infrastructures where other weather variables and their resulting natural disasters have some effect on the traffic condition. This research proposes a traffic prediction model that incorporates the aforementioned weather variables present in Manila, and other features that describe the trends in traffic and weather for both normal and disrupted periods. Following data analysis, it was observed that heavy rain disrupts the normal trend of traffic and that the collected weather variables have weak correlation with traffic. From such findings, features were engineered from traffic and weather to be used in the models, such as temporal information of traffic, previous and current traffic conditions, rolling and expanding features, working day and peak hour, and weather effects. A traffic-based model and weather-based model were implemented using DBN and RNN, while the fusion model at both feature and decision level were implemented using DBN, RNN, and WA using Least Square Estimate. The various combinations of features, the different fusion approaches and algorithms, and the sensitivity of the models were evaluated. Results show that the traffic-based prediction outperforms weather-based traffic prediction. Moreover, fusing at decision level have better results than fusing at fusion level. After implementing various fusion algorithms, it was found that RNN, especially at decision level, outperforms the other fusion algorithms.

Keywords: Traffic modeling, weather information, deep learning, data fusion

Contents

1 Research Description	1
1.1 Background of the Study	1
1.2 Research Objectives	3
1.2.1 General Objective	3
1.2.2 Specific Objectives	3
1.3 Scope and Limitations of the Research	4
1.4 Significance of the Research	4
1.5 Research Methodology	5
1.5.1 Review of Related Literature	5
1.5.2 Data Collection and Processing	5
1.5.3 Data Analysis	5
1.5.4 Design and Implementation of Traffic Model	6
1.5.5 Verification and Validation of Traffic Model	6
1.5.6 Documentation	6
2 Review of Related Literature	7
2.1 Materials	7
2.1.1 Traffic Data	7

2.1.2	Weather Data	8
2.2	Research Methodology	9
2.3	Modeling Approach	12
2.4	Evaluation Strategy	16
3	Theoretical Framework	19
3.1	Traffic-related terms	19
3.1.1	Traffic Congestion	20
3.2	Weather-related terms	20
3.3	Historical Data	22
3.3.1	Traffic Data from MMDA's Traffic Monitoring System . .	23
3.3.2	Weather Data from World Weather Online	23
3.4	Working Day	24
3.5	Peak Hour	25
3.6	Weather Disruptions	25
3.7	Traffic Model	25
3.8	Linear Interpolation	26
3.9	Correlation	26
3.10	Feature Engineering	29
3.11	Fusion Techniques	30
3.11.1	Fusion Levels	30
3.12	Neural Networks	32
3.12.1	Artificial Neural Network	33
3.12.2	Deep Belief Network	35

3.13	Weighted Average	37
3.14	ParseHub	38
3.15	Performance Indices	38
3.15.1	RMSE and MAE	38
3.15.2	Sensitivity Analysis	38
4	Research Design	40
4.1	Data Collection	41
4.1.1	Traffic Dataset	41
4.1.2	Weather Data	42
4.2	Pattern Analysis	42
4.2.1	Traffic Analysis	43
4.2.2	Weather Analysis	44
4.2.3	Weather Disruption	45
4.2.4	Traffic Disruption	45
4.3	Correlation Analysis	45
4.3.1	Correlation of Engineered Traffic Features with Traffic Condition	45
4.3.2	Correlation of Immediate Traffic Features with Traffic Condition	46
4.3.3	Correlation between Connected Road Segments	46
4.4	Model Implementation	47
4.4.1	Prediction Models	47
4.4.2	Data Fusion Model	49
4.5	Training	50

4.5.1	TOM Training Dataset	51
4.5.2	WOM Training Dataset	52
4.5.3	Fusion Model Training Dataset	53
4.6	Evaluation	53
4.6.1	Prediction Model Evaluation	53
4.6.2	Sensitivity Analysis	54
5	Results and Discussion	56
5.1	Pattern Analysis	56
5.1.1	Connected Road Segments	56
5.1.2	Traffic Analysis	59
5.1.3	Weather Analysis	64
5.1.4	Weather Disruption	69
5.1.5	Traffic Disruption	71
5.2	Correlation Analysis	72
5.2.1	Correlation of Engineered Traffic Features with Traffic Condition	72
5.3	Prediction Model Evaluation	78
5.3.1	Traffic-Only Model	78
5.3.2	Weather-Only Model	81
5.3.3	Fusion Analysis	85
5.3.4	Sensitivity Analysis	90
6	Conclusion	95
7	Future Works	98

A Research Ethics Documents	100
B Turnitin Similarity Report	105
C Research Project Timeline	106
D Preliminary Results	107
D.1 Data Pre-processing	107
D.1.1 Traffic Dataset	107
D.1.2 Weather Dataset	108
D.2 Input Dataset	109
D.3 Developing the Model	109
D.3.1 Preparing the Data	109
D.3.2 Defining the Training and Testing Dataset	110
D.3.3 Building the Model	110
D.3.4 Training the Model	111
D.3.5 Evaluation of the Model	112
References	113

List of Figures

2.1	Two states in the BML model. The red arrows are for eastward vehicles, while the blue arrows denote northward vehicles.	12
2.2	ANN Framework used in More et al., 2016	14
3.1	Dasarathy's Decision In - Decision Out (DEI-DEO)	32
3.2	(a) Structure of the Fincher's Pre-Detection Approach, and (b) Structure of the Fincher's Post Detection Approach	34
3.3	Network graph of a One-Hidden layer ANN	34
3.4	Network graph of RBM given n hidden units, and m visible units.	36
4.1	Research Framework	40
4.2	Structure of DBN Training Process	49
4.3	A summary on the contents of the Traffic Only Model Training and Testing Dataset	52
5.1	Correlation heatmap of traffic for both southbound and northbound of Roxas Boulevard	57
5.2	Correlation heatmap of traffic for both southbound and northbound of Espana	57
5.3	Daily average of all working days in one month in all road segments in Roxas Boulevard showing its intensity relationship	58

5.4	Daily average of all working days in one month in all road segments in Espana showing its intensity relationship	58
5.5	Autocorrelation plot of (a) Pablo Ocampo and (b) Antipolo revealing its daily and weekly seasonality	59
5.6	Autocorrelation plot of (a) Pablo Ocampo and (b) Antipolo showing a decaying weekly seasonality	59
5.7	Comparison of the average traffic of (a) Pablo Ocampo's southbound and (b) Antipolo's northbound in one month between working and non-working revealing the lack of intense traffic for non-working days	60
5.8	Comparison of peak hours of the average traffic of (a) Pablo Ocampo's southbound and (b) Antipolo's northbound in one month between working and non-working	61
5.9	Examples of one-month average working day traffic of Pablo Ocampo's southbound illustrating the issues in the peak hour detection in terms of short-term (a) below-peak hour and (b) above-peak hour condition change	62
5.10	Examples of one-month average working day traffic of Pablo Ocampo's southbound showing the improved peak hour detection, fixing the issues for short-term (a) below-peak hour and (b) above-peak hour condition change	62
5.11	Monthly comparison of the average non-working day traffic of (a) Pablo Ocampo's southbound and (b) Antipolo's northbound . . .	63
5.12	Comparison between the two-day-ago pattern and one-week-ago pattern of (a) Pablo Ocampo's southbound and (b) Antipolo's northbound traffic pattern showing that the week before traffic is more similar despite its difference in terms of days	64
5.13	Correlation heatmap of traffic (Pablo Ocampo and Antipolo) and weather variables showing a weak correlation between them . . .	65
5.14	Autocorrelation of weather variables showing the presence of daily seasonality	66

5.15 Comparison of the normal pattern of temperature, heat index, feels-like and wind chill with the normal pattern of Pablo Ocampo's southbound and Antipolo's northbound traffic	67
5.16 Comparison of the normal pattern of pressure with the normal pattern of Pablo Ocampo's southbound and Antipolo's northbound traffic	68
5.17 Comparison of the normal pattern of humidity with the normal pattern of Pablo Ocampo's southbound and Antipolo's northbound traffic	68
5.18 Comparison of the normal pattern of dew point with the normal pattern of Pablo Ocampo's southbound and Antipolo's northbound traffic	69
5.19 Wet and dry season based on the average precipitation per month from 2015 to 2017 defined by the 0.15mm threshold	70
5.20 Autocorrelation of traffic comparing the daily and weekly seasonality per season showing that its pattern is disrupted during the wet season	71
5.21 Comparison between the current traffic and its previous week pattern showing a disrupted pattern	72
5.22 One-day visualization of the relationship between the current traffic and the mean of the traffic 6 weeks ago and 2 weeks ago	74
5.23 One-day visualization of the relationship between the current traffic and the mean of the traffic 6 weeks ago and 2 weeks ago after a week of Typhoon Goring	74
5.24 Autocorrelation of traffic for working days	75
5.25 Standard Deviation of Traffic per Window Size for the Wet Season in Pablo Ocampo	76
5.26 Comparison of Rolling and Expanding windows 4 and 96 to original Northbound traffic in Pablo Ocampo	77
5.27 Average Correlation of Rolling and Expanding Mean to All Southbound Roads in Roxas Blvd.	78

5.28 Comparison between performance of DBN TOM on Roxas Boulevard and Espana using different feature combinations	79
5.29 Performance of DBN TOM on Roxas Boulevard and Espana using OTWP traffic feature combination	80
5.30 DBN TOM Prediction for Normal (left) and Disrupted (right) trends for Pablo Ocampo and Antipolo	81
5.31 Comparison between RNN TOM and DBN TOM	82
5.32 RNN TOM Prediction for Normal (left) and Disrupted (right) trends for Pablo Ocampo and Antipolo	82
5.33 Performance of DBN WOM on Pablo Ocampo and Antipolo using weather feature combinations	83
5.34 Performance of DBN WOM using OW weather feature combination for all road segments	84
5.35 DBN WOM Prediction for Normal (left) and Disrupted (right) trends for Pablo Ocampo and Antipolo	85
5.36 RNN WOM Prediction for Normal (left) and Disrupted (right) trends for Pablo Ocampo and Antipolo	86
5.37 Comparison of DBN models in predicting the southbound of Pablo Ocampo for the wet season	87
5.38 Comparison of RNN models in predicting the southbound of Pablo Ocampo for the wet season	88
5.39 Final Prediction generated by RNN Feature Fusion model for Normal (left) and Disrupted (right) trends for Pablo Ocampo and Antipolo using DBN Decision Fusion	89
5.40 Sensitivity of TOM with different feature combinations	91
5.41 Sensitivity of WOM with different feature combinations	92
5.42 Change in performance in different feature combinations	93
B.1 Turnitin Similarity Report	105

C.1	Research Project Timeline	106
D.1	Predict Southbound Traffic without Feature Fusion	110
D.2	Predict Southbound Traffic with Feature Fusion	110
D.3	ANN Model for Predicting Southbound Traffic without Feature Fusion	111
D.4	ANN Model for Predicting Southbound Traffic with Feature Fusion	112

List of Tables

2.1	Summary of Traffic Models	18
3.1	Sample of Traffic Data from MMDA's Traffic Monitoring System .	23
3.2	Sample of Weather Data from World Weather Online	24
3.3	Results of Pearson and Spearman	27
4.1	Traffic speed equivalent of traffic conditions	42
4.2	DBN Models Network Architecture	48
5.1	Comparison of traffic condition distribution between working and non-working	61
5.2	Transition distribution of traffic condition of (a) Pablo Ocampo and (b) Antipolo for all non-working days	63
5.3	Transition distribution of traffic condition of (a) Pablo Ocampo and (b) Antipolo for all working days	64
5.4	Comparison between previous day and week traffic with the traffic mean 4-weeks-ago showing significant increase in strength in its relationship	73
5.5	Comparison of correlation values on the traffic mean of a range of weeks	73
5.6	Comparison between Prediction Models and Fusion Models	86

Chapter 1

Research Description

Several traffic models were already developed to alleviate traffic congestion, while also considering weather as an effect. However, they were not designed and tested in countries with substandard drainage system, low traffic infrastructure investments, and underdeveloped roads. Moreover, these traffic models made use of information on traffic flow represented as continuous data, compared to categorical traffic data. This research aims to adapt a weather-aware traffic model that will be able to predict traffic given categorical data on traffic, and data on weather. This chapter gives a background on the problem of traffic congestion in countries with and without poor drainage management, traffic infrastructure investment, and developed roads, as well as brief overview of the existing state-of-the-art traffic models and their limitations. This chapter also details the research objectives, scope and limitations, and the significance of the research.

1.1 Background of the Study

Traffic congestion has been a natural occurrence in urban centers in past decades (Bando et al., 1995; Zhao et al., 2005) as the number of vehicles steadily increase and outgrow existing road infrastructures, further delaying traffic flow (J. Lee et al., 2015). Aside from traffic signals and accidents, slight commotions (Bando et al., 1995), weather conditions, road accidents, road constructions, and the behavior of drivers (Mahmud et al., 2012) are also considered major causes. Additionally, in developing and newly industrialized countries, traffic congestion is compounded by poor driver discipline, private transit inflation, archaic traffic management, poor road planning, and low traffic infrastructure investment (Jain et al., 2012).

In order to address this problem without curbing urban growth, several countries have developed various traffic models using approaches like a cellular automata-based model, a knowledge-based model, artificial neural networks, and a hybrid model. Inspired by the Biham-Middleton-Levine (BML) model, Hu et al. (2016) developed a cellular automata-based model that maps and predicts traffic jams at intersections in real-time by simulating traffic volume with certain evolution rules. Machine learning techniques were also used to forecast traffic condition. More et al. (2016) used artificial neural networks (ANN) to predict traffic flow using real-time traffic data such as traffic volume, ensuring a smooth flow using a dynamic synchronization of traffic signals. Meanwhile, W.-H. Lee et al. (2009) developed a knowledge-based model that uses location-based services (LBS) to collect data through data mining technologies. Lastly, Pan et al. (2012) created a Historical ARIMA (H-ARIMA) model, a hybrid traffic prediction model that makes use of historical traffic data together with the current traffic data, specifically traffic volume, speed, and occupancy.

These traffic models do indeed predict traffic congestion. However, they did not consider the weather which has a crucial impact on traffic congestion. In fact, adverse weather conditions, such as precipitation, may reduce the visibility of vehicles, loss of stability, and loss of control (Zhao et al., 2005). From all mentioned factors that affect traffic congestion, weather, by itself, is by far the most disruptive, especially in places with poor drainage systems and road infrastructures. In a heavy rainfall, water is not properly managed and usually overflows the roads above the ground. This produces loss of visibility and control of the drivers, causing them to slow down their vehicles in the roads, which, in turn, causes heavy traffic congestion (Varangis et al., 2003).

The effects of weather in predicting traffic congestion have gained the attention of researchers in recent years (Zhao et al., 2005). Thus, different models have been developed to incorporate weather conditions in predicting traffic condition. For instance, Koeswiady et al. (2016) created a model that incorporates Deep Belief Network (DBN) and data fusion that cross-correlates historical traffic data and current weather data variables making use of a modified ANN to generate a prediction. Y. Jia (2017) used and compared both DBN and Recurrent Neural Network (RNN) using Long Short-Term Memory (LSTM). Both models uses both historical traffic data and rainfall data. In Dunne and Ghosh (2013), on the other hand, they created an Auto-Correlated Neural Network (ACNN) taking transformed data using Stationary Wavelet Transform (SWT) as input to produce a prediction. Besides the use of Neural Networks, one model used multiple linear regression (MLR) to analyze traffic congestions using weather data (J. Lee et al., 2015). This model concludes that temperature affects the traffic congestion, while rainfall does not.

As the recent traffic models were designed and evaluated in countries having exceptional drainage system and fair traffic infrastructure investments (e.g. England (M-BML), Ireland (ANN and SWT-ACNN), USA (H-ARIMA and DBN with Data Fusion), Taiwan (Knowledge-based), and South Korea (MLRA), China (RNN)), using them as is might not yield accurate predictions as countries that have substandard drainage system, underdeveloped roads, and low traffic infrastructure investment, such as Manila experience extreme weather conditions on a fairly regular basis and other scenarios not present in other countries. Additionally, the existing studies on traffic modeling made use of data on traffic flow represented as continuous data on traffic volume. Countries that have low traffic infrastructure, insufficient approach on traffic data collection, such as Manila, have data on traffic conditions represented as categorical data. Hence, the analysis of categorical traffic data, and approaches that can be used to extract information on the effects of all weather variables present in the country from such data, was explored.

1.2 Research Objectives

1.2.1 General Objective

The research aims to develop a traffic model that considers data on traffic condition and weather variables such as wind speed, wind gust, temperature, humidity, dew point, precipitation, visibility, pressure, cloud cover, heat index, and feels-like.

1.2.2 Specific Objectives

Specifically, this research aims:

1. To analyze the relationship and effects of weather variables on traffic congestion;
2. To adapt an existing approach on traffic modeling that considers weather variables in predicting traffic congestion; and
3. To test the accuracy of the model's prediction as compared to the actual traffic data and to test the sensitivity of the model to different settings

1.3 Scope and Limitations of the Research

This study used two different publicly available datasets: traffic and weather. The traffic dataset was obtained from the Metro Manila Development Authority (MMDA). This includes traffic conditions, which were collected in a 15-minute time interval in 14 road segments at Manila for both the northbound (NB) and southbound (SB). On the other hand, the weather dataset was obtained from the World Weather Online (WWO) and generalizes the weather for the entire city of Manila in a 1-hour time interval. This dataset includes weather variables such as wind speed, wind gust, temperature, humidity, dew point, precipitation, visibility, pressure, cloud cover, heat index, and feels-like. The description of each weather variable is shown in Chapter 3. Analysis on traffic and weather were performed to determine the set of features that would be integrated into the model. The traffic and weather datasets were collected from January 2015 to December 2016.

From the approaches and techniques of the existing traffic models that were reviewed (see Chapter 2), this research followed the model framework of Koesdwiady et al. (2016) which will implement data fusion models, and prediction models. This framework was followed based on the similarity of data used and accuracy. The prediction models adapted Koesdwiady et al. (2016)'s DBN, and Y. Jia (2017)'s RNN. The fusion models also adapted Koesdwiady et al. (2016)'s framework implemented in DBN, RNN, and Weighted Average.

To evaluate the proposed model's performance, two statistical error measures were used, namely, the root mean squared error (RMSE) and mean absolute error (MAE). Furthermore, RMSE was also said to be a good aid for decision making because it describes the enormity of errors (Armstrong & Collopy, 1992). Sensitivity analysis was also performed through the comparison of the model's performance with changing inputs to give insight on the relevance of inputs for the model, and the model's responsiveness to the inputs' changes.

1.4 Significance of the Research

Predicting traffic remains to be a challenging problem in the field of complex systems. On a macroscopic scale, patterns of traffic congestion must be derived from traffic flow, density, and speed (Hueper et al., 2009). However, given that weather also affects traffic, as applied in previous weather-aware traffic models, it is verified that weather factors can be aggregated as a traffic contributing factor. This study would provide further analysis on the trends present on categorical traffic data, and extract information on the effect of weather on traffic. Furthermore, given

that weather has an effect on traffic, this study will develop a weather-aware traffic model capable of predicting especially on time periods where weather significantly disrupted traffic, on urban centers with underdeveloped roads and substandard drainage systems.

In transportation, the proposed traffic model could be integrated with existing multi-modal trip planners so that commuters could know how unexpected weather conditions would affect the operations of road-based public transportation. Similarly, for private transits, they could also plan and optimize their trip, and contribute less to the traffic by taking the less congested route.

1.5 Research Methodology

1.5.1 Review of Related Literature

In this phase, existing studies on traffic modeling approaches were reviewed and compared. These approaches could be classified into two: traffic modeling that does not consider weather, and traffic modeling that does consider the weather. To further understand the motivations behind these approaches, and to recognize the factors that build traffic, researches on traffic congestion and the weather's effect on traffic congestion were also reviewed.

1.5.2 Data Collection and Processing

During this phase, historical traffic and weather data were collected. One year of traffic and weather data were collected from publicly available resources. These data were cleaned of missing records and processed to match needs for further analysis.

1.5.3 Data Analysis

To understand the trends and relationships present in both the traffic and weather data, data was analyzed through comparative and correlation analysis. Findings in this phase were used to determine the features to use in the model.

1.5.4 Design and Implementation of Traffic Model

Based on the availability of similar data and accuracy, two traffic models and three fusion models were adapted as the base models for this study. We prioritized traffic models where similar data is accessible for replication before its accuracy. After the replication of the model, it was extended to support other correlated weather factors. These additional factors were integrated into the model either by deriving features out of other traffic models that use it or through experimentation.

1.5.5 Verification and Validation of Traffic Model

In this phase, the performance of the developed traffic model was evaluated using RMSE and MAE. Further on, the performance of different fusion approaches was evaluated to determine what approach is best in predicting traffic. Aside from measuring the performance of the traffic model, its sensitivity to the diversity of the data, and the variety of its hyperparameters was evaluated to determine the most optimal setting for the model.

1.5.6 Documentation

This phase was done alongside other phases. All findings and developments throughout the research process were documented. The documentation was used to keep track of the progress and implementation of each phase.

Chapter 2

Review of Related Literature

This section surveys two types of traffic models: (a) those that do not consider weather data, and (b) those that do consider weather data. For each traffic model, we compare the data used, their research methodology, the modeling approach, and their evaluation strategy.

2.1 Materials

2.1.1 Traffic Data

The surveyed traffic models used different types of traffic data for training their models. The modified Biham-Middleton-Levine (M-BML) model used real-time traffic density and evolution rules as its input (Hu et al., 2016). On the other hand, an artificial neural network (ANN) model used real-time traffic volume per 5-minute interval as its input (More et al., 2016). Aside from the ANN model, an H-ARIMA model also used traffic volume together with speed data (Pan et al., 2012). These data were collected from 800 loop detectors different stationed at different highways in Los Angeles, California.

On the other hand, the knowledge-based model used vehicle GPS data and intersection delay (W.-H. Lee et al., 2009). This model used location-based services such as GPS to collect data in real time. The data collected were the position of the vehicle (cartesian coordinates), traveling speed, direction, and status (idle or not). In addition, intersection delay, the average time it takes for a vehicle to make its turn in intersections, was also taken into account as an input for this

model.

The Deep Belief Network (DBN) with Data Fusion model, the rainfall integrated Recurrent Neural Network the Stationary Wavelet Transform - Auto-correlation Neural Networks (SWT-ACNN) model also collected traffic volume (Koesdwiady et al., 2016; Dunne & Ghosh, 2013). In the DBN with Data Fusion model, traffic volume is measured every 15 minutes for four months to generate a 15-minute traffic prediction. In the SWT-ACNN model, traffic volume is measured hourly in 14 days to generate a 1-hour traffic prediction. The RNN using LSTM was initially collected in 2-minute traffic volume for 2 months (Y. Jia, 2017). Traffic data was resampled from 2 minutes and 30 minutes to generate 10 and 30-minute prediction. The DBN with Data Fusion and LSTM in RNN collected traffic data from freeways in USA and China, respectively. The SWT + ACNN collected traffic data from city roads in Ireland. Meanwhile, the MLRA model collected traffic volume together with traffic speed and travel time in road segments in surrounding Ocean Beach in Seoul, South Korea from July and August 2013 (J. Lee et al., 2015).

2.1.2 Weather Data

The weather data used in weather-aware models also differ from one to the other depending on the presence of these variables in their data, and the correlation between weather and traffic. The DBN with Data Fusion collected weather data from 16 different weather stations for 4 months (Koesdwiady et al., 2016). The weather data includes information for different weather variables such as weather condition, temperature, humidity, wind gust and speed, visibility, dew point, and cloud layer height. After correlating weather variables with traffic condition, the DBN with Data Fusion model made use of temperature, wind gust, and weather condition as their final weather input data.

RNN that uses LSTM used historical hourly rainfall intensity data (Y. Jia, 2017). The study's weather data was resampled to fit the traffic data sampled from 2 to 30 minutes.

In training the SWT-ACNN model, historical weather data is collected from one weather station (Dunne & Ghosh, 2013). The weather data consisted of hourly rainfall record of rainfall level measured in millimeters per hour during the weekdays in 14 days. However, in the actual run time of the model, current weather condition is collected real-time.

In training the MLRA model, 48 individual weather variables were analyzed

through regression. In addition, dummy variables, such as the days of the week, were used. Because there are too many highly-correlated independent variables, regression analysis was used to remove these, avoiding redundancy. Their final input for weather variables is temperature, humidity, and rainfall.

2.2 Research Methodology

The procedure of predicting traffic of the M-BML model can be summarized in three steps (Hu et al., 2016). First, traffic data input is initialized. Based on the traffic density of each road segment in the route, they obtained the average traffic density of each route. Then, the number of vehicles in the M-BML model is initially distributed based on the traffic density of each route.

Second, the M-BML model runs the system. After the model is initialized, a set of evolution rules on how the M-BML model runs is defined: (1) If the next cell is empty, only the vehicles heading *east* can move through one cell at an odd step time; and if the next cell is empty, only the vehicles heading *north* can move through one cell at an even step; and (2) to conserve the number of vehicles in each line, the boundary conditions are periodic. After defining all evolution rules, the system sets a threshold to confirm the jammed area and gradually decreases it to confirm the jammed cells.

Third, different mapping strategies are used to plot the coordinates of the jammed cell in the M-BML model to the intersections in the real-life traffic network. When the model stops running, then the jam value of each cell is confirmed.

Meanwhile, the knowledge-based model undergo four phases as part of its prediction process. The first phase involves the generation of traffic information. This involves the collection and transformation of mined data. This is collected through reports sent to the onboard unit (OBU) of the location-based service application. The mined data will be used to generate real-time traffic information, which is stored and be used as part of the model's real-time predictor's inference.

The next phase involves the mining of the traffic patterns. Using the data from the first phase, traffic patterns will be derived from the historical database. The traffic information generation module will then aggregate these data from the same vehicle and classify them based from four traffic patterns: right-turn delay (RTD), left-turn delay (LTD), spatial and temporal aggregation (STA), and through delay (TD). These processed data will be stored into a journey set table for the model's historical predictor's inference.

After the raw data have been preprocessed and patterns have been mined, an inference engine for the model is developed. This phase will involve the rule construction of the model. These will be based on traffic patterns and meta-rules defined by domain experts. Rules derived from the historical journey set are converted to an if-else ruleset. Meanwhile, meta-rules defined by domain experts include real-time external traffic events such as road accidents.

Lastly, an expert system is developed to make use of these generated and pre-processed traffic information. Three inputs are used in the expert system: an origin-destination pair, start time, and external event module. These are used together with the historical and real-time predictor for the knowledge-based model.

More et al. (2016), on the other hand, have developed a model using ANN approach. For their training, four inputs were taken and the output was predicted. Then, together with the input from the input layer, this predicted output is stored in the context layer which is fed in next iteration for predicting the next one. The process of prediction consists of two subprocesses: feed-forward and backpropagation. During backpropagation, the weights are adjusted depending upon the error.

In the H-ARIMA model, Pan et al. (2012) used traffic parameters like traffic volume and speed to analyze an auto-regression algorithm called Auto-Regressive Integrated Moving Average (ARIMA) and a model that uses average historical data called Historical Average Model (HAM). They were able to infer that because ARIMA uses real-time data, it is only optimal for short-term future prediction while HAM is better to use when doing long-term prediction because it uses the average historical data of a given day of week and time of day. Trying to utilize both models' advantages, they developed a hybrid model that distinguishes whether it is more suitable to use ARIMA or HAM given a situation. In training the model, it first initializes the dataset of all historical data on a given day at a given time. This dataset is then used to test both models to determine their prediction error. From there, the model can determine which submodel to use.

In Dunne and Ghosh (2013), the SWT-ACNN model decomposes input data, either traffic or weather or both, using Stationary Wavelet Transform (SWT) into approximations, and feeds these into the ANN, and generates an output which is recombined using Inverse SWT (ISWT). This generated and recombined output is the predicted traffic flow. Before feeding the decomposed data into the neural network, the decomposed data is auto-correlated to determine the correlation between observations at different lags and to determine the most influential point of the approximations. Additionally, the coefficients for both the weather data and traffic flow are used as input to the neural network at each level of decomposition.

The model framework of the SWT-ACNN is comprised of two parts, the Dry Model and the Wet Model Dunne and Ghosh (2013). The model first determines whether it is currently raining. If it is, the Wet Model, which involves the weather data in decomposition and prediction, is activated. Otherwise, the Dry Model which only involves the traffic data in decomposition and prediction is activated. The correlation, generated by auto-correlation and the neural network, between traffic flow and weather indicates the effect of the latter to traffic

In Koesdwiady et al. (2016), the DBN with Data Fusion model first determines weather variables that truly affect traffic by cross-correlation the different weather variables to the traffic flow. After determining the most influential weather variables, these factors and the traffic flow data is fed into the DBN for training. Traffic and weather are predicted separately. These predictions are fused using Data Fusion techniques to generate an enhanced and accurate traffic flow prediction.

Traffic flow data and weather data used by the DBN with Data Fusion are pre-processed to align data with the model Koesdwiady et al. (2016). Traffic flow data was originally sampled every 30 seconds until aggregating the data into 15 minutes. On the other hand, the weather data was originally sampled every 1 hour. Linear Interpolation was used to resample the weather into 15-minute data. There were observable fluctuations and patterns of the traffic flow especially the differences in traffic during weekdays and weekends. Thus, the data was preprocessed into a detrended version, and a weekday/weekend version. Detrending was used to remove fluctuations caused by variation of the hours and days of each week. The research conducted observed accuracy between the original, detrended and weekday/weekend version.

Y. Jia (2017) used DBN and RNN using LSTM to predict 10 and 30-minute traffic volume. The study used traffic data and weather data together in its training dataset. Deep learning methods DBN and LST were used in predicting 10 and 30-minute prediction in order to learn effective features of traffic flow and rainfall data. The study's training dataset consist of June to August 2013 data, and used the same months of 2014 as its testing data. Using the study's training dataset, the architecture of the study's DBN was determined by testing different input dimensions, layer size, hidden units size per layer, and epochs. Testing dataset was used to compare the differences between DBN and LSTM in RNN. The models without integrating rainfall was considered as benchmark.

J. Lee et al. (2015), on the other hand, suggested a model that uses multiple linear regression analysis (MLRA) model. Before everything else, the weather data was cleaned. Because there are too many independent variables in the model that are highly correlated with one another, regression analysis was used to re-

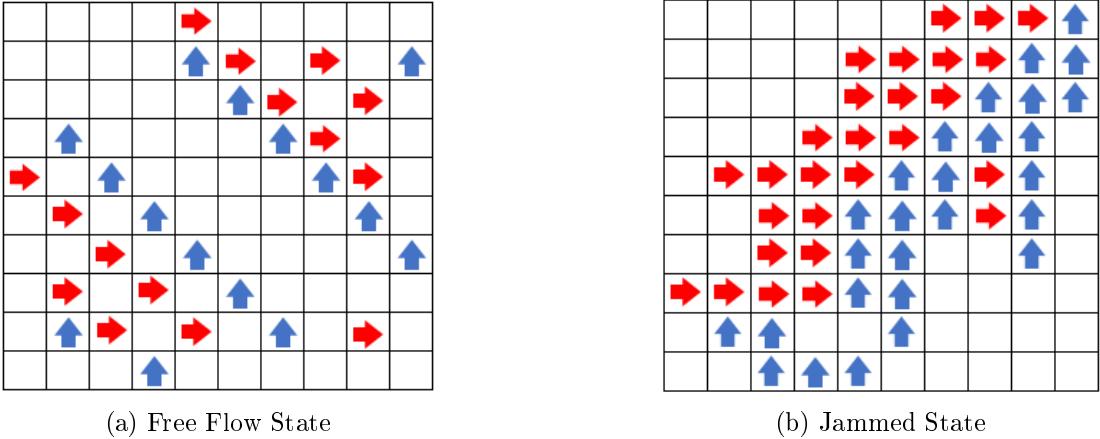


Figure 2.1: Two states in the BML model. The red arrows are for eastward vehicles, while the blue arrows denote northward vehicles.

move these variables. This method of removing variables comprises of three steps. First, this step is called *Backward*, where the model is simplified by removing unnecessary variables one by one. After removing 18 variables, there remain unnecessary independent variables. Hence, their multicollinearity will be diagnosed to remove them again. Second, this step is called *MultiCollinearity*, where the independent variables are removed again based on their multicollinearity (level of linear relationship) between them. 18 more variables were removed after this step. Third, this step is called *Significant Probability (p-value)*, wherein the remaining weather variables are thoroughly filtered.

2.3 Modeling Approach

Different modeling approaches have been used by the models. The M-BML model was inspired by Biham, Middleton, and Levine's model called the BML (Hu et al., 2016). The latter model was the first two-dimensional cellular automaton (CA) model ever developed for simulating traffic in urban road networks (Biham et al., 1992). Each lattice in the two streets, northwards and eastwards. To simulate movement, eastward vehicles move one unit at each odd step time, while northward vehicles move one unit at each even step time, shown in Figure 2.1a. A vehicle cannot move if the next square lattice is occupied by another vehicle. Thus, a traffic jam can be simulated, as shown in Figure 2.1b.

However, Hu et al. (2016) modified the BML in such a way that it improved its performance. While the BML distributed the number of vehicles in eastwards

and northwards equally, the M-BML distributed at random to be more realistic. In addition, current urban networks can be mapped immediately into the M-BML model for predicting traffic congestion.

W.-H. Lee et al. (2009), meanwhile, developed a knowledge-based real-time travel time prediction model that uses location-based services (LBS) collected through data mining technologies. These LBS are collected from vehicles equipped with GPS and mobile data communication module to report its current speed, traveling direction and its current position. It also uses intersection delay patterns, discovered through sequential pattern mining, which is used to estimate the time to turn to an intersection. The model makes use of a dynamic linear combination of two weight predictors: the historical predictor and real-time predictor. Historical predictors are based on historical traffic information. It is used to estimate link travel time and predict intersection delays. On the other hand, the current predictor is based on real-time traffic information. It is used to incorporate external events into the travel time prediction of the model. The concept of dynamic linear combination allows the model to shift between these predictors. For instance, in the case of an external event (e.g. car accident), the model will reduce the weight of the historical predictor because the current predictor may be more reliable since the effect of this incident will immediately affect the traffic condition.

The H-ARIMA model, on the other hand, makes use of 2 different submodels: ARIMA and HAM (Pan et al., 2012). The ARIMA is an autoregressive moving average model that heavily relies on the combination of previous data collected just before the current time in determining the traffic condition for the next time series. Because it considers recent instances, the ARIMA is more optimal to use for short-term prediction. The HAM, on the other hand, relies more on the average of the previous data given that the data is on the same day of the week and at the same time of the day. In order to distinguish the most suitable approach for a given situation, The researchers trained a decision tree that selects which approach to use. Once given an input, the H-ARIMA feeds the input to both approaches and then gets the overall rate of the prediction error of both approaches. The overall rate of the prediction error is computed as the prediction error of the ARIMA divided by the sum of prediction errors of both approaches. If for instance, the rate of the ARIMA is less than the set threshold (0.5), it means that the ARIMA is to be used for the given situation.

Saputri and Lee (2013) believed, however, that using ANN is the best method of forecasting amongst all others. Inspired by the nonlinear characteristics of Biological Brain System, the work performance of ANN can be compared to the workings of the human brain system. Besides its simple computation and fast performance, More et al. (2016) concluded that ANNs minimize the error in limited

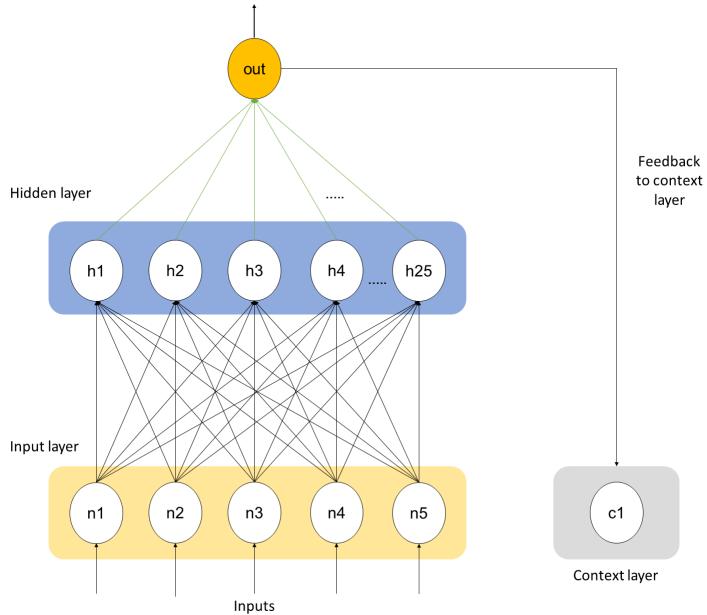


Figure 2.2: ANN Framework used in More et al., 2016

time; hence, it improves the efficiency and accuracy of the system.

There were two models that used ANNs in their approach. One of them developed a traffic model that uses Jordan's Sequential Neural Network, which has a good ability of generalization (More et al., 2016). The structure of this kind of ANN is such that the distribution of nodes in the hidden layer should be the square of the number of nodes in the input layer. For example, if there are 5 nodes found in the input layer, then there must be 25 nodes in the hidden layer. The Jordan's Neural Network contains four layers: (a) context layer, which acts as a memory and stores previous information, (b) input layer, which constitutes the input for the next processing, (c) hidden layer, which gets input from the “true” input layer and the context layer, and (d) output layer, which outputs the result or feedbacks to the context layer to be processed again. Figure 2.2 shows a Jordan's Sequential Neural Network with 5 inputs in the input layer.

The ANN algorithm in the SWT + ACNN model, on the other hand, uses the structure of FeedForward (FF) Back Propagation (BP) algorithm for training (Dunne & Ghosh, 2013). The FF phase receives the input and passes it to the output layer through the hidden layer. As discussed earlier, the input fed into the neural network of the SWT + ACNN model is generated from auto-correlation. The output values are calculated from the input layer passing through the hidden layer, and is summed with the weights of the neural network units through activation functions. The BP phase compares the generated to the desired value.

This phase optimizes the error function through a number of iterations until the error function is close to optimal. The ANN used by the SWT + ACNN, which takes in auto-correlated inputs, have been labeled as the Auto-Correlation Neural Network (ACNN).

In the developed model of Koesdwiady et al. (2016), Deep Belief Network (DBN) and data fusion techniques are used to enhance the generated prediction. DBN, unlike ANN, is composed of multiple layers of hidden units. The DBN of this model makes use of Restricted Boltzmann Machines (RBM), and stacks RBM together within the hidden layer. RBM is an unsupervised learning algorithm that can learn useful features of the data. It takes the input and translates them into a set of numbers that represents them. Then, these numbers can be translated back to reconstruct the inputs. This neural network is trained through multi-task learning to predict several traffic flow predictions at each level at the same time to reach the final traffic flow prediction. Koesdwiady et al. (2016) further discusses that the optimal architecture for the DBN in traffic prediction consists of three hidden layers with 250 in the first, 200 in the second, and 100 in the last hidden layer. Additionally, Koesdwiady et al. (2016) adds that 100 epochs is optimal for training the DBN. The separately predicted traffic flow and weather data will be fused using data fusion techniques to generate an enhanced and accurate traffic flow prediction. The DBN with Data Fusion makes use of Decision In - Decision Out (DEI-DEO) which fuses input data considered as the decision to generate a new or enhanced decision (Koesdwiady et al., 2016).

Y. Jia (2017) used RNN using LSTM to capture time series characteristics during its training and prediction phases. RNN uses memory cells to save information from previous time intervals. LSTM can adjust its hyperparameters to automatically adjust its hyperparameters from the data. The LSTM model consist of one input layer, one hidden layer, and one output layer. The hidden layer performs as the network's memory block that memorizes the long and short term temporal features.

J. Lee et al. (2015), on the contrary, suggested a traffic model that makes use of multiple linear regression analysis (MLRA) employing both weather forecast data and traffic congestion data. MLR analysis is used to explain the relationship between one continuous dependent variable (traffic congestion data) and two or more independent variables (weather data). In this model, the traffic congestion is influenced by 48 independent variables. However, in their research, some of those independent variables are highly correlated to each other, and therefore should be removed to prevent the increase of correlation.

2.4 Evaluation Strategy

Before computing the accuracy of each traffic models, different experiments and case studies were first performed. All traffic models were tested to predict the traffic congestion at a given time period.

In evaluating the knowledge-based model, (W.-H. Lee et al., 2009) collected five months of location-based service (LBS) raw data. The LBS raw data was collected through an online taxi dispatch system (TDS), consisting of around 500 taxis operating 24-7 in a Taipei urban area. The first four months are used for mining traffic patterns, whereas the fifth is used for verifying the accuracy of the model. In the experiment, a random origin-destination pair is selected at two peak hour sections. The model produced a precision of 10.8% *relative mean error* (RME) and *root mean squared error* RMSE of 15.92%. To further challenge its reliability, the experiment was performed with the same set of input, having the intersection delay replaced with a turning delay estimate from a human expert. The model produced a precision of 20% RME and 30.55% RMSE, which, in comparison with the pattern generated intersection delay, is relatively unreliable.

In evaluating the accuracy of the H-ARIMA model, the researchers compared results with other baseline approaches given two situations: short-term prediction and long-term prediction (Pan et al., 2012). RMSE and *mean absolute percentage error* (MAPE) were used to measure the accuracy of the traffic prediction. Although the H-ARIMA model was able to yield better results than the other baseline approaches for short-term prediction, the researchers were not able to see the edge of the H-ARIMA model against them. Similar to that, the H-ARIMA model was also able to produce a better result for long-term prediction compared to the baseline approaches. It was observed that its MAPE is lower compared to others because it considers historical traffic data in predicting traffic. Overall, the H-ARIMA model was able to produce around 95-96% accuracy.

To measure the accuracy of the predictions of the DBN with Data Fusion, performance indexes RMSE and MAE are used (Koesdwiady et al., 2016). These performance indices calculate the error value of the prediction by comparing the actual and predicted output at a certain time t . The research compared the performance of different neural networks of ARIMA and ANN with DBN. After experimentation, the DBN outperformed the other neural networks in predicting traffic flow. The performance of the DBN generated an average MAE of 0.07 and average RMSE of 0.05. On the other hand, ANN generated an average MAE of 0.08, and an average of RMSE of 0.06, and ARIMA generated an average MAE of 0.27 and an average RMSE of 0.23.

To examine the performance of the neural network with low, medium and heavy traffic, three different freeways that experience the mentioned traffic conditions are chosen (Koesdwiady et al., 2016). The detrended version of the data was more accurate in predicting heavy traffic, and the original data was more accurate in predicting low and medium traffic. Medium traffic flow using original data achieved an MAE of 0.041 and RMSE of 0.06. Low traffic flow using original data achieved MAE of 0.034 and RMSE of 0.045. On the other hand, detrended version of the data performed best in predicting high traffic flow achieving an MAE of 0.06 and RMSE of 0.09. Moreover, using weekday/weekend version of the data generated a higher average error. Furthermore, the model better predicts the medium traffic flow with consideration to weather information.

For Y. Jia (2017), they evaluated the model, and its effectiveness in predicting traffic with consideration of rainfall, through comparing the performances of DBN and LSTM models with and without rainfall consideration. The test dataset used for evaluating consist of instances when rainfall was significantly present. The study used MAE, MAPE and RMSE as the evaluation metrics. Results show that predicting 10-minute traffic volume is more accurate than predicting a 30-minute traffic volume. Moreover, the LSTM model performed better than DBN with or without considering rainfall, showing the advantage of LSTM to capture time series patterns of the traffic data. The LSTM model achieved an RMSE (vel/h) of 240.98 and 269.91 for the 10-minute and 30-minute prediction, respectively, while the DBN model achieved an RMSE (vel/h) of 255.79 and 365.49, showing a significant change from the performance of LSTM.

The model's performance was compared to ANN that takes in undecomposed data to observe the differences in performance. To measure the accuracy and performance, RMSE and MAPE were used. The SWT-ACNN outperformed the non-wavelet model significantly by approximately 5% of MAPE, and 40 of RMSE. Additionally, the wet model is superior to the dry model achieving a MAPE of more than 30% than the dry model.

To compare the results of J. Lee et al. (2015)'s MLRA model with the actual values, present traffic congestion data were used. As discussed in the previous section, the weather data used in their research are temperature, humidity, rainfall. In their analysis, they used MAPE to assess the developed MLRA model. When they predicted the traffic congestion from July and August 2013, the traffic model got an accuracy of 94.1%. However, when they predicted the traffic congestion in 2014 for the same months, they have arrived at 84.8%.

Table 2.1: Summary of Traffic Models

Author (Year)	Modeling Approach	Traffic Data Input	Weather Data Input	Coverage	Evaluation Strategy	Accuracy
Hu et al. (2016)	Cellular Automata (CA)	- traffic density - evolution rules	none	- road segment - Birmingham, England	not indicated	94.00%
More et al. (2016)	Artificial Neural Network (ANN)	traffic volume	none	- road segment - Dublin, Ireland	not indicated	92.00 - 98.00%
W.-H. Lee et al. (2009)	Knowledge-based	- vehicle GPS data - intersection delay	none	- whole city - Taipei, Taiwan	- RMSE - RME	84.08%
(Pan et al., 2012)	HAM and ARIMA (H-ARIMA)	- traffic volume - speed	none	- road segment - Los Angeles, USA	- RMSE - MAPE	95.99%
Koesdwiyadi et al. (2016)	Deep Belief Network with Data Fusion (DBN with Data Fusion)	- traffic volume	- temperature - wind gust - weather condition	- road segment - San Francisco, USA	- RMSE - MAE	95.95%
Dunne and Ghosh (2013)	Stationary Wavelet Transform and Auto-Correlation Neural Networks (SWT-ACNN)	- rainfall - traffic volume		- road segment - Dublin, Ireland	- RMSE - MAPE	91.45%
J. Lee et al. (2015)	Multiple Linear Regression Analysis (MLRA)	- speed - travel time - traffic volume	- temperature - traffic volume	- whole city Seoul, South Korea	- MAPE	84.80%

Chapter 3

Theoretical Framework

3.1 Traffic-related terms

Traffic flow

According to May (1990), traffic flow studies how travelers interact with infrastructures and with each other, in order to understand the movement of traffic and how can it be improved with less congestion. These travelers include drivers, pedestrians, among others, while infrastructures include roads, signages, stop lights, and other devices that control traffic.

Traffic speed

The speed of a vehicle can be computed by measuring the distance it traveled per unit time. Because the speed of each vehicle may be different from its neighboring vehicles, traffic speed is the average of the speed of each vehicle in the given environment.

Traffic volume

Traffic volume refers to the number of vehicles present in a certain road at a given time.

Traffic density

Given a length of a road, traffic density is measured by the number of vehicles present. This means that if the traffic density is low, then there is no traffic congestion because the vehicles are apart from each other. In reverse, if the traffic density is high, then the vehicles are close to each other; thus, a traffic congestion.

Traffic condition

Traffic conditions refer to the states of traffic at a certain point at a certain time, with respect to traffic flow, speed, volume, and density. It has three major states: light, moderate, and heavy traffic.

3.1.1 Traffic Congestion

Traffic congestion, according to (Vuchic et al., 1994), happens when traffic volume on a particular road goes beyond the road's capacity. (Bovy et al., 2002) define traffic congestion as the state of traffic flow on a particular road with low speeds and high densities compared to some other state with high speeds and low densities.

Road and road segments

A road is a wide path from one place to another, usually paved for the vehicles to drive on (Wang et al., 2013). Typically, a road is created for vehicles to head two opposite directions, northbound and southbound. A road segment, on the other hand, is a portion of a road heading in one direction, separated by infrastructures (e.g. train stations, landmarks, intersections).

3.2 Weather-related terms

Temperature

Temperature is the measure of the hotness and the coldness of an object. There are three major scales that are being used internationally, *Celsius*, *Fahrenheit*,

and *Kelvin*.

Dew point

Dew point is the temperature wherein moisture or *dew* appears on solid surfaces. This is caused by condensation, in which the water vaporizes into its liquid form at certain amounts of pressure.

Humidity

Humidity refers to the quantity of the water vapor contained in the air. Measured in percentage, relative humidity, on the other hand, is the quantity of water vapor in relation to how much the air can hold at a certain temperature. If the air is warm, it has high relative humidity since the air holds more water vapor than cold air.

Wind speed

Wind speed is the average wind speed in the indicated amount of time. Because of the changing temperature, wind speed results from the air going from above average temperature to a lower temperature.

Wind Gust

Wind gust is the short, rapid rise of wind speed before quickly calming. The wind is forced to change its direction and speed quickly because of sudden decrease in temperature, wind shears, and friction.

Precipitation

Precipitation refers to any result of air condensation that falls due to the pull of gravity. This includes, but not limited to, rain, snow, and hail. Usually, precipitation is measured in terms of millimeters (mm).

Visibility

Visibility is the measure of how long can we distinguish light or an object at a certain distance.

Pressure

Pressure, also called atmospheric pressure, is the amount of force exerted by the air molecules in a particular surface area of the earth. Meteorologists use millibars (mb) to measure pressure.

Cloud Cover

Cloud cover is defined as the amount of clouds in a fragment of the sky in a particular location. This contributes to the weather condition and visibility. This is usually measured by *okta*.

Heat Index

Heat index is the temperature of how hot the human body feels like. This is directly related to air temperature and relative humidity.

Feels-like

Feels-like is the temperature of how cold the human body feels like when the wind touches the skin.

3.3 Historical Data

Historical data is an extensive archive of data that can be utilized to detect regularities or pattern for predicting future outcomes. It ranges from months-worth to years-worth of past data. The following section features sources whose historical data will be used for the research.

Table 3.1: Sample of Traffic Data from MMDA’s Traffic Monitoring System

Date and Time	Road	Segment	Condition (Northbound)	Condition (Southbound)
2015-01-01 00:00:00	EDSA	Quezon Ave.	L	L
2015-01-01 00:00:00	EDSA	Taft Ave.	M	M
2015-01-01 00:00:00	ESPAÑA	Welcome Rotunda	L	L
2015-01-01 00:15:00	EDSA	Quezon Ave.	N	N
2015-01-01 00:15:00	EDSA	Taft Ave.	M	M
2015-01-01 00:15:00	ESPAÑA	Welcome Rotunda	L	L

3.3.1 Traffic Data from MMDA’s Traffic Monitoring System

The traffic dataset includes traffic conditions for nine major roads in Metro Manila, collected in a 15 minute time interval. The traffic condition can either be *light* (L), *moderate* (M), or *heavy* (H). However, if no information is available, it can also appear as *none* (N).

Major roads from this dataset include EDSA, Commonwealth, Quezon Avenue, España, C5, Ortigas, Marcos Highway, Roxas Boulevard, and SLEX. Each road consists of a number road segments, which includes a northbound lane and a southbound lane. For instance, EDSA consists of 37 road segments (e.g. Balintawak, Kaingin Road, Muñoz).

Table 3.1 shows a sample raw data collected from MMDA’s traffic monitoring system. From the sample data, it can be observed that despite not having a traffic condition entry, the interval is still being recorded as part of the dataset, having a traffic condition record of *none* (N).

3.3.2 Weather Data from World Weather Online

The weather dataset from World Weather Online includes temperature (in both Celsius and Fahrenheit), humidity (in percentage), pressure (in millibars), wind speed (in both miles per hour and kilometers per hour), and dew point (in both Celsius and Fahrenheit), cloud cover amount (in percentage), heat index (in both Celsius and Fahrenheit), visibility (in kilometers), wind chill temperature (in both Celsius and Fahrenheit), wind gust (in both miles per hour and kilometers per hour), feels-like temperature (in both Celsius and Fahrenheit), and precipitation (in millimeters). This data is sampled every one hour of every day and is a generalized reading for the whole city of Manila.

Table 3.2: Sample of Weather Data from World Weather Online

Property	Sample Value
Date	2015-10-01
Time	0
Weather Condition	Moderate or heavy rain shower
Temperature (°C)	27
Temperature (°F)	81
Wind Speed (m/h)	2
Wind Speed (km/h)	4
Humidity (%)	87
Visibility (km)	8
Pressure (mb)	1013
Cloud Cover (%)	27
Heat Index (°C)	31
Heat Index (°F)	88
Dew Point (°C)	25
Dew Point (°F)	76
Wind Chill (°C)	27
Wind Chill (°F)	81
Wind Gust (m/h)	4
Wind Gust (km/h)	7
Feels Like (°C)	31
Feels Like (°F)	88
Precipitation (mm)	2.8

Table 3.2 shows a sample raw data collected from World Weather Online. It could be observed that the conversion of some variables to different units has already been performed as part of the data. Furthermore, missing data is not evident from the samples collected.

3.4 Working Day

A working day refers to a day in which people are assigned on duty in an organization (e.g. company, government, school, etc.) each week (J. Liu, Zhou, & Chen, 2008). For most organizations, working day is defined to be from Mondays to Fridays. Non-working days, meanwhile, are from Saturdays to Sundays. As people are on duty during working days, this implies an increase in demand on transportation when going to their respective organizations (Z. Liu et al., 2016).

Thus, there is an increase in traffic volume due to the demand during weekdays as compared to weekends.

Aside from weekends, there are also instances in which a weekday can be classified as a non-working day. This occurs during holidays or whenever a public-sector or government announces class or work suspension.

3.5 Peak Hour

A peak hour, or rush hour, is a time of the day where the congestion of traffic in roads or inflation of people in public transports are at its highest peak (Downs, 2005). There are two peak hours each weekday: the morning peak hour and the afternoon or evening peak hour. These are the times when majority of the people travel and commute to go to work or school. The morning peak hours depict the time when employees and students travel towards their workplace or school, while the evening peak hours suggest the time when they return to their respective homes. These periods may last for more than one hour, and may vary from road to road, city to city, country to country, and seasonally.

3.6 Weather Disruptions

Weather disruptions such as typhoons and low-pressure areas have brought heavy and prolonged precipitation which often causes flooding in some areas. One example of these extreme weather disruptions is Typhoon Goring that occurred from July 22, 2015 until July 26, 2015. Weather disruptions typically produce a significant amount of precipitation in just one day. These prolonged rain periods usually last for days, thus building up the effects it brings as time goes by.

3.7 Traffic Model

Mathematically, a traffic model is a representation of traffic in the real-world (Mahmud & Town, 2016). These models exist to help researchers understand how traffic works and how can the congestions be minimized by simulating them in a way that researchers can explore and manipulate.

There are two major types of traffic models: *macroscopic* and *microscopic* traf-

fic models (Mahmud & Town, 2016). A macroscopic traffic model deals with the properties of transportation elements in the bigger picture. It describes the circulation of traffic without going into its individual components. Macroscopic traffic models usually describe traffic using flow-rate, volume, density, speed, among others. A microscopic traffic model, on the other hand, deals with characteristics of the individual transportation elements. This covers driver behavior, how the vehicles move, element interaction, among others. These kinds of traffic models use various learning algorithms like regression, neural networks, clustering, decision trees, among others.

3.8 Linear Interpolation

Using surrounding data points, interpolation can be used to determine the value of an unknown point in a line. Linear interpolation is one method of interpolation where it assumes a linear or straight line relationship between two known points. It is used to approximate value through the weighted average of two points. The equation for Linear Interpolation is defined as:

$$y = y_1 + \frac{y_2 - y_1}{x_2 - x_1}(x - x_1) \quad (3.1)$$

3.9 Correlation

The Spearman's rank correlation coefficient is an approach for statistical dependence between two independent variables while not consider the parameters of a frequency distribution (nonparametric) (Zar, 1972; D. Liu et al., 2010; Gauthier, 2001). The rank correlation coefficient, r_s , can be expressed using a monotonic function as:

$$r_s = 1 - \frac{6 \sum a^2}{N(N^2 - 1)} \quad (3.2)$$

where r_s represents the Spearman's rank correlation coefficient, a denotes the ranked difference between the i th measurements for the two random variables, and N is the number of measurements in each of the two random variables in the correlation (Zar, 1972). r_s measures the strength and course of the *monotonic* relationship between ranked variables. Hauke and Kossowski (2011), meanwhile,

Table 3.3: Results of Pearson and Spearman

Correlation Relationship	Value
very strong positive correlation	$0.9 < x \leq 1.0$
strong positive correlation	$0.7 < x \leq 0.9$
moderate positive correlation	$0.5 < x \leq 0.9$
low positive correlation	$0.3 < x \leq 0.5$
no correlation	$-0.3 < x \leq 0.3$
low negative correlation	$-0.5 < x \leq -0.3$
moderate negative correlation	$-0.7 < x \leq -0.5$
strong negative correlation	$-0.9 < x \leq -0.7$
very strong positive correlation	$-1.0 < x \leq -0.9$

explain that r_s can be considered as the correlation coefficient of Pearson that deals with ranks.

Pearson's product moment correlation coefficient, commonly Pearson's correlation coefficient or Pearson's r, is the most commonly used correlation statistic to measure the strength and course of the *linear* relationship between two continuous variables (Ahlgren et al., 2003). It is expressed using this function:

$$r = \frac{\sum(A - \bar{A})(B - \bar{B})}{\sqrt{\sum(A - \bar{A})^2 \sum(B - \bar{B})^2}} \quad (3.3)$$

where r represents the Pearson's r, A and B denote the two variables being observed, and \bar{A} and \bar{B} are the averages of the two variables respectively.

Both correlation analysis outputs a value between -1 to +1. If the result of a correlation is close to +1, then variable A has a positive relationship with variable B; vice versa, if the result is close to -1, then variable A has a negative relationship with variable B. If the result is approaching 0, then variable A has no relationship with variable B. Table 3.3 shows the correlation relationships with their corresponding ranges, where x is the exact correlation result.

Although Spearman is considered a Pearson's r measure in terms of ranks, there are advantages that enable Spearman to be a more powerful measurement over Pearson (Gauthier, 2001). Spearman's rank correlation coefficient is not affected by the distribution of the values, unlike Pearson's r, which normal distribution is analyzed. Furthermore, instead of the raw data, it does not care for outliers because it deals with the ranks of the data. In addition, the data does not need to be in time-series, where the intervals are regular. In contrast, since

Spearman disregards the outliers when it turns the data into ranks, there is a loss of information. Moreover, it is less powerful than the Pearson's r if the data is normally distributed.

Seasonality

Seasonality refers to the characteristic of a time series in which the data experiences regular and predictable changes that recur every number of intervals. In trend analysis, determining the data's seasonality is significant as it could define a "normal pattern" by getting the mean of several samples per seasonal interval.

Autocorrelation

Autocorrelation, sometimes called *serial correlation* or *lagged correlation*, measures the similarity or correlation of an observation in a time series and itself shifted in a specific time *lag*. The series of numbers arranged in time is correlated to the values of its own past and future. The purpose of autocorrelation is to find out if there is a pattern repeating in the data. The formula for autocorrelation is as follows:

$$r_k = \frac{\sum_{i=1}^{N-k} (X_i - \bar{X})(X_{i+k} - \bar{X})}{\sum_{i=1}^N (X_i - \bar{X})^2} \quad (3.4)$$

where k denotes the lags, N as the number of observations in the series, and X as the data.

Lag

Lag refers to the amount of delay between a given observation. For instance, a comparison between Tuesday's 12 PM and the last week's Tuesday's 12 PM is indicated as a one day lag.

Autocorrelation plot

Autocorrelation plot is a collection of autocorrelation coefficient values from a range of time lags. It is commonly used for evaluating the randomness of the

dataset. It can be used to measure seasonality as it reveals how many intervals does it take for the pattern to reappear.

It consists of three parts: the y-axis, the x-axis, and the reference lines. The y-axis consists of correlation coefficient values, while the x-axis consists of time lags defined as t where $t = 1, 2, 3, \dots, n-1, n$.

3.10 Feature Engineering

Feature engineering is important for any system that uses machine learning. The performance of machine learning algorithms depends on how the data was presented to them. If they accept raw data directly, they would not give the intended results since machine learning algorithms do not have the capacity to extract insightful features from raw data automatically. This is where feature engineering comes in. It is using the domain knowledge of and from the raw data and create insightful features which would help machine learning algorithms to perform better.

A feature is a property that is common with all the independent units in the raw data. Choosing the right features for the model is of utmost necessity. To yield better results, models should be simple and be more flexible, which better features would produce.

The process of feature engineering is difficult and exhaustive. At first, a lot of features need to be decided and created regardless of its relevance. Afterwards, these features would be checked with the model to identify how and which features would help the model. Then, to avoid overfitting, feature selection should be used. This process would repeat until certain features are finalized and used with the model. The steps to follow look like this:

1. Brainstorm features. Understand the problem, explore the data, and find studies that are similar to your problem and how they used feature engineering to solve their problem.
2. Devise features. Decide on what features to create based on the problem at hand.
3. Create features. Use different feature selection methods and feature importance scorings to create feautes.
4. Test features with the model. Estimate the accuracy of the model on unseen data using the chosen features.

5. Improve features. Modify the features depending on the result of the model's accuracy.
6. Repeat Step 1 until the work is done.

3.11 Fusion Techniques

To achieve the best performance, fusion techniques were made for designing systems which recognize patterns. By combining data, features, or decisions from a set of sensors, better inferences are made and accuracy is improved (Sohn & Lee, 2003). Fusion techniques are applied in the field of military, where targets are automatically recognized (Bossé et al., 2006), in the field of image processing for medicine (Constantinidis et al., 2001), face recognition (Mangai et al., 2010), robotics (Jimenez et al., 1999), among others. There are three levels for fusion techniques: *data fusion*, *feature fusion*, and *decision fusion*. In this paper, only the feature fusion and decision fusion will be discussed. In addition, there are numerous techniques to solve fusion problems, but in this paper, only neural networks and weighted average will be discussed.

3.11.1 Fusion Levels

Feature Fusion

Features are the most essential information needed to accomplish any classification task. Although important, not all features contribute to the performance of a classifier. Features that do not match the rest of the dataset can have an effect to the pattern recognized by the classifier. Thus, they should be removed from the dataset (Mangai et al., 2010). The process of improving or obtaining new features is called feature fusion (Castanedo, 2013).

Dasarathy (1997) broke down the common hierarchy of fusion into five levels. In the said breakdown, he defined feature fusion as the Feature In- Feature Out Fusion (FEI-FEO). This fusion process accepts and outputs features. Feature fusion can be divided into three methods: feature ranking and selection, feature extraction, and combination (Mangai et al., 2010).

Mangai et al. (2010) described feature ranking and selection as the soul of feature fusion. It aims to find the optimal subset that can represent the entire dataset. In feature extraction, on the other hand, features are reduced and ranked

for a better analysis Dasarathy (1997). Lastly, feature combination derives new features from at least two selected features.

Another fusion level that accepts features is the Feature In-Decision Out Fusion (FEI-DEO). Its difference with the FEI-FEO Fusion is that instead of having features as its output, it outputs a decision instead. Some researchers refer to this as either feature fusion because of its input or decision fusion because it outputs a decision. It all depends on the researcher's view (Dasarathy, 1997). It is commonly used by researchers for pattern recognition systems that generates a decision based on inputs from different sensors (Castanedo, 2013).

With the issues involving the validity of decision fusion for the affective field, D'Mello and Graesser (2010) used feature fusion for a multimodal affect detection system. The researchers combined features to generate a better distinction between common human experiences such as confusion, frustration, engagement, delight, boredom, and neutral. They concatenated features from three sensory channels to produce a multichannel feature set. As a result, they were able to generate four multichannel models: Facial-Dialogue (FD) model, Facial-Posture (FP) model, Dialogue-Posture (DP) model, and Facial-Dialogue-Posture (FDP) model. They used feature selection to filter out a number of features that have the highest F-ratio. These features were then combined with the set of features selected from the other channel.

Geetha and Radhakrishnan (2013) were able to get satisfactory classification results after fusing fingerprint and palmprint features for a multimodal biometric authentication system. It aims to identify the set of most important features that can be used for a better recognition accuracy. The researchers claimed that fusing the features extracted from 2D Gabon filter, stationary wavelet transform (SWT), and principal component analysis (PCA) by concatenation would result into a large feature set. This makes computing match scores more laborious. Hence, they used a wavelet-based fusion algorithm to fuse the extracted features. After using SWT to extract line information, the researchers used the mean-max fusion method to fuse the said features.

Decision Fusion

A decision is a conclusion stemmed from facts of a discerned events and activities (Castanedo, 2013). As the high-level fusion technique, the decision fusion is more complicated since it inputs decisions from multiple classifiers to obtain one accurate decision (Mangai et al., 2010). Dasarathy (1997) defines decision fusion as the Decision In - Decision Out (DEI-DEO) fusion in his five-step hierarchy

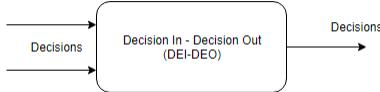


Figure 3.1: Dasarathy's Decision In - Decision Out (DEI-DEO)

of fusion based on input and outputs (see Figure 3.1). This combines multiple decisions from the input and outputs a more appropriate decision.

Dasarathy (1997) also argues that while DEI-DEO fusion does not always trump data or feature fusion, the whole system does not fail if one of the sensors fail, unlike the other fusion techniques. He further explains that the DEI-DEO has less computational demands than the data or feature fusion, and that the bandwidth for communication is not important.

Castanedo (2013) states one of the most used methods for decision fusion. The first method is the *Bayesian Method*. This technique combines facts from probability theory rules, where the input and the outputs are probabilities in between $[0, 1]$. This method is derived from the Bayes rule:

$$P(B|A) = \frac{P(A|B)P(B)}{P(A)}, \quad (3.5)$$

which gives us the probability of B given A . However, because the probabilities $P(A|B)$ and $P(A)$ are not always known, it may not be applicable to some cases. Furthermore, Hall and Llinas (2001) state that the Bayesian method has a complexity problem if there are more than one possible result for $P(B|A)$.

Other than Bayesian method, there are other techniques that can be applied to decision fusion, such as the Dempster-Shafer inference, abductive reasoning, semantic methods (Castanedo, 2013), logistic function, weighted decision methods (Sohn & Lee, 2003), projection pursuit, majority voting, fuzzy logic, and neural networks (Jimenez et al., 1999).

3.12 Neural Networks

Neural Networks can be used as either a prediction model or a classifier. Koesdwiady et al. (2016); Dunne and Ghosh (2013) used neural networks, specifically Deep Belief Network and Auto Correlation Neural Network, respectively. They used historical traffic data as input, and outputs the predicted traffic volume. Their

neural networks extract and learn patterns present in their data.

Neural Networks can also be used as a data fusion center (Fincher & Mix, 1990), specially in fusing data at the decision level. The advantage of having neural network as a technique for fusion over statistical approaches, such as Bayesian Method, is that it does not need to know certain probability errors beforehand. It can train itself with the current facts at hand and still get accurate results. Fincher and Mix (1990); Dai and Khorram (1999); Jimenez et al. (1999) used neural networks in fusing outputs generated by separate models. Fincher and Mix (1990) used neural network-based data fusion for recognizing patterns between handwritten and computer-made numbers. Handwritten Patterns are first pre-classified, and compared with computer-made numbers using a number of classifying algorithms. The different output of the different classifying algorithms are then fused into one improved classification. Figure 3.2 illustrates the pattern recognition approach of the study. Dai and Khorram (1999) used neural networks for image processing to recognize changes between pictures of the same location of different times. The changing pictures were used as inputs, and their fusion center takes care of extracting patterns and changes in the picture, and outputs a single picture that features the changes between the inputs. Jimenez et al. (1999), much like Fincher and Mix (1990), generates decisions from separate classifier models, and fuses them into one decision through neural networks.

3.12.1 Artificial Neural Network

Inspired from the nonlinear characteristics of Biological Brain System, the work performance of artificial neural networks (ANNs) can be compared to the workings of the human brain system (More et al., 2016). While handling uncertainty and non-linearity at the same time, ANNs provide “intelligent processing functions” in order to predict, learn, and memorize (Sommer et al., 2013). ANN can be applied to every situation where the input variables have a relationship with the output variables. The network for ANN consists of 3 layers in order, the input layer, hidden layer and output layer. Each layer consists of 1 or more units or neurons.

Figure 3.3 shows a the network graph of a One-Hidden layer ANN. Each set of inputs is modified by unique weights in unit connections, and biases in unit. Training in ANN involves adjusting all the weights and biases to have the correct output. A conventional ANN uses backpropagation for its training algorithm (Hamad et al., 2017). Backpropagation is a training algorithm which trains the neural network from the input layer to the output layer initializing the weights and biases, and then propagate back from the output layer to the input layer to adjust the weights and biases from the differences between the generated output

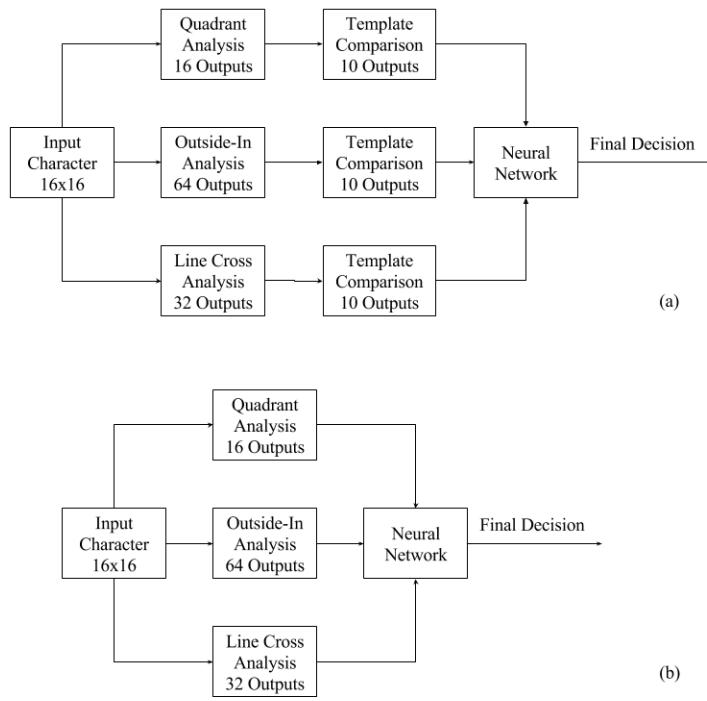


Figure 3.2: (a) Structure of the Fincher's Pre-Detection Approach, and (b) Structure of the Fincher's Post Detection Approach

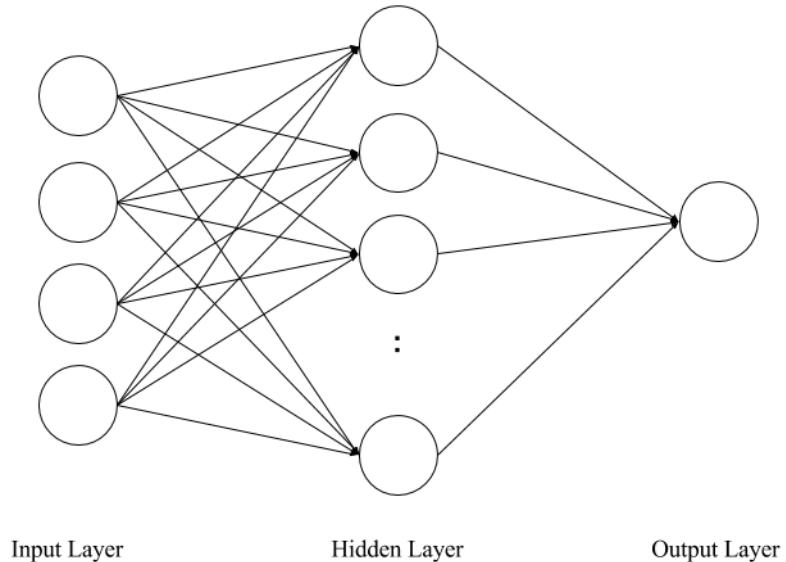


Figure 3.3: Network graph of a One-Hidden layer ANN

to the expected output. In backpropagation, each unit that receives a value gets adjusted using an activation function. This training process is repeated a number of times until training error is close to optimal, or until the network reaches the maximum number of epochs. Once backpropagation is finished, the network is trained. The weights (w) are adjusted by many learning algorithms such as the Error Correction Learning where the connection weights between unit i and unit j are adjusted in terms of the difference between the desired and the computed value. A multilayer error correction weight adjustment formula is defined as

$$w_{ij}^{new} = w_{ij}^{old} - \eta \frac{\partial E}{\partial w_{ij}^{old}} \quad (3.6)$$

where η is the learning rate - the percentage the network minimizes the error rate in each iteration and E is the square of errors of the desired output and actual output which can be defined as

$$E = \frac{1}{2} \sum_{j=1} (b_j - z_j)^2 \quad (3.7)$$

where b is the desired output value, and z is the actual output value.

3.12.2 Deep Belief Network

Koesdwiady et al. (2016) states that the training algorithm for ANN suffer from the problem of local minima, wherein the training algorithm may get stuck in the local minima during backpropagation. Deep Belief Networks (DBN) solve this problem by adding an extra step called pre-training which is done before backpropagation that can lead to an error rate not far from optimal. Backpropagation can be used then to slowly reduce the error rate from there. Additionally, other techniques and learning algorithms cannot extract and learn features without prior knowledge of specific domains. Deep Learning could learn features with less prior knowledge.

The training process of DBN consists of two phases, the pre-training and fine-tuning. In the pre-training process, the hidden layers of the DBN are trained greedy layer-wise. Pre-training generates the initially trained DBN with initialized weights and biases for each layer and unit. Fine-tuning further adjusts these weights and biases via backpropagation training algorithm using a labeled input data.

DBNs are made up of stacks of Restricted Boltzmann Machines (RBM). It is a building block for multi-layer learning models of Deep Belief Networks. A DBN

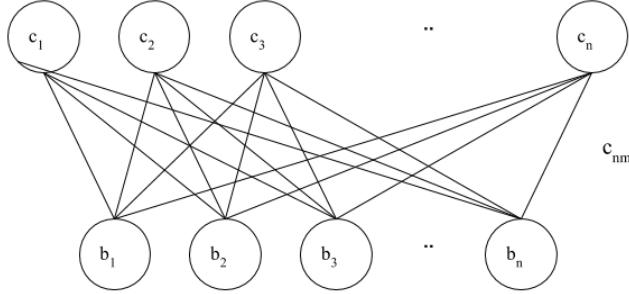


Figure 3.4: Network graph of RBM given n hidden units, and m visible units.

stack RBMs to learn features to features to arrive at a high-level representation. An RBM consists of 2 layers which are the visible layer with i visible units, and a hidden layer with j hidden units. The RBM is an unsupervised learning algorithm that can learn useful features of the data. It takes the input and translates them into a set of numbers that represents. Then, these numbers can be translated back to reconstruct the inputs. Through several forward and backward passes, the RBM will be trained. A trained RBM can reveal which features are the most important ones when detecting patterns (Zhang et al., 2017; Fischer & Igel, 2014). The hidden units of a trained RBM represent relevant features of observations. These features can also serve as input for another RBM. The network graph of an RBM is illustrated in 3.4.

RBM defines a probability distribution, via the energy function, between each units' weights and biases. This distribution is defined as

$$p(v, h) = \frac{e^{-E(v, h)}}{Z} \quad (3.8)$$

where Z is the partition function, and $E(v, h)$ is the energy function defined as

$$E(v, h) = \sum_{i=1}^V \sum_{j=1}^H w_{ij} v_i h_j - \sum_{i=1}^V a_i v_i - \sum_{j=1}^H b_j h_j \quad (3.9)$$

where the v_i is the visible unit i , h_j is the hidden unit j , w_{ij} is the weight between v_i and h_j , a_i and b_j are their biases. V and H represent the number of visible and hidden units, respectively. The distribution of the visible units' weights and biases is defined as

$$p(v) = \sum_H p(v, h) = \sum_H \frac{e^{-E(v, h)}}{Z} \quad (3.10)$$

In RBMs, the units of the same layer are independent which do not have any connection with each other. In terms of probability, this means that the hidden

variables are independent given the state of the visible variables and vice versa. Thus, the condition distributions of $p(h|v)$ and $p(v|h)$ are defined as

$$p(h_j = 1|v) = \sigma \left(\sum_{i=1}^V w_{ij} v_i + b_j \right) \quad (3.11)$$

$$p(v_i = 1|h) = \sigma \left(\sum_{j=1}^H w_{ij} h_j + a_i \right) \quad (3.12)$$

where $\sigma(x) = \frac{1}{1+e^{-x}}$, the sigmoid function of x , the feature, element-wise.

In DBN's pre-training, each RBM is trained individually, greedy layer-wise. The weights of each units' connections, and each layer's biases, are computed within this phase and saved for fine-tuning. This learning is repeated, from RBM to another, until all hidden layers are trained. This process can be expressed as follows

$$p(h_j^{(l-1)} = 1|v) = \sigma \left(\sum_{i=1}^V w_{ij}^{(l)} v_i^{(l)} + b_j^{(l-1)} \right) \quad (3.13)$$

where l corresponds to the current layer. The formulas and equations for RBM are based from the papers of Koesdwiady et al. (2016); Fischer and Igel (2014); Zhang et al. (2017).

3.13 Weighted Average

The Weighted Average is a signal-level fusion method that takes the weighted average of repeating information from the original inputs (King et al., 2017; Yan et al., 2011; Meurant & Meurant, 1992). King et al. (2017) claimed that using this method will ease the effect of unwanted data in the final estimation. This method can be used to estimate user activity details such as intensity, postures, and fundamental static for activity recognition systems.

Yan et al. (2011) proposed the use of the weighted average method on ships traffic flow data. They used data fusion to produce a higher estimation accuracy from multiple sensors. The researchers multiplied the number of ships with its corresponding weight then obtained the average of the produced weighted inputs. They then applied a distribution method to the original data to eliminate the unwanted data.

3.14 ParseHub

ParseHub is a free web scraping tool that collects from any JavaScript or AJAX site. This web scraping tool can also export the collected data in CSV and JSON files. The tool also has the ability to cloud host which enables the data scraped to be saved through the cloud, and schedule a run to a future time. ParseHub can scrape from hundreds of pages depending on the pricing. The Free ParseHub may only collect 200 pages worth of data in under 40 minutes. It also can run 200 pages per run. Lastly, ParseHub retains data collected for 14 days.

3.15 Performance Indices

3.15.1 RMSE and MAE

To evaluate a model's performance, many studies have employed using two of the most used performance indexes: the root mean squared error (RMSE) and the mean absolute error (MAE) (Chai & Daxler, 2014). The RMSE is used as a standard statistical system of measurement to calculate a model's performance, especially in air quality, meteorology, and climate research studies. It is defined using this function:

$$r = \sqrt{\frac{1}{n} \sum_{i=1}^n (x_i - y_i)^2} \quad (3.14)$$

where n is the number of samples, x_i and y_i are the errors being observed at a certain i . On the other hand, MAE is a measure of the absolute difference between the errors. It is defined using this function:

$$r = \frac{1}{n} \sum_{i=1}^n |x_i - y_i| \quad (3.15)$$

3.15.2 Sensitivity Analysis

Sensitivity analysis is a study of how much the input variables clearly affect the outcome of a model (Saltelli et al., 2000). It is also called the simulation analysis,

wherein the results are predicted based on a range of input variables. Calculating the sensitivity that is dependent on time, we calculate the sensitivity relative to the initial parameters, inputs, or conditions in the model.

The “time-dependent” sensitivities of output Y relative to every input variable are “time-dependent” derivatives is given by the equation:

$$\left| \frac{\partial Y}{\partial X_i} \right|_{X^0} \quad (3.16)$$

where, Y is the output and X_i is the input factor. X^0 indicates that the derivative is taken at some fixed point in the space of the input. This shows that per input of the model, the ratio of its derivative with respect to its output is computed to get the sensitivity.

Several researchers have been applying sensitivity analysis to their models, particularly to the models which uses neural networks. In Hunter et al. (2000), they applied sensitivity analysis of neural network inputs to their trauma survival prediction model to analyze the Trauma and Injury Severity Score (TRISS) variables used in their model. Their experiments on the variable’s sensitivity show that age is the most prominent variable in predicting survival. The researchers defined three approaches to sensitivity analysis. First is to introduce noise to every input variable and to observe its effects to the results. Second is to examine the derivatives of the weights of the input variables. Last is the proposed form of analysis based from the missing value problem approach.

In Refenes et al. (1994), they performed sensitivity analysis to evaluate their model on stock performance using neural networks. They used scatter plots to visually analyze the change in their network output (the likelihood of a sample being a target) with respect to the network input (stock factors). Based on their result, they were able to explain the predictive behavior of their neural network output by using sensitivity analysis. Furthermore, they were able to conclude that compared to regression models, their model can model the situation more convincingly.

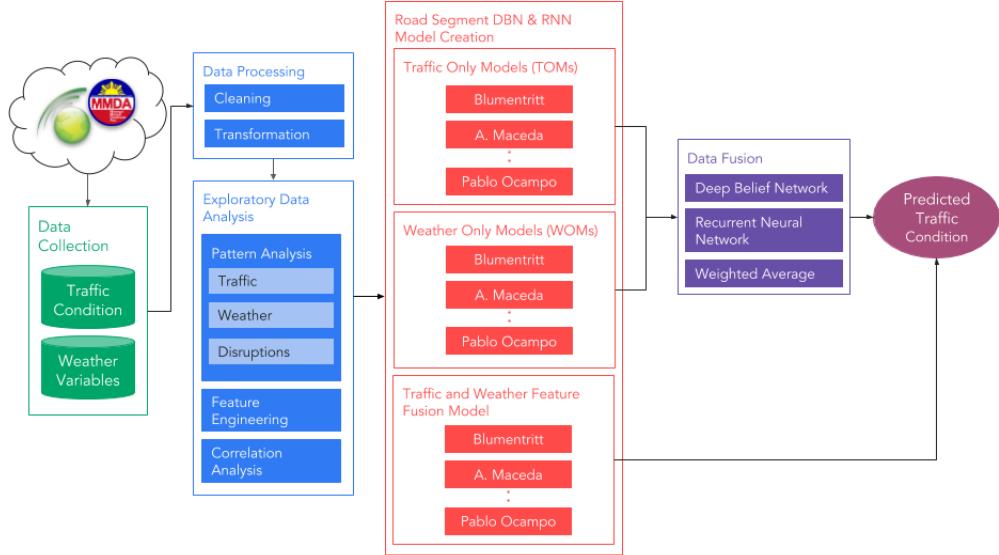


Figure 4.1: Research Framework

Chapter 4

Research Design

Figure 4.1 illustrates the whole framework for the research. First, this research collected historical traffic condition from MMDA and historical weather variables from WWO. These raw data were cleaned and re-sampled to match the time intervals of the data using linear interpolation and was transformed to their normalized values. The data was explored and analyzed to identify seasonality and trends present for both traffic and weather. Analyses and insights collected were used to select and engineer features to use in the model to predict traffic. These features include rolling and expanding window features, which are in-depth statistical features of traffic such as the mean, minimum, and maximum values of past traffic

of a certain time period.

The final variables and engineered features were fed into the Traffic-Only Models (TOM) and Weather-Only Models (WOM), which were developed in DBN and RNN, for the 14 road segments in Manila for both wet and dry season. Additionally, analyses were evaluated through the training of the models. Two different fusion levels were tested in this model, specifically at the feature level and at the decision level. For the decision level, three fusion techniques were tested, particularly DBN, RNN, and WA. The model was evaluated using RMSE and MAE. The model's sensitivity was also explored to analyze the relevance of input variables.

4.1 Data Collection

There were two public datasets collected: one for traffic and one for weather. The traffic dataset was obtained from Metro Manila Development Authority (MMDA) traffic monitoring system, while the weather dataset was collected from World Weather Online (WWO). Both datasets were collected from January 2015 to December 2015.

4.1.1 Traffic Dataset

There were two limitations found from the traffic dataset. First is that the traffic conditions were only represented as *light* (L), *moderately light* (ML), *moderate* (M), *moderately heavy* (MH), and *heavy* (H). Since this dataset only had five values to classify the traffic condition in a particular road segment, this might cause underfitting in our model since it was used as input for a regression problem. Moreover, it could also contribute to poor correlation as these five values were correlated with continuous weather variable values. Instead, they were converted to their equivalent estimated traffic speed provided by the MMDA (see Table 4.1). These speeds are further converted to condition intensity, represented as their reciprocal so that the trend of the data would be negated, thus would be easier to interpret such that increase in traffic would indicate increase in traffic condition intensity. It is important to note, though, that the limitation of this approach is that, visually, the gaps between *heavy* (H) and *moderately heavy* (MH) would be more emphasized due to the nature of fractions that the larger the denominator, the lower the value is.

Another limitation was that the traffic dataset contains missing records. Out of 935,200 records, there were 93 rows wherein the traffic condition of that road

Table 4.1: Traffic speed equivalent of traffic conditions

Traffic Condition	Equivalent Speed (kph)
Light (L)	36 - 60
Moderately Light (ML)	31 - 35
Moderate (M)	16 - 30
Moderately Heavy (MH)	11 - 15
Heavy (H)	0 - 10

segment in that particular time interval was not recorded as indicated by *none* (N) condition. Furthermore, having only 935,200 records from a sample from 2015, having a 15-minute interval for 14 road segments, meant that 45,920 records were missing as well. This implied that inconsistencies may occur as the missing data would need to be filled to make the data continuous. To do this, those missing values were replaced through linear interpolation. Apart from the limitations, there were other factors considered in this study. Since this study is only concerned road segments from Manila, only the road segments under it were used. As a result, 14 out of 142 road segments were only considered: 7 roads from Roxas Boulevard and 7 roads from España.

4.1.2 Weather Data

The collected weather dataset from WWO featured a complete hourly reading of the weather variables for Manila. One downside of this dataset, however, was that the weather data generalizes the weather for the whole city. This implied inconsistencies when correlating the traffic condition to the weather variables as the weather at one road is not the same as the weather of another, despite being in the same city.

Additionally, the hourly weather dataset needed to be matched with the 15-minute interval of the traffic dataset. This was done by resampling and linear interpolating the dataset to have a 15-minute time interval.

4.2 Pattern Analysis

To be able to determine the relationship of weather to traffic, it is important to understand the underlying pattern between these two datasets. In the following analyses, traffic will be treated as the dependent variable and weather as the

independent variable. These are approached in four steps. First, patterns of traffic with itself are analyzed by its seasonality and daily trend. Second, weather is analyzed with respect to traffic, likewise, in terms of seasonality and daily trend. With the relationship of weather and traffic identified, weather disruptions are characterized and identified as a prerequisite for the next step. As weather disruptions are determined, disruptions on the normal traffic pattern could be identified.

4.2.1 Traffic Analysis

Before understanding the effects of weather to traffic, it is necessary to understand the underlying pattern of traffic as it may have its own existing pattern that might neglect the effects of weather. On an average day, traffic could be linked with the people's daily transportation demand. One example of these is the daily commute of people, attributed to their organizational duties (i.e. 9 to 5 jobs) and academical duties. Built upon these expected demands, traffic could be expected to be daily seasonal on working days. Given this statement, to understand traffic, two terms must be understood: seasonality and working days.

Seasonality refers to a predictable pattern of a time series data that regularly repeats after a number of intervals. To identify the seasonality of a variable, the similarity between an observation and time lags between them were analyzed through autocorrelation. *Lags* refer to the time delay of one observation on another. For instance, the delay between the traffic observations at June 18 and June 19 is indicated by a one-day lag.

Understanding seasonality is significant to determine the duration of a certain pattern which could be used as a guide in predicting an incoming observation. In terms of traffic, it is known to be seasonal with its previous day (e.g. Tuesday with Monday) and its previous week (e.g. Monday with the previous Monday) (Kumar & Vanajakshi, 2015).

Traffic's **previous day** seasonality could be perceived as causal, such that the traffic of yesterday could be attributed to the traffic of today. For instance, having an intense traffic yesterday morning could be linked with the incoming morning traffic of today. In inheriting the factors of previous days, nonetheless, we also need to take into consideration the concept of working and non-working day.

A *working day* refers to a day in which people are assigned on duty in an organization (J. Liu et al., 2008). For most organizations, it is defined to be on weekdays, Mondays to Fridays, while non-working days are on weekends, Sat-

urdays to Sundays. Aside from weekends, though, non-working days also occur during holidays and government-announced class/work suspension. In the following analyses, those days are treated as outliers to our data as the traffic pattern for that particular day is irregular compared with the other weekday working day records. These are important to consider as the transportation demand during working days are higher compared with non-working days (Z. Liu et al., 2016). For example, the transportation demand of Monday is significantly different from Sunday, thus referencing Sunday for the expected pattern of Monday would be erroneous.

With the difference of the transportation demand during working days and non-working days, the concept of peak hour must also be considered (De Fabritiis et al., 2008). Peak hour refers to the busiest hour where traffic is expected to rapidly rise (Downs, 1962). In the case of Metro Manila, peak hours are expected to occur from 7 AM to 10 AM, when people leave their home to go to their respective organizations, and 4 PM to 7 PM, when they depart their organizations and return home (Regidor, 2013).

On the other hand, traffic's **previous week** seasonality could be perceived as occasional. Monday (Rakha & Van Aerde, 1995) and Friday (Datla & Sharma, 2008) traffic could be observed as more congested as compared with the other weekday traffic. Unlike previous day traffic, it does not matter if it is a working day or a non-working day as Mondays are based on the pattern of previous Mondays. The advantage of this, in fact, is that traffic is no longer causal, thus a normal pattern could be derived using its pattern from the succeeding weeks.

4.2.2 Weather Analysis

With the pattern of traffic taken into consideration, the relationship between weather and traffic could now be better understood. To have an overview of the relationship between traffic and weather variables, Spearman's rank correlation is performed to measure the non-linear relationship between these two. Although given that traffic has its own pattern and weather generally has a one-way relationship with traffic, it is expected for these two to not have a direct relationship (Tanner, 1952).

To verify this, an exploratory analysis was performed by examining the commonalities of traffic and each weather variables through its seasonality and trend. From this, a normal trend will be defined based on their average per time interval on a given common seasonality. Then, a more specific relationship could be defined by relating their trends.

4.2.3 Weather Disruption

With the general relationship between traffic and weather examined, the effects of weather on traffic could now be assessed. These are primarily focused on rainfall potentially disrupting the normal trend of traffic. To identify these, climate seasonality is classified, and rainy weather conditions are utilized.

The classification of seasons is significant to determine the months when precipitation is rampant. This is measured by getting the average of precipitation on a given month. In conjunction, rainy weather conditions may also provide a more general insight with regards to the rainfall intensity at a given time period. These are classified into 11 conditions: patchy rain possible, patchy light rain, light rain, light rain shower, light rain, moderate rain at times, moderate rain, moderate or heavy rain shower, heavy rain at times, heavy rain and torrential rain showers.

4.2.4 Traffic Disruption

As weather disruption dates are identified, verification whether rainfall really does affect traffic could be performed. As mentioned in the earlier analysis of traffic seasonality, traffic is said to be daily seasonal and weekly seasonal. Since it is expected that rainfall may potentially disrupt the normal trend of traffic, then it is expected that this seasonality would be affected. In general, this is examined by comparing the seasonality of traffic between different climate seasons through autocorrelation.

4.3 Correlation Analysis

4.3.1 Correlation of Engineered Traffic Features with Traffic Condition

Given the initial seasonality analysis and findings on how different a disrupted traffic pattern is compared to its normal pattern, a potential weakness of using one instance of its seasonal day alone is that it may be a disrupted pattern, hence it would not be a reliable guide for the incoming traffic. With that in mind, more reliable features are engineered with the aim of minimizing the identified weakness.

To address this problem, a concept of normal pattern for a given day must be

defined. One way to approach this is by getting the average traffic per time interval from a number of instances of seasonal days. For instance, having the mean of one disrupted day and one normal day is a better basis than one disrupted day. Scaling up the range, getting the mean of a number of normal days with the inclusion of one disrupted day can override the effects of the single disruption.

4.3.2 Correlation of Immediate Traffic Features with Traffic Condition

Lastly, the relationship between the engineered traffic features to the current traffic feature was explored. Before exploring this relationship, traffic features were engineered from the current traffic feature in order to give information of the immediate past traffic, and its relationship with the current traffic. These engineered traffic features include rolling and expanding window features, statistical description of past time period such as the mean traffic six weeks ago, and flags for significant traffic patterns such as the work day and peak hours. Exploring the relationship between these engineered traffic features with the current traffic feature also give a better representation of the effect of disruptions present in the immediate past to the current traffic.

As mentioned, rolling and expanding window features were engineered to represent the immediate past traffic. Rolling and expanding traffic features were generated for window sizes *4, 8, 24, 48, and 96*, with each window representing a 15-minute time interval. Thereby, the generated window sizes translates to *1, 2, 6, 12, and 24*-hours time interval. The statistical features such as the mean, minimum, and maximum for both rolling and expanding windows were generated to describe the immediate past traffic conditions given a specific window size.

4.3.3 Correlation between Connected Road Segments

There are a number of factors contributing to traffic. For instance, given a point-to-point road segment, traffic in one road segment could be due to its connected road segment carrying over its traffic. As the road segments in the utilized dataset are just samples from a larger road network, a road segment may be skipped through their connected intersections. With road segments analyzed with their own pattern, the next step is to analyze them as part of a whole road.

Identifying the relationship between connected road segments are significant as it allows a certain road to have a generalized description based on their com-

mon characteristics. Furthermore, this is necessary as this relationship defines if the effect of weather on one road segment is the same with its neighboring road segments. To verify this, given that these road segments have a matching seasonality, the average of their traffic per time interval based on their seasonality could be evaluated. Then, their correlation could be evaluated by using Pearson correlation coefficient to analyze their linear relationship.

4.4 Model Implementation

Features were engineered in order to represent the immediate past traffic, and other trends and patterns of traffic. Additionally, weather features were selected through correlation analysis. These features are as follows:

1. Temporal Information of the respective traffic record represented as Month, Day, Hour, Minute, Day of Week,
2. Traffic a Day before represented as L, ML, M, MH, H
3. Traffic 6 weeks ago represented as L, ML, M, MH, H
4. Current Traffic represented as L, ML, M, MH, H
5. Rolling and Expanding Traffic Features (mean, max, and minimum) for windows 4, 8, 24, 48, and 96 represented as L, ML, M, MH, H,
6. Weather Variables (wind speed, wind gust, temperature, humidity, dew point, precipitation, visibility, pressure, cloud cover, heat index, and feels-like) represented in their respective measurements

Two models were implemented with Deep Belief Network (DBN) and Recurrent Neural Network (RNN) with Long Short-Term Memory (LSTM). These models used these features that represent past traffic to predict the current traffic condition intensity.

4.4.1 Prediction Models

According to the framework in 4.1, two models were implemented in the algorithms of DBN and RNN: the Traffic-Only Model (TOM) and the Weather-Only

Table 4.2: DBN Models Network Architecture

	Pre-Train Epochs	Fine-Tune Epochs	Activation Function	Batch Size	Hidden Layer Structure
TOM	7	80	relu	192	[14, 375]
WOM	5	88		96	[20, 85, 170]
FEI-DEO	7	80		192	[14, 375]
DEI-DEO	8	350		192	[20, 50, 100]

Model (WOM). The TOM considers historical traffic condition intensity to predict traffic, while the WOM only considers historical weather variables to predict traffic. In this study, these models were implemented with the open source machine learning framework in Python, *tensorflow* and *keras*. The TOM and WOM network architectures using both DBN and RNN are shown in 4.2.

DBNs are made up of stacks of Restricted Boltzmann Machines (RBM). The training for DBN consists of two phases: pre-training and fine-tuning. In pre-training, each RBM is trained individually, and the weights and biases of layers are fixed. In fine-tuning, the weights and biases of the whole network are updated via back propagation using labeled input data.

Figure 4.2 shows the process of how the TOM and the WOM using DBN was trained for prediction. The training process consists of three phases. In the first phase, the stacks of RBM (sRBM) within the network are trained individually. At the end of this phase, the weights and biases of the whole DBN are initialized. In the second phase, the DBN fine-tunes the initialized weights and biases using the backpropagation algorithm. The network after stage 2 is the trained and enhanced DBN. In the third phase, the network predicts the future traffic condition using a testing dataset.

For the pre-training phase, the sRBM performs a number of forward and backward passes until the reconstructed data is close to the original input. The process of backward and forward passes is performed using the equations 3.11 and 3.12 to compute for the conditional probability of the hidden unit h_j and visible unit v_i , respectively.

For the fine-tuning phase, the loss function and activation function is defined. The loss function for the softmax layer to improve the learning rate uses the cross-entropy equation between the visible and hidden units. The cross-entropy function is defined as

$$C = -\frac{1}{n} \sum_x [y \ln a + (1 - y) \ln(1 - a)] \quad (4.1)$$

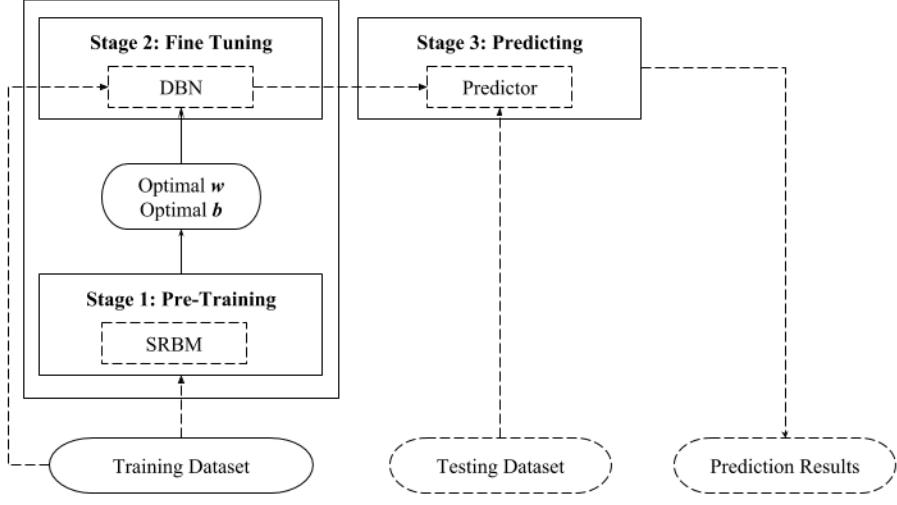


Figure 4.2: Structure of DBN Training Process

where n is the size of the training data, x is the training input, y is the desired output, and a is the unit's output. For the activation function in the fine-tuning phase, the rectifier function was used for its nonlinearity activation capability. The rectifier function is defined as

$$f(x) = x^+ = \max(0, x) \quad (4.2)$$

4.4.2 Data Fusion Model

Data fusion is significant to see the effectiveness of adding weather as a factor in predicting traffic. This study evaluated two fusion approaches: Feature In-Decision Out (FEI-DEO) and Decision In-Deci-sion-Out (DEI-DEO). In the FEI-DEO approach, traffic and weather features are fused in one dataset first before being used by the model to predict traffic. The DEI-DEO approach, meanwhile, predicts traffic through TOM and WOM, and fuses the prediction of both models into one final prediction. DBN and RNN were used in the FEI-DEO approach, while three algorithms are tested in the DEI-DEO approach which are Weighted Average (WA), RNN and DBN.

Weighted Average

The weighted average data fusion method used the predicted traffic from TOM and WOM. Both predictions were multiplied with its corresponding weight. Each

weight was assigned based on the importance of the variable considered while keeping in mind the sum of the weights should be equal to 1. Then, the mean of the weighted predictions of both TOM and WOM will be calculated. The result will be the fused final traffic prediction.

Neural Network

The fusion model was also developed in two neural networks: Recurrent Neural Network (RNN) and Deep Belief Network (DBN) in evaluating DEI-DEO fusion approach. Only DBN and RNN were implemented in evaluating FEI-DEO approach.

In FEI-DEO, the traffic congestion intensity and weather variables were fused into one dataset before feeding it into the prediction model. The network will be trained to predict the traffic condition based on both traffic and weather in one model for the current time period t . The training of the network will continuously adjust weights and biases from comparing the generated output with the actual traffic condition.

In DEI-DEO, the traffic congestion intensity was predicted first with two prediction models, TOM and WOM. The prediction of these two prediction models was used into another model that will fuse the two predictions into one improved final prediction. The network will be trained to predict the traffic congestion intensity for the current time period t through backpropagation by comparing the generated traffic condition prediction to the expected prediction, and adjusting the weights and biases of units and layers to fuse the two decisions to arrive at a prediction close to the expected. The input layer will have the predicted traffic condition of TOM and WOM.

The DBN model network architecture for both FEI-DEO and DEI-DEO fusion are also shown in 4.2. The RNN for DEI-DEO fusion have only have 1 input layer, 1 hidden layer, and 1 output layer. The number of units for the hidden layer of the RNN will be determined through trial and testing starting from 5 to 100 units.

4.5 Training

The collected dataset for traffic and weather was divided into two subsets; wet and dry season. The wet season dataset consists of data from the months of May to October 2015, while the dry season dataset consists of data from the months

of November to April 2015. The models were tested on these datasets to evaluate the inclusion of weather variables.

Datasets were split into training and testing datasets. The training dataset was used during the pre-training and fine-tuning of the model. In the fine-tuning phase of the training of the model, the training dataset was labeled with the expected output so as to verify and adjust the weights and biases back from the pre-training. The label consists of the expected traffic condition given the input data. All data fed into the network are already normalized.

The training dataset for both prediction models TOM and WOM consists of data from the months of May to August was used for evaluating wet season, and months of January to April was used for evaluating the dry season. In turn, the testing dataset made use of the remaining months of the season: September to October for the wet season, and November to December for the dry season.

4.5.1 TOM Training Dataset

Training datasets for TOM include traffic features in a 15-minute time interval that were derived from insights in the exploratory data analysis. These traffic features include the following:

1. Temporal information of the respective time period (i.e. month, hour, minute, day, and day of week);
2. Traffic condition intensity a day before the respective traffic;
3. Flags on working day and peak hour of the respective time period;
4. Rolling and expanding window features (which consist of the minimum, maximum, and mean for each window) for the immediate past traffic of the respective traffic; and
5. Average traffic 2 weeks before the respective traffic.

Different combinations of these traffic features are generated as separate training datasets to compare the performance of the model with the respective feature combination. These feature combinations are denoted as the following:

1. *OT* - Features that only consist of the past traffic a day before the current;

Traffic Only Model Training and Testing Dataset

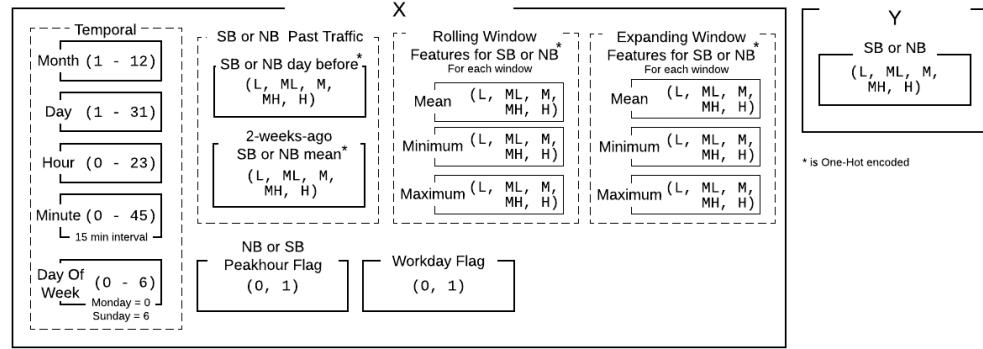


Figure 4.3: A summary on the contents of the Traffic Only Model Training and Testing Dataset

2. *OTWP* - Features including past traffic a day before the current, and flags on the workday and peak hour, and;
3. *WPRE*- Features including OTWP, plus the addition of rolling and expanding features of the traffic 15 minute in the past of the current. In subsequent discussions, any number following this notion pertains to the window size of both the rolling and expanding features (e.g. WPRE 4 pertains to the features that include rolling and expanding features of window size 4).

The label for the training dataset consists of actual the 15-minute time interval of the traffic condition intensity of the respective time of the bound of the road segment to be predicted. For visualization purposes, the input including the labels is illustrated in Figure 4.3

4.5.2 WOM Training Dataset

Training datasets for WOM include weather features in a 15-minute time interval that were derived and selected from insights in the exploratory data analysis. These weather features include the following:

1. Temporal Information of the respective time period (i.e. month, hour, minute, day, and day of week); and

2. Current weather variables (e.g. temperature, precipitation, wind speed, etc.) of the respective time period.

Different combinations of these weather features are generated as separate training datasets to compare the performance of the model with the respective feature combination. These feature combinations are denoted as the following:

1. Original Weather (OW) - all weather variables
2. All Correlated Weather (ACW) - all weather variables that have correlation between 0.1 to 0.3
3. Correlated Weather (CW) - all correlated weather variables excluding the redundant ones

The label for the training dataset consists of the actual 15-minute time interval of the traffic condition intensity of the respective time of the bound of the road segment to be predicted.

4.5.3 Fusion Model Training Dataset

For the FEI-DEO model, the training dataset consists of merged training dataset used in the TOM and the WOM. The months for the training and testing datasets for this fusion model is also the same.

For the DEI-DEO model, the training dataset consists of the predicted traffic generated by TOM and WOM. The months for the training consists of the months of May to September for the wet season and January to April and November to December for the dry season. The testing dataset consists of the predicted traffic for the month of October and December. The label for the training dataset will consist of the 15-minute time interval of the actual traffic condition intensity of the respective time of the bound of the road segment to be predicted.

4.6 Evaluation

4.6.1 Prediction Model Evaluation

The performance of all models and algorithms (DBN, RNN, and WA) were evaluated using RMSE and MAE. To evaluate TOM and WOM, the performance of the

TOM and the WOM with different feature combinations are compared with each other to see which input variables are needed in predicting the traffic condition intensity for the current time period t . The performance of the fusion models in the feature level (FEI-DEO) and in the decision level (DEI-DEO) was also evaluated. In evaluating DEI-DEO, the performance of the TOM and the WOM were initially evaluated before the fusion model/s. Then, three fusion techniques, namely WA, RNN, and DBN, were compared and evaluated to see the accuracy of the final prediction. In evaluating FEI-DEO, feature combinations used in evaluating TOM and WOM were used in the model. Additionally, the performance of the TOM and the final prediction of the DEI-DEO and FEI-DEO fusion models were evaluated to see the relevance of the inclusion of weather variables as a factor in predicting traffic.

4.6.2 Sensitivity Analysis

The model's sensitivity was also explored to analyze the relevance of input variables. Sensitivity analysis is also performed to achieve higher accuracy through calibration of hyperparameters. Specifically, the sensitivity for the models TOM, WOM and DEI-DEO and FEI-DEO fusion center in DBN were evaluated. Different combinations of input variables were evaluated to see how much the inclusion and removal of a variable affect the final prediction.

First, the sensitivity of the models with changing input variables was evaluated. The different input variables were removed per experiment to see the effect of its inclusion. The combination of input variables was done in the feature combination in earlier evaluations of the model (e.g. OTWP, OT, WPRE, OW, etc). For example, variables of the OTWP feature combination were tinkered. Then, the variables of OT combination were evaluated, and so on. The base model, with all the features including temporal and past traffic, as compared with the model with the removed variables (with or without temporal information or past traffic), and its change in performance was evaluated. The changes in performance describe the sensitivity of the model. Change in performance is calculated by getting the difference between the base and new input, and dividing with the base input. Formula in performance change is defined as

$$C = \frac{x_{base} - x_{new}}{x_{base}} \quad (4.3)$$

In evaluating TOM, two sets of test-cases were considered, (1) the effect of temporal information in consideration of traffic features, and (2) the effect of past traffic with and without the consideration of temporal information. The

first test-case removes temporal information one-by-one, testing the performance of the model with only the selected temporal information, and traffic features. This traffic features include working day and peak hour flags, and rolling and expanding features, and mean traffic 6 weeks before, and traffic a day before. The second test-case removes traffic features one-by-one without or without temporal information.

Much like TOM, two sets of test-cases were considered in evaluating WOM, (1) the effect of temporal information in consideration of weather features, and (2) the effect of each weather features with and without the consideration of temporal information. The first case is similar to TOM's first case. Instead of traffic features, weather features were experimented with. The second case removes weather features one-by-one, and compares other combination of weather features (i.e. all weather variables, all correlated weather variables with redundant variables, correlated weather variables without redundant variables).

Chapter 5

Results and Discussion

This chapter discusses the exploratory data analysis of the collected traffic and weather data to identify seasonalities, disruptions, and correlations. It also discusses the experiments performed in building the prediction model, as well as its evaluation. The traffic data includes traffic conditions for the whole year of 2015. The weather data includes weather variables such as wind speed, wind gust, temperature, humidity, dew point, precipitation, visibility, pressure, cloud cover, heat index, and feels-like, for the three years 2015 to 2017.

5.1 Pattern Analysis

5.1.1 Connected Road Segments

To be able to identify if there is a direct relationship between connected road segments, we first perform an initial correlation on their traffic for all working days in one month. Figure 5.1 illustrates the correlation heatmap of the traffic of road segments in Roxas Boulevard. From this, we could observe a consistent strong relationship between each road.

This strong relationship remains true with the traffic for both southbound and northbound for Espana (see Figure 5.2). Compared with Roxas Boulevard, however, there are certain road segments in Espana that have relatively weak relationship with its nearby road segments.

After analyzing the pattern of an individual road segment, we now analyze it as a part of a road. Exploring the working day traffic of all road segments in Roxas

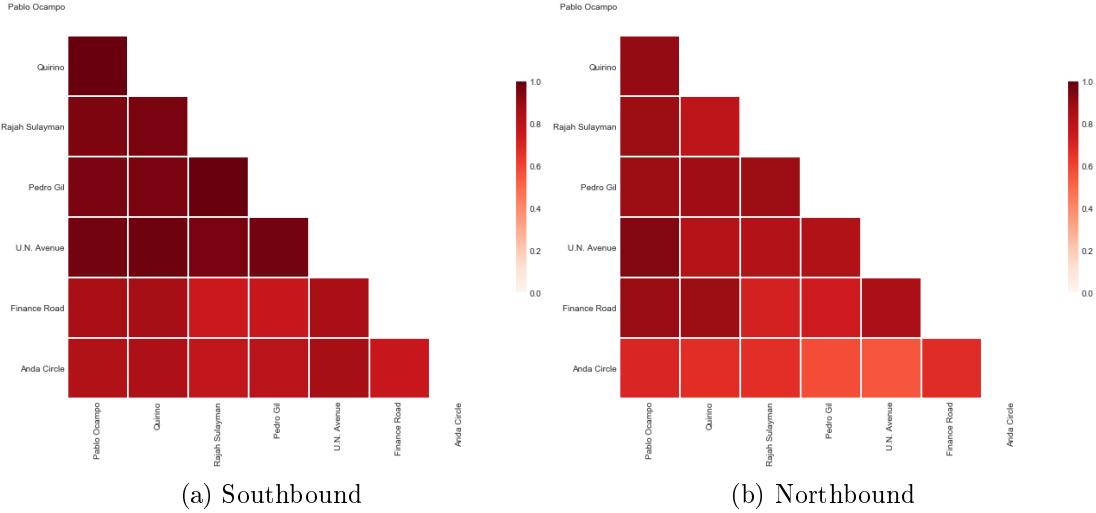


Figure 5.1: Correlation heatmap of traffic for both southbound and northbound of Roxas Boulevard

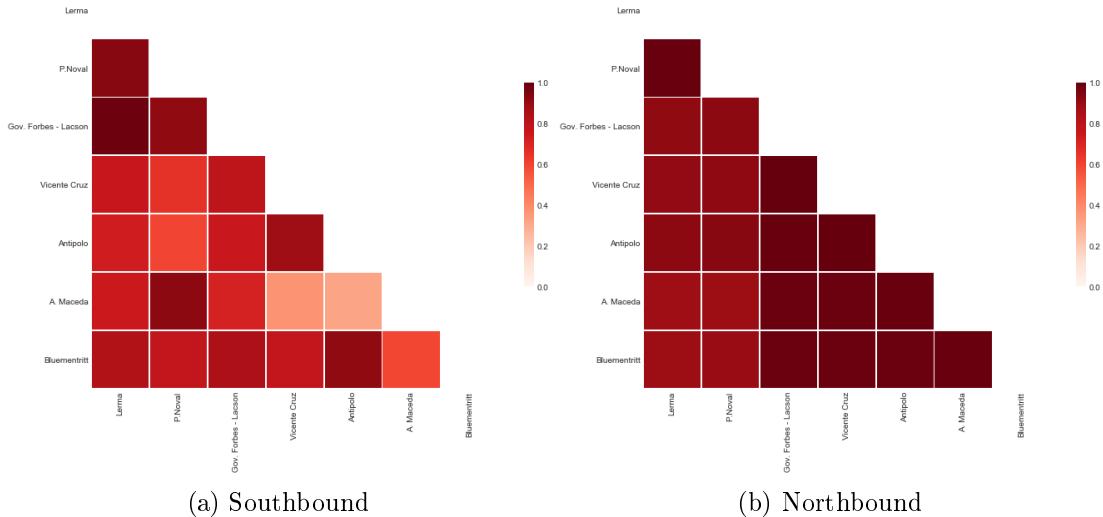


Figure 5.2: Correlation heatmap of traffic for both southbound and northbound of Espana

Boulevard in one month, it could be observed that there is an intensity relationship between these southbound road segments such that their peaks remain the same yet their intensity differs (see Figure 5.3). This is also the case in the northbound of the road segments in Roxas Boulevard. The intense traffic of Pablo Ocampo is carried over to Quirino in a similar intensity yet continuously decays as we go

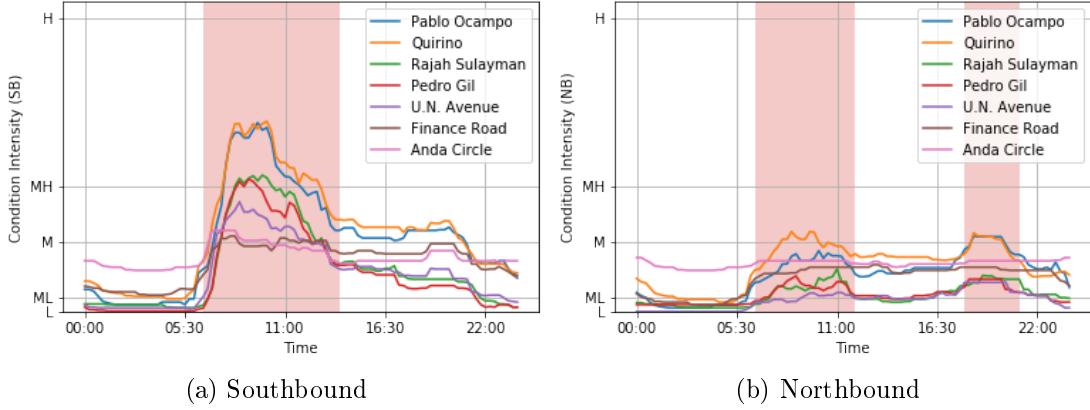


Figure 5.3: Daily average of all working days in one month in all road segments in Roxas Boulevard showing its intensity relationship

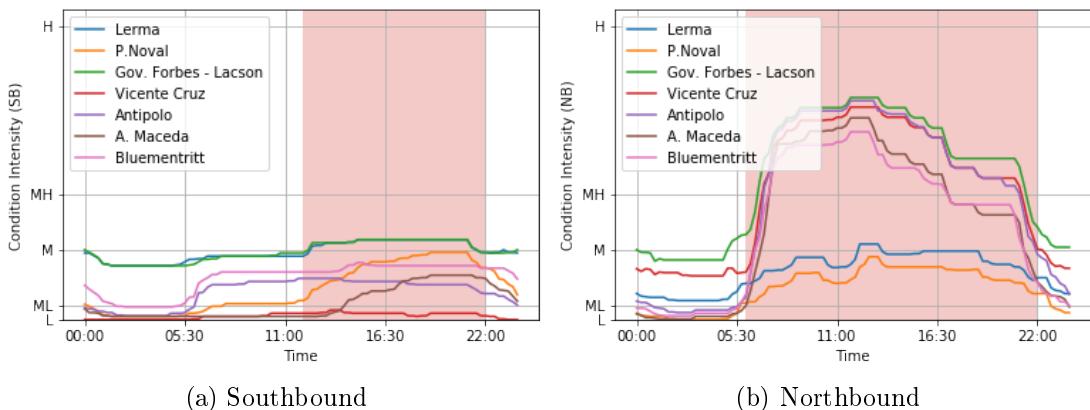


Figure 5.4: Daily average of all working days in one month in all road segments in Espana showing its intensity relationship

further to Anda Circle.

Likewise, in road segments of Espana, it follows a similar trend (see Figure 5.4). The intensity of the traffic at the northbound of Blumentritt rises as we approach Antipolo then decays as we go further to Lerma.

In summary, in consideration with the strong correlation between connected road segments, and dynamic traffic intensity, it can be concluded that the road segments which can generally describe the other road segments in the same road are Pablo Ocampo, for Roxas Boulevard, and Antipolo, for Espana.

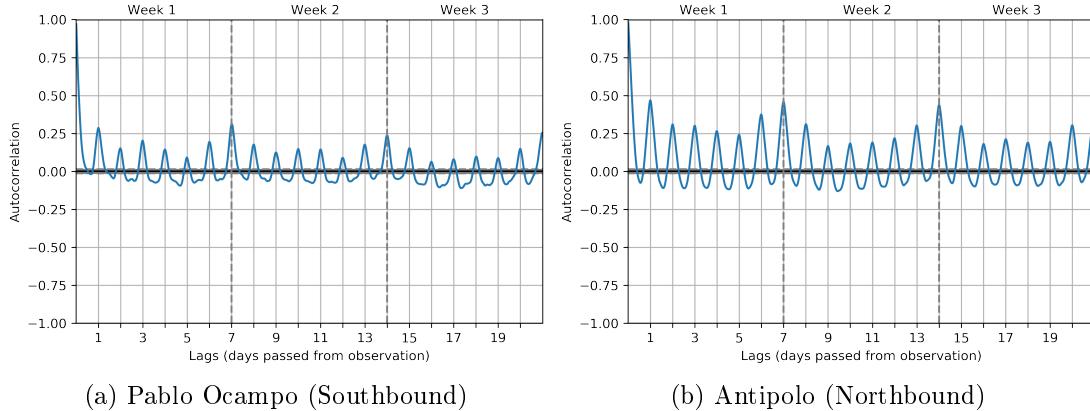


Figure 5.5: Autocorrelation plot of (a) Pablo Ocampo and (b) Antipolo revealing its daily and weekly seasonality

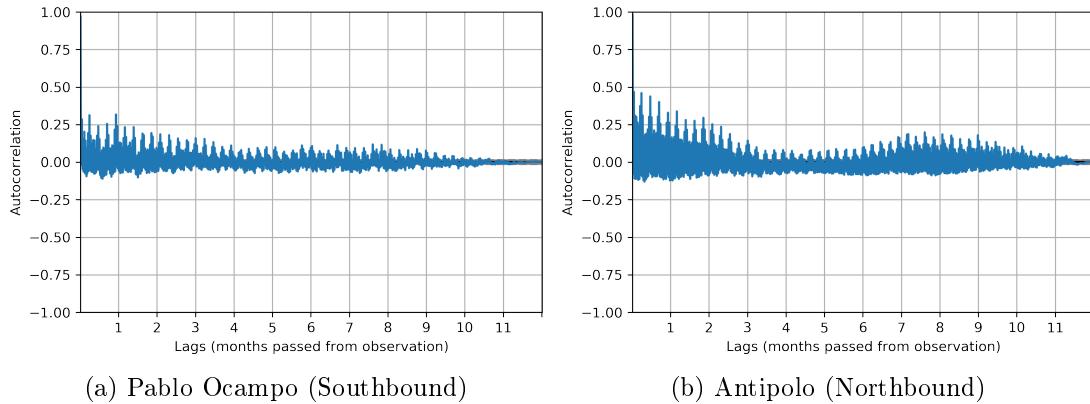


Figure 5.6: Autocorrelation plot of (a) Pablo Ocampo and (b) Antipolo showing a decaying weekly seasonality

5.1.2 Traffic Analysis

Analyzing the autocorrelation plot of traffic (see Figure 5.5) for both Pablo Ocampo and Antipolo, it could be observed that in spite of its daily pattern, its succeeding days are loosely correlated with the present one. Notably, it is noticeable how the seasonality the day before (e.g. similarity of a Tuesday observation with yesterday's Monday) and the week before (e.g. similarity of a Monday observation with last week's Monday) are relatively stronger compared with the other days (e.g. 2 days ago, 3 days ago).

Viewing their pattern in a longer term (e.g. month-long), nevertheless, its

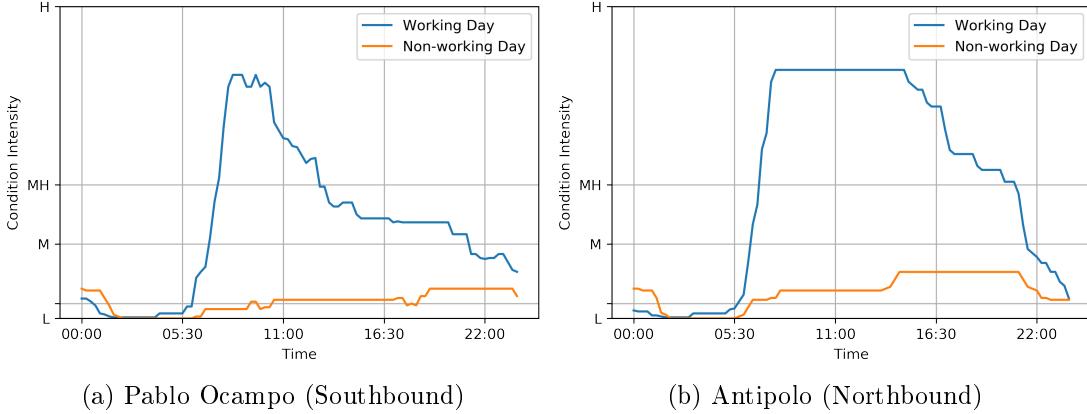


Figure 5.7: Comparison of the average traffic of (a) Pablo Ocampo’s southbound and (b) Antipolo’s northbound in one month between working and non-working revealing the lack of intense traffic for non-working days

weekly pattern becomes looser as months go by (see Figure 5.6). In other words, traffic patterns must not be analyzed by segmenting it by month. Instead, it must be analyzed weeks prior to the current observation as mutations in the traffic pattern may just be caused by a change in pattern carrying over to the succeeding days.

Day Before

Comparing the average traffic between working days and non-working days in one month, we could see a significant difference in terms of intensity and pattern (see Figure 5.7). Majority of intense traffic occurs at working days. Table 5.1 shows that heavy traffic consists 17.8% and 35.3% of the working day of Pablo Ocampo’s southbound and Antipolo’s northbound respectively, while having none during non-working days for both road segments. Moreover, light traffic consists only 30.5% and 26.1% of the working day traffic of Pablo Ocampo’s southbound and Antipolo’s northbound respectively, while it accounts for 73.7% and 61.6% of the non-working day traffic.

This, in terms of trends, indicates that the working day traffic may follow the peak hour-driven traffic pattern. In this study, the researchers considered the mean of heavy and moderately heavy traffic as the threshold in detecting the peak hour (see Figure 5.8). Coming from nominal categorical data, however, there are instances when traffic changes its condition but only for a short while (see Figure 5.9). With these problems present, discontinuous and false peak hours might be

Table 5.1: Comparison of traffic condition distribution between working and non-working

	Pablo Ocampo (Southbound)		Antipolo (Northbound)	
Traffic Condition	Working Day	Non-working Day	Working Day	Non-working Day
L	30.5%	73.7%	26.1%	61.6%
ML	6.1%	5.9%	5.0%	3.1%
M	41.4%	20.2%	31.3%	35.3%
MH	4.2%	0.3%	2.2%	0.0%
H	17.8%	0.0%	35.3%	0.0%

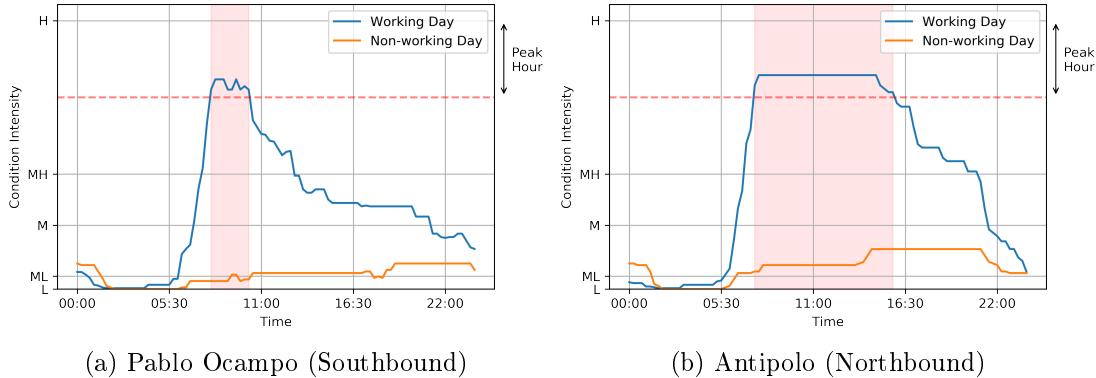


Figure 5.8: Comparison of peak hours of the average traffic of (a) Pablo Ocampo's southbound and (b) Antipolo's northbound in one month between working and non-working

identified. Therefore, to alleviate these problems, an allowance threshold of 1 hour or 4 intervals is considered such that if there is a below-peak hour threshold condition change that occurred for only an hour or less, these would be recognized as part of the peak hour. Similarly, if an above-peak hour threshold condition change that occur for only an hour or less, these will not be recognized as part of the peak hour. The results of the improved peak hour detection is illustrated in Figure 5.10.

Contrary to working day traffic, non-working day traffic does not have a context of peak hour. Its traffic trend only settles between near light and around moderately light due to the abundance of light traffic condition (see Figure 5.7). To further support this, Figure 5.11 shows a visualization of the monthly average of non-working day traffic for Pablo Ocampo's southbound and Antipolo's northbound. Unlike working day traffic (see Table 5.3), patterns are less recognizable

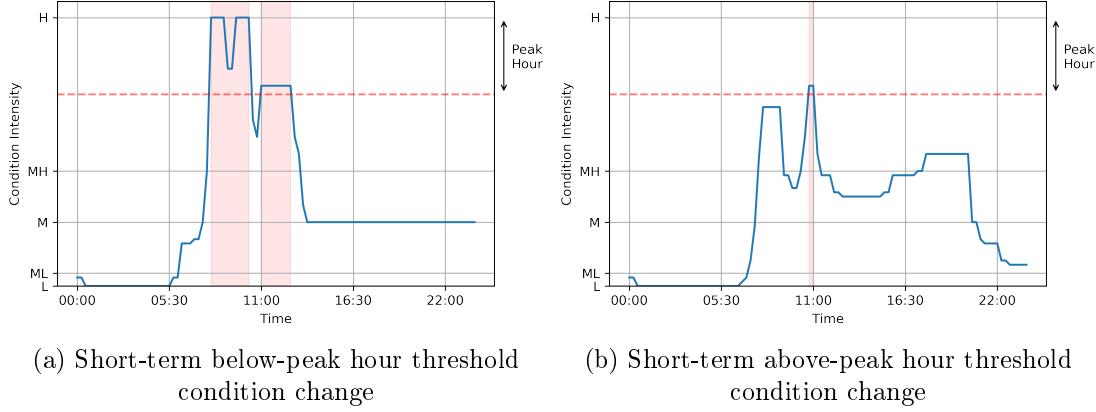


Figure 5.9: Examples of one-month average working day traffic of Pablo Ocampo's southbound illustrating the issues in the peak hour detection in terms of short-term (a) below-peak hour and (b) above-peak hour condition change

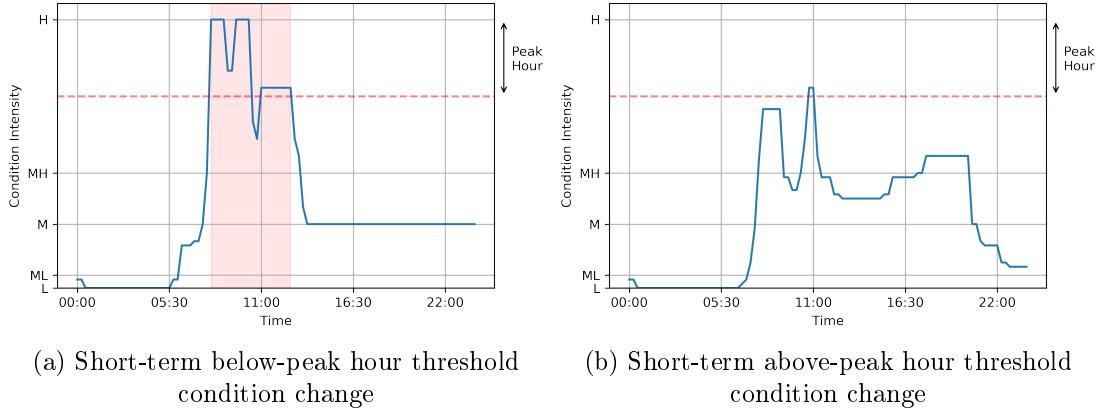


Figure 5.10: Examples of one-month average working day traffic of Pablo Ocampo's southbound showing the improved peak hour detection, fixing the issues for short-term (a) below-peak hour and (b) above-peak hour condition change

due to the lack of variation of conditions for non-working day traffic (see Table 5.2).

Week Before

In Figure 5.12, it could be observed how closer the traffic pattern is with its week before pattern compared with its two-days-ago pattern. Referring at the identified

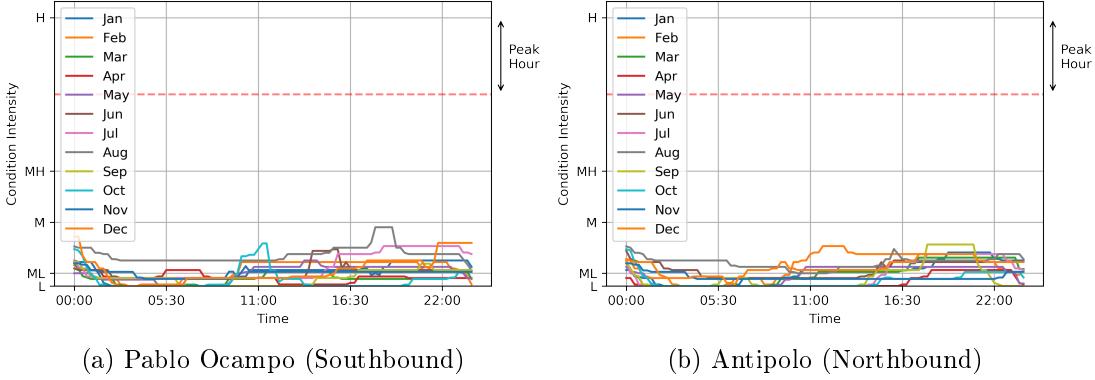


Figure 5.11: Monthly comparison of the average non-working day traffic of (a) Pablo Ocampo's southbound and (b) Antipolo's northbound

Table 5.2: Transition distribution of traffic condition of (a) Pablo Ocampo and (b) Antipolo for all non-working days

(a) Pablo Ocampo (Southbound) distribution (%)

		To				
From		L	ML	M	MH	H
	L	76.1	0.5	0.2	0.0	0.0
	ML	0.6	2.1	0.4	0.0	0.0
	M	0.0	0.6	19.0	0.1	0.0
	MH	0.0	0.0	0.1	0.1	0.0
	H	0.0	0.0	0.0	0.0	0.3

(b) Antipolo (Northbound) distribution (%)

		To				
From		L	ML	M	MH	H
	L	56.2	0.9	0.2	0.0	0.0
	ML	1.0	2.3	0.8	0.0	0.0
	M	0.0	1.6	36.4	0.1	0.0
	MH	0.0	0.0	0.0	0.4	0.1
	H	0.0	0.0	0.1	0.0	0.6

traffic seasonality in Figure 5.5, we could see how an observation in traffic appears to be more seasonal with its previous weeks as compared with the preceding days, with exception to the day before a specific observation.

Table 5.3: Transition distribution of traffic condition of (a) Pablo Ocampo and (b) Antipolo for all working days

(a) Pablo Ocampo (Southbound) distribution (%)

		To				
From		L	ML	M	MH	H
	L	46.7	1.1	0.0	0.0	0.0
	ML	1.0	2.2	1.2	0.0	0.0
	M	0.1	1.1	31.9	0.8	0.0
	MH	0.0	0.0	0.5	0.6	0.7
	H	0.0	0.0	0.3	0.4	11.4

(b) Antipolo (Northbound) distribution (%)

		To				
From		L	ML	M	MH	H
	L	29.5	1.1	0.0	0.0	0.0
	ML	1.0	2.2	1.1	0.0	0.0
	M	0.1	1.0	41.0	0.6	0.0
	MH	0.0	0.0	0.6	0.5	0.6
	H	0.0	0.0	0.1	0.5	20.1

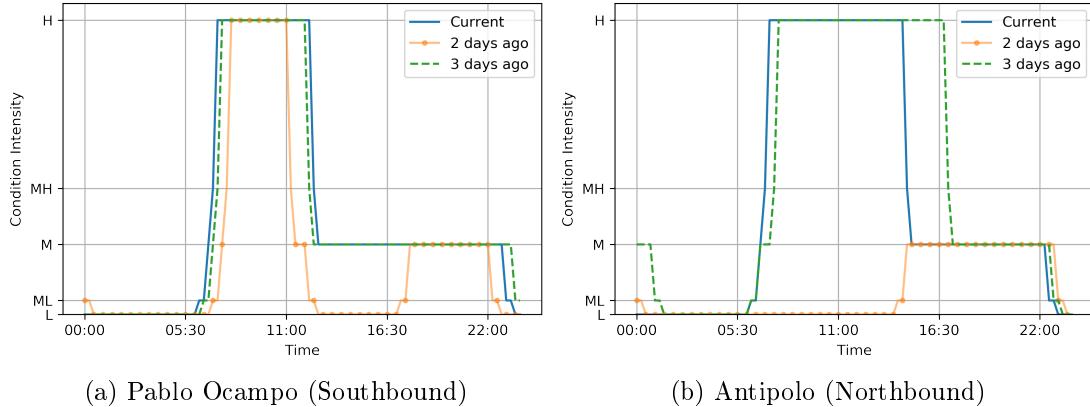


Figure 5.12: Comparison between the two-day-ago pattern and one-week-ago pattern of (a) Pablo Ocampo's southbound and (b) Antipolo's northbound traffic pattern showing that the week before traffic is more similar despite its difference in terms of days

5.1.3 Weather Analysis

Performing Spearman's rank correlation on weather variables against traffic, in general, reveals that they have a weak correlation (see Figure 5.13). One possible

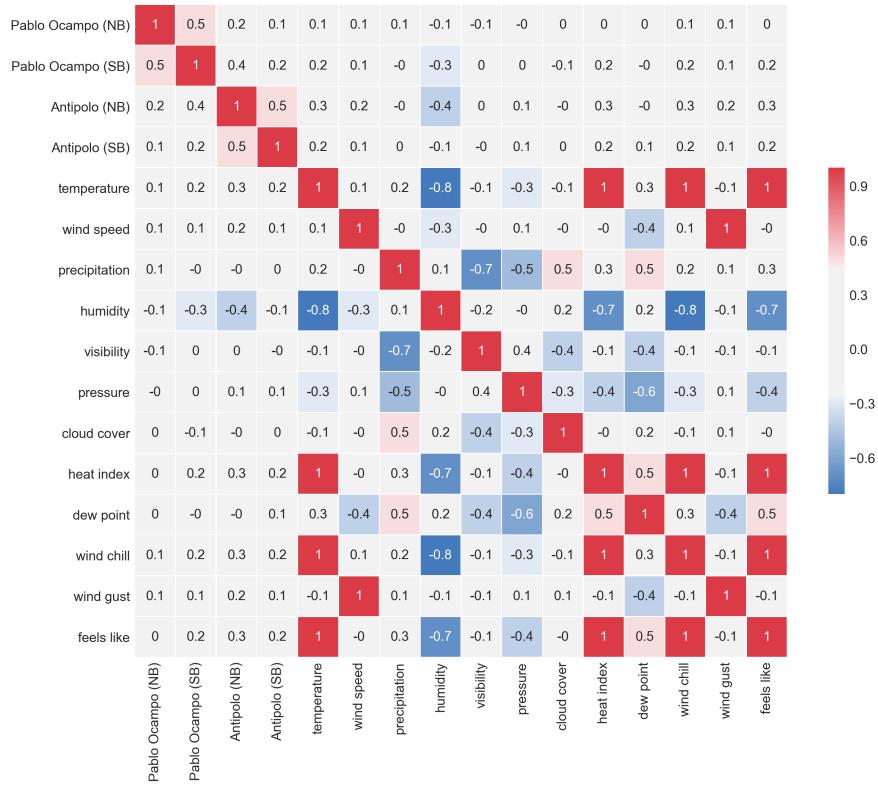


Figure 5.13: Correlation heatmap of traffic (Pablo Ocampo and Antipolo) and weather variables showing a weak correlation between them

reason for this is the effects of weather to traffic is not immediate. For instance, changes in traffic pattern are not immediately seen upon the start of precipitation. Instead, it can be seen after a while as precipitation continues building up. To address this problem, an exploratory analysis between each weather variables and traffic are conducted, exploring their commonalities in terms of seasonality and trends.

Seasonality

Similar to traffic, the autocorrelation of each weather variable reveals that all of them have a daily seasonality (see Figure 5.14). Notably, the majority of them are able to maintain their seasonality for days or even a week. Nevertheless, these are not true for weather variables such as precipitation, visibility, wind speed, and wind gust, which are seasonal to their previous day yet have a weak relationship with it.

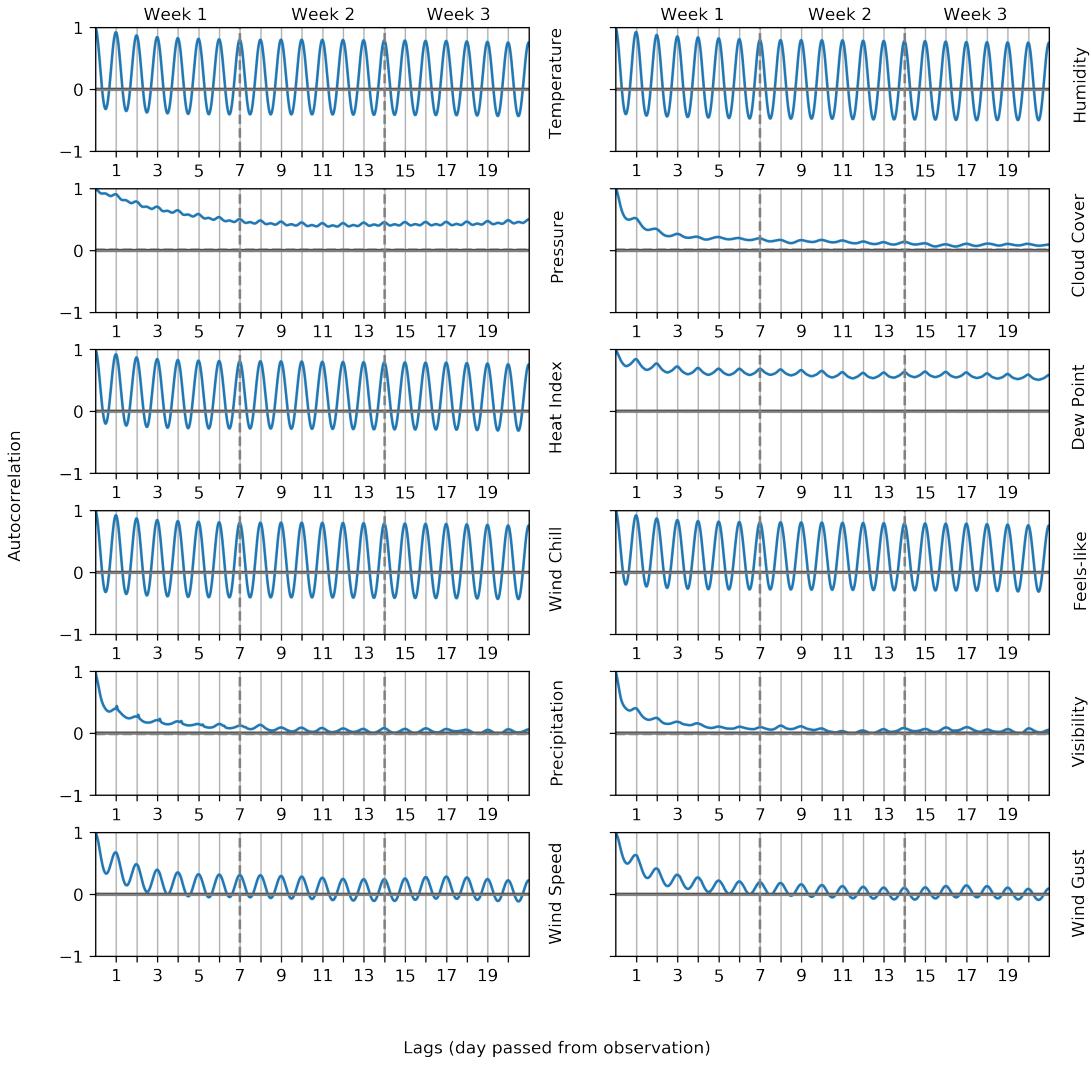


Figure 5.14: Autocorrelation of weather variables showing the presence of daily seasonality

Trend

As traffic is able to maintain a relatively moderate seasonality with its previous days, weather variables whose seasonalities are characterized similarly will be explored. These will include temperature, pressure, heat index, wind chill, humidity, dew point, and feels-like. To define their normal trend, their daily average per time intervals will be utilized, given by its daily seasonality. In consideration for the case of traffic, however, priority will be given to the SB traffic as it has a relatively stronger relationship with other weather variables as compared with NB traffic, and only working days on a given month will be considered with respect

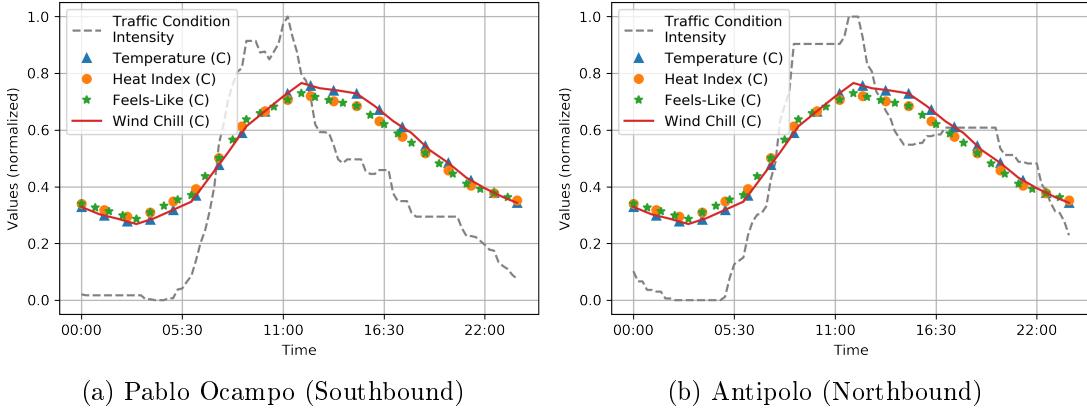


Figure 5.15: Comparison of the normal pattern of temperature, heat index, feels-like and wind chill with the normal pattern of Pablo Ocampo's southbound and Antipolo's northbound traffic

to its previous day seasonality.

Temperature, Heat Index, Feels-Like and Wind Chill Figure 5.15 illustrates a one-month visualization of the normal trend of temperature, heat index, feels-like and wind chill against traffic. From the initial correlation analysis mentioned earlier (see Figure 5.13), temperature, heat index, feels-like and wind chill has a weak correlation of 0.2 and 0.3 with Pablo Ocampo's southbound and Antipolo's northbound traffic respectively. A reason for this is despite that they match in terms of their morning trend, their evening trend significantly differs. Moreover, interpreting this relationship, it only shows the transition of dawn to morning, or simply the beginning of the morning peak hour.

Pressure Figure 5.16 shows a one-month visualization of the normal trend of pressure and traffic. At initial glance, it resembles the traffic pattern in a subtle way. However, looking at the initial correlation analysis earlier (see Figure 5.13), pressure appeared to have a significantly weak correlation with traffic, at 0.033. One notable difference between pressure and traffic is that pressure rises again during the evening up to dawn, following its relationship with temperature (Aguado et al., 2007).

Humidity Figure 5.17 illustrates a one-month visualization of the normal trend of humidity and traffic. Basing on the initial correlation (see Figure 5.13), humidity has a weak correlation of -0.260 with traffic. Comparatively, this could be

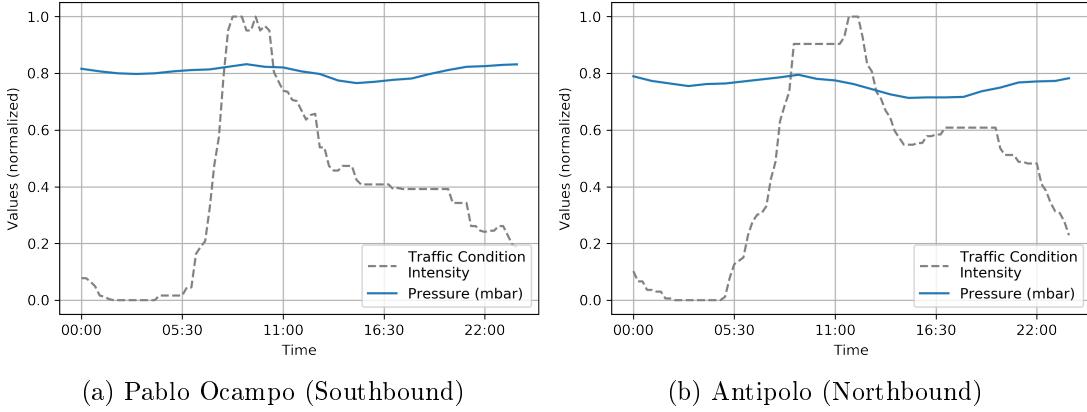


Figure 5.16: Comparison of the normal pattern of pressure with the normal pattern of Pablo Ocampo's southbound and Antipolo's northbound traffic

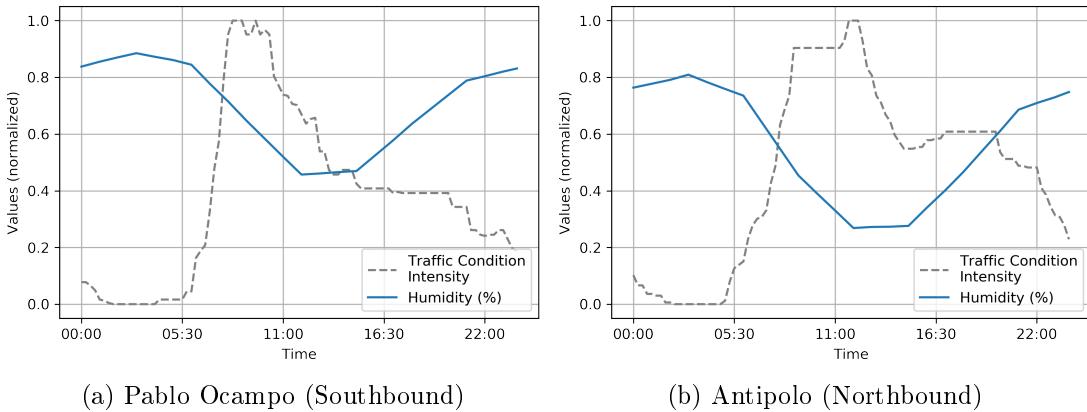


Figure 5.17: Comparison of the normal pattern of humidity with the normal pattern of Pablo Ocampo's southbound and Antipolo's northbound traffic

interpreted in the same way as temperature yet reversed due to its negative relationship, following the relationship of temperature and humidity (Paull, 1999). This is further supported by the strong negative relationship between temperature and humidity with a value of -0.810.

Dew Point Figure 5.18 shows a one-month visualization of the normal trend of dew point and traffic. Upon initial inspection, there is a subtle similarity between its pattern with the pattern of traffic. However, referring to the initial correlation (see Figure 5.13), dew point has a significantly weak correlation of -0.037 with traffic. Rather, this similarity in terms of form may be due to its relationship

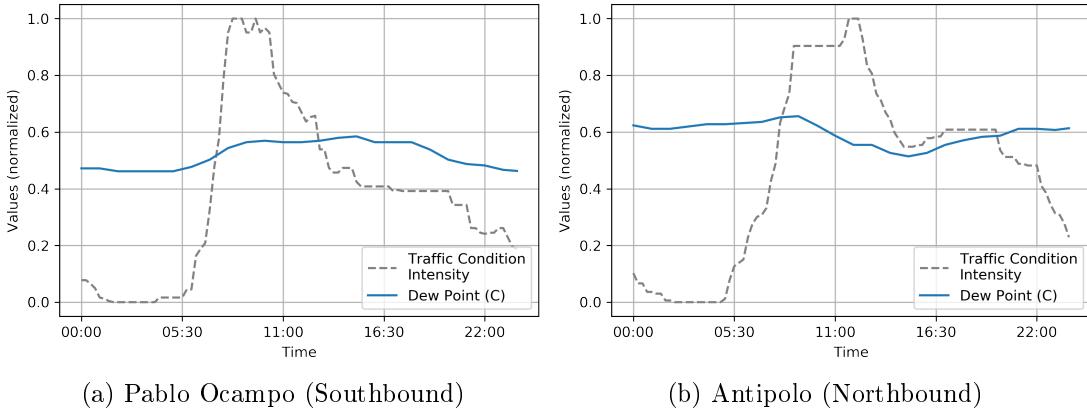


Figure 5.18: Comparison of the normal pattern of dew point with the normal pattern of Pablo Ocampo's southbound and Antipolo's northbound traffic

with pressure (Gaul & Underwood, 1952).

In summary, based on exploratory analysis, there is no derivable relationship between weather variables and traffic. This might be due to the fact that contributing factors to traffic are already embedded in its respective conditions, or traffic, itself, has its own pattern to follow. As the examined variables gradually change, as characterized by their consistently strong week-long seasonality, there is no abrupt or noticeable impact in terms of the daily traffic pattern.

5.1.4 Weather Disruption

As there was no established relationship between weather variables and normal traffic pattern, another way to analyze the relationship of weather to traffic is by exploring its special cases, particularly when there are extreme weather conditions such as typhoons and low-pressure areas that may disrupt the usual pattern of traffic. To assess this, the criteria for classifying a weather-disrupted day are identified.

Climate Season

According to *Climate of the Philippines* (n.d.), dry and wet season occurs from December to May and June to November respectively. However, contrary to this, the precipitation data from 2015-2017 shows that the dry season occurs from January to April, and wet season strongly occurs from May to October (see Figure

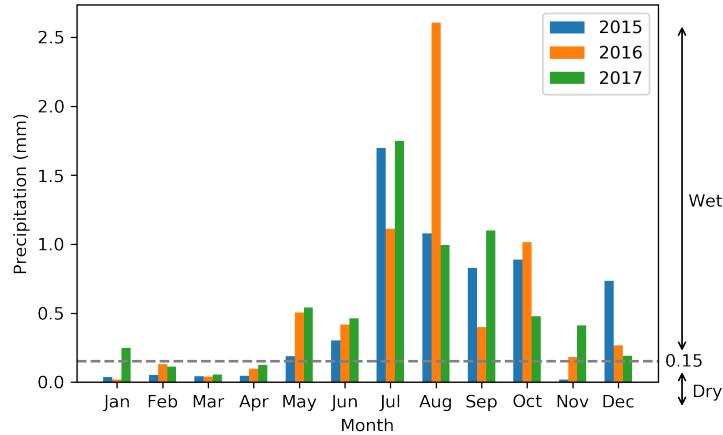


Figure 5.19: Wet and dry season based on the average precipitation per month from 2015 to 2017 defined by the 0.15mm threshold

5.19).

Disrupted Day

It is important to note that when defining disrupted days in respect to traffic, there are two factors to consider. First, it has been established by analyzing the traffic trends that increase in traffic mostly occur around 6:00. Thus, to observe the effects of prolonged rainfall to traffic, the instances of precipitation during the evening should be disregarded as its effect is more likely to decay when it is expected to effect during the morning. In the following experiments, only weather instances from 0:00 to 21:00 will be observed.

Second, only working days are considered as these are the days when traffic is significantly dynamic, hence disruption on its pattern can be observed. Given this, similar in our previous experiments in traffic, holidays and suspensions are considered as outliers as its traffic pattern would be inconsistent with its usual working day pattern.

Meanwhile, for weather, a threshold should be made with respect to the number of intervals per day. Given that a day is defined by 96 15-minute intervals, a cumulative minimum of 28 intervals or 7 hours of rain condition will be set as the threshold in classifying a disrupted day.

With these criteria set, a total of 69 disrupted days have been identified, in which 44.92% came from working days under the typhoon. As expected, the

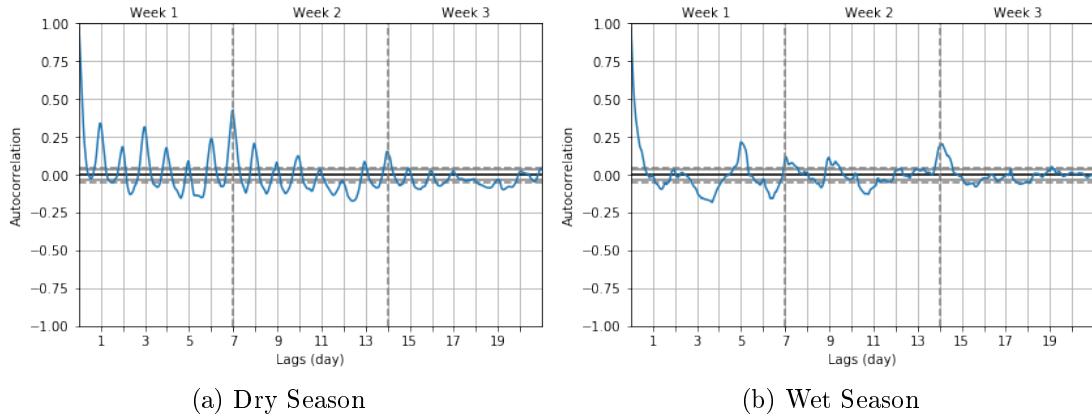


Figure 5.20: Autocorrelation of traffic comparing the daily and weekly seasonality per season showing that its pattern is disrupted during the wet season

majority of these are taken from the wet season, more specifically 94.20% of it.

5.1.5 Traffic Disruption

Comparing the autocorrelation between dry and wet season, it could be observed that the daily seasonality of traffic becomes less evident during the wet season (see Figure 5.20). This could be due to the abundance of precipitation, disrupting the normal pattern of traffic.

To verify this, we compare one observation of traffic (a week before Typhoon Goring) with its previous week (on the week of the typhoon). Basing from the seasonality of traffic, it is expected that the current traffic pattern would be similar to its previous week (see Figure 5.21). However, visualizing the current traffic pattern with its previous week, it could be observed that there is a significant increase in traffic as compared with the previous week of traffic.

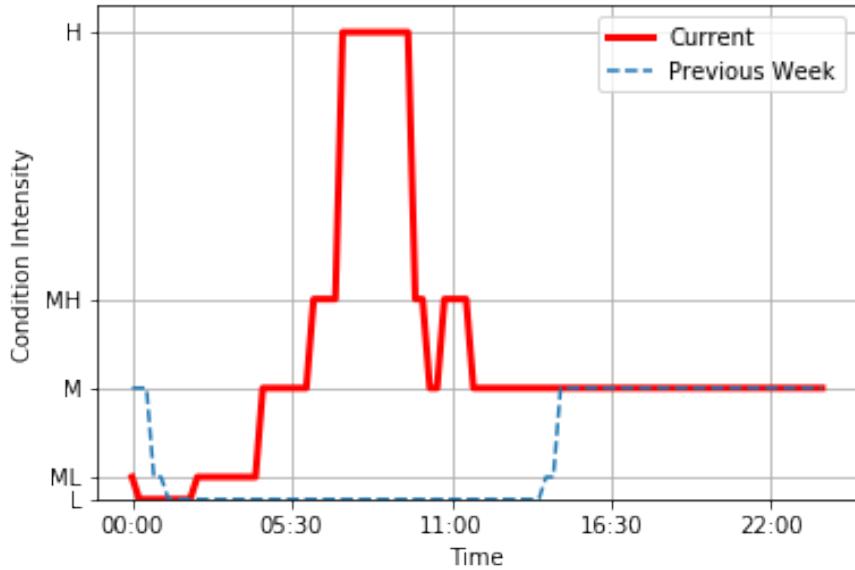


Figure 5.21: Comparison between the current traffic and its previous week pattern showing a disrupted pattern

5.2 Correlation Analysis

5.2.1 Correlation of Engineered Traffic Features with Traffic Condition

Mean of Previous Weeks

As the weekly seasonality of traffic remains consistent in both dry and wet season, the previous weeks could be potentially used to override the disrupted pattern of the previous week of a specific observation. In identifying this pattern, the mean of the traffic for the past weeks are taken. Correlating against the previous day and previous week seasonality, we could immediately observe an increase in the strength of its relationship with the present traffic (see Table 5.4).

Further experimenting with the strength of its relationship, we examined the correlation of from 2-weeks-ago traffic up to 7-days-ago traffic (see Table 5.5). From this, we have identified the ideal range to be 6 weeks ago, as the relationship already starts to fade when 7 weeks ago is reached. Interestingly, the traffic mean 2-weeks-ago has a weaker relationship to the current traffic than the succeeding number of weeks. This could be due to the fact that at 2 weeks, there exist only the traffic of the previous week and the traffic 2 weeks ago. Considering the

Table 5.4: Comparison between previous day and week traffic with the traffic mean 4-weeks-ago showing significant increase in strength in its relationship

	Correlation value
Previous Day Traffic	0.265
Previous Week Traffic	0.282
Traffic Mean 4-weeks-ago	0.391

Table 5.5: Comparison of correlation values on the traffic mean of a range of weeks

Traffic Mean N-weeks-ago	Correlation value
2	0.293
3	0.327
4	0.391
5	0.399
6	0.418
7	0.411
8	0.405

observation at the previous week is disrupted, then the effect of it is not minimized as you're only aggregating it against one more value.

To verify this finding, Figure 5.22 illustrates an observation from an undisrupted time span, comparing the similarity of the current pattern with the traffic mean 6 weeks ago and 2 weeks ago. From this, it could be observed how close the current pattern with the mean of the traffic 6 weeks ago, specifically from 6:00 to 13:00.

This observation holds true even in disrupted days. Figure 5.23 shows an observation after a week of Typhoon Goring. It could be seen in this visualization that the 6-weeks-ago traffic mean appeared to be more similar to the pattern of the current traffic as compared with the 2-weeks-ago traffic mean. As mentioned earlier, this could be due to the fact that getting the mean of just two observations where one is disrupted may not be enough to capture the undisrupted relationship of the previous weeks of traffic.

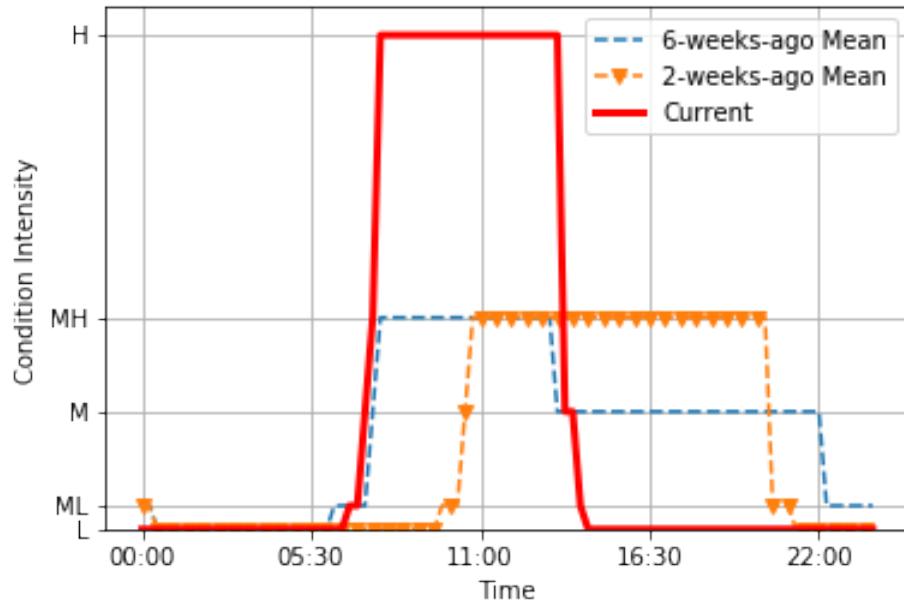


Figure 5.22: One-day visualization of the relationship between the current traffic and the mean of the traffic 6 weeks ago and 2 weeks ago

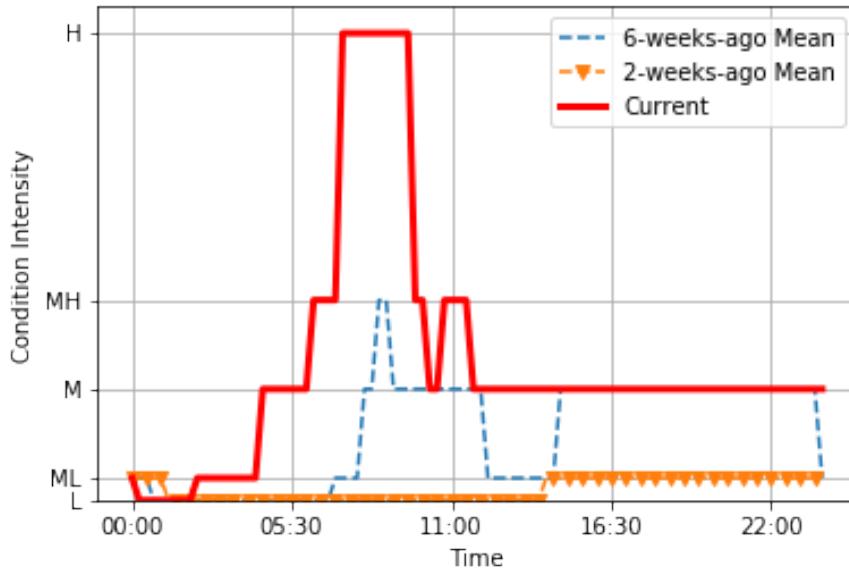


Figure 5.23: One-day visualization of the relationship between the current traffic and the mean of the traffic 6 weeks ago and 2 weeks ago after a week of Typhoon Goring

Rolling and Expanding Features

The data only describes the traffic condition per timestep and the seasonality of traffic. Although traffic has pattern, there are instances when a certain disrupt-

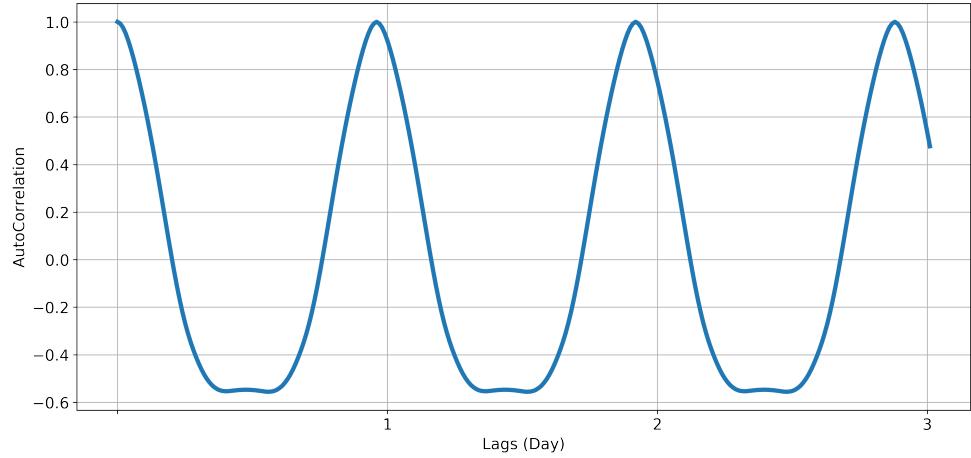


Figure 5.24: Autocorrelation of traffic for working days

tion in traffic may cause congestion build up. Therefore, considering how the immediate past traffic conditions may affect the current traffic condition can be considered as a factor for predicting traffic. Data from the previous timestep can be used as a reference in predicting the current traffic condition. However, the change in traffic in a 15-minute timeframe may not be significant. As seen in Figure 5.24, autocorrelation reveals that a traffic condition is highly likely to reoccur every 15 minutes. In other words, the traffic condition of the previous time step is highly likely to be the traffic condition of the current time step. However, this does not capture the effects of sudden outliers to the build up or decay of traffic. Thus, it does not fully describe how the past traffic conditions might affect the current traffic condition.

Generating rolling and expanding features based on a specific window size gives a bigger look as to what the current traffic might be based from the previous traffic conditions. Rolling and expanding window traffic features such as the mean, the minimum, and the maximum with window size 4, 8, 24, 48, and 96 were generated from the original traffic data. To summarize the possible effects of sudden changes in traffic, the mean of the past traffic conditions based on a window size was generated. Figure 5.25 shows the standard deviation values of traffic for every window size. Standard deviation shows the variability or the distance of the data from the mean. From this, it can be observed that there is a rising pattern in the growth of the standard deviation as the window size increases. The low standard deviation of smaller window sizes signifies that there is only a little to no change in traffic condition within that time frame. Meanwhile, large window sizes like window 96 which yield a relatively larger standard deviation value of 0.03531 than of window 4, implies that the traffic conditions in a 1-day time frame are more varied or are more widely spread. With small window sizes, the values generated

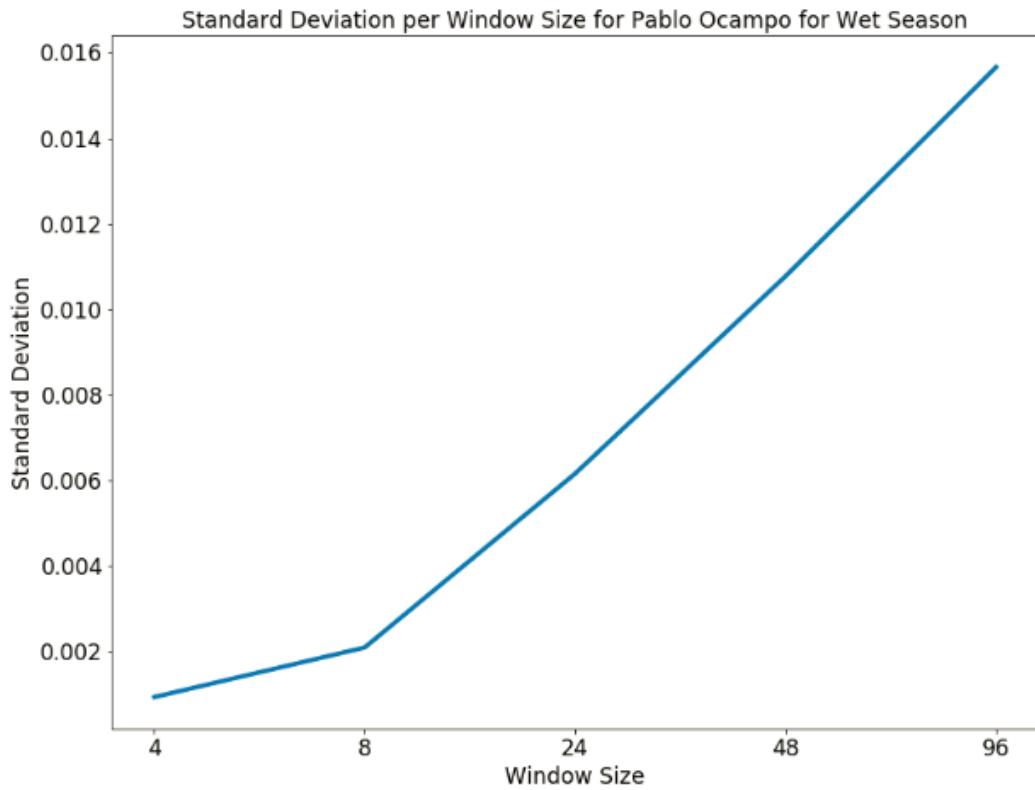


Figure 5.25: Standard Deviation of Traffic per Window Size for the Wet Season in Pablo Ocampo

captures less of the trifile changes in traffic and gets more affected by outlier values which then results in a more generic information. However, as the window size increases, the effect of outlier values also get more neutralized because of the number of data considered, giving a broader summary of the past traffic.

The minimum and maximum features, on the other hand, reveals the range of x in the dataset. Being sensitive to outliers, they provide outlier detection when compared to the average value of that specific set of data. A big difference between the values of the minimum and the maximum signifies a large progression in traffic condition. Although as the window size used gets bigger, it becomes harder to determine whether the sudden change in traffic condition occurred just a few timesteps before or if it is because of a farther instance which may have less to no effect to the current traffic condition.

Figure 5.27 shows the average correlation of southbound road segments of Roxas Boulevard per window size in relation to traffic for both rolling and expanding windows. On average, the original traffic has a strong relationship with rolling features having small window size, specifically window 4 with a correlation

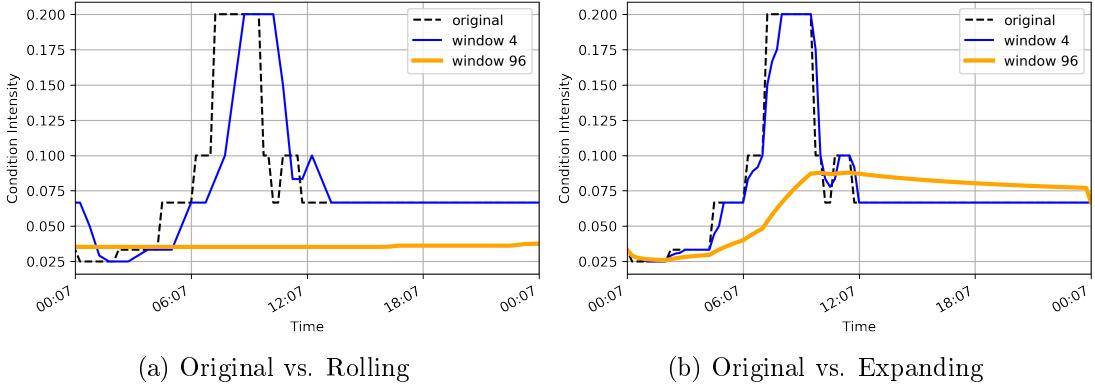


Figure 5.26: Comparison of Rolling and Expanding windows 4 and 96 to original Northbound traffic in Pablo Ocampo

value of 0.7501. It is noticeable, however, that the strength of the relationship dwindles down as the window size increases. This reveals that although having a bigger window size means being able to capture various changes in traffic condition, it does not give importance to the most recent traffic conditions. Big changes in traffic conditions that occurred way back and may not have any effect on the current traffic are being considered. Thus, causing its misalignment to the original data.

In the case of expanding windows, the strength of the relationship to the original traffic also decreases as the window size increases, albeit not so much as the rolling mean do. Looking into both graphs, the strength of the relationship given by window 4 for both rolling and expanding is distinctly stronger compared to the ones with larger window size. This might be because as mentioned earlier, traffic does not usually change significantly within a small window. Furthermore, a smaller window size means that its frequency of reverting back to the original value, making its generated value more accurate. Meanwhile, the farther from the past that it considers, the less it captures changes in traffic. This is shown in Figures 5.26a and 5.26b, where rolling and expanding at window 96 generalizes the high condition intensities into information that is no longer close to reality. Furthermore, the plodding decrease of correlation strength in expanding features as compared to rolling features is caused by limiting the number of windows that the feature grows to and considers and the restarting of its window size. Not limiting the window size growth of expanding features would produce values that are very far away from reality because it would consider every data from the previous days. It would contain values that consider data that are not relevant in predicting the future traffic.

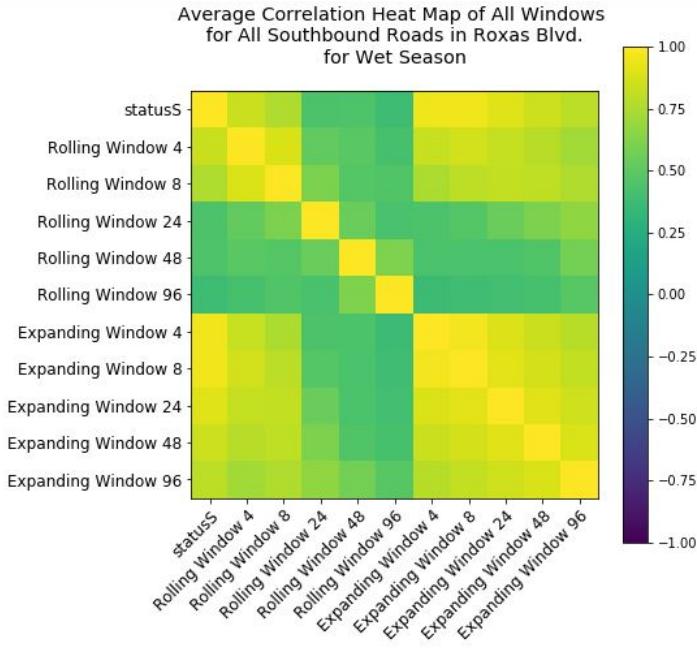


Figure 5.27: Average Correlation of Rolling and Expanding Mean to All Southbound Roads in Roxas Blvd.

5.3 Prediction Model Evaluation

5.3.1 Traffic-Only Model

Traffic-Only Model implemented in DBN was first evaluated. As seen in Figure 5.28 the inclusion of the information about working days and peak hours for all road segments improved the performance of the model by only 22% having originally an RMSE of 0.167 which improved to 0.113. As discussed earlier on the trend and patterns of traffic, though there is a difference between the trends of working days and non-working days, light and moderate traffic are most frequent in both trends in the majority of the road segments. This implies that the mean traffic condition intensity for both working and non-working days are similar. This similarity attributes to the small improvement in the prediction. Furthermore, including rolling and expanding window features for traffic significantly improved the prediction by around 53%, from having an RMSE of 0.129 to 0.061 by window 4. Rolling and Expanding window features present a generalized information regarding the trend of the immediate past traffic. As discussed earlier, average traffic does not change significantly within a small window. Moreover, increasing the window size of both features As such, the performance of the model decreases as the window increases.

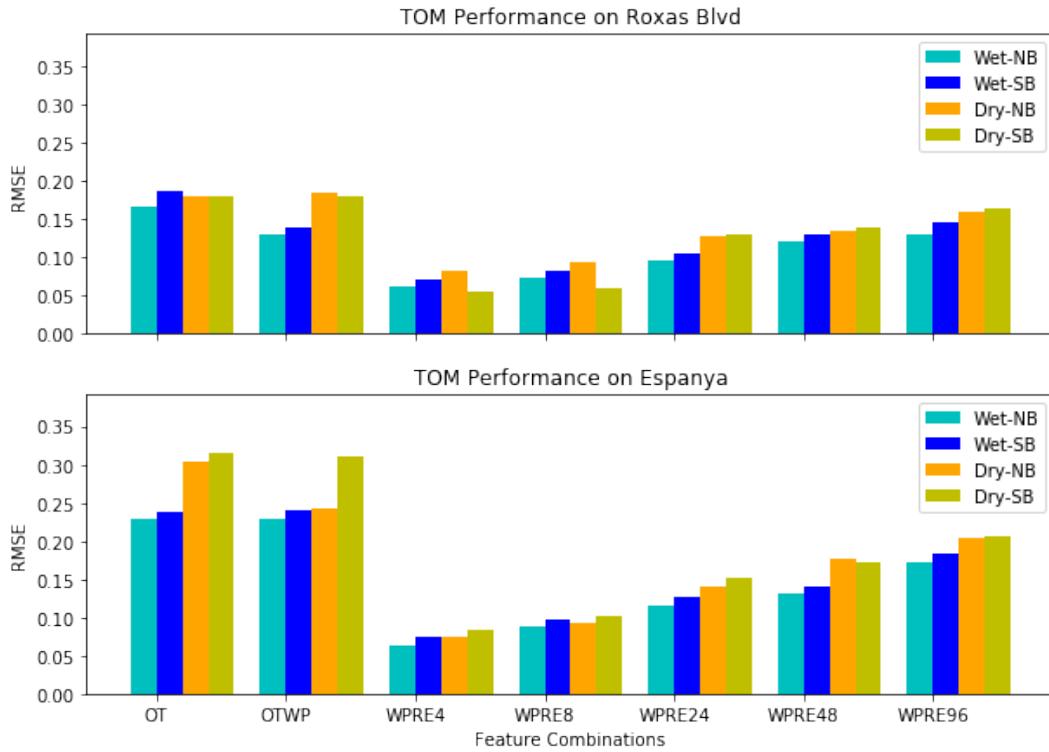


Figure 5.28: Comparison between performance of DBN TOM on Roxas Boulevard and Espanya using different feature combinations

To evaluate if the model can successfully identify the trends present for each road segment, and its ability to predict its traffic, the performance of the model using OTWP or Original Traffic with the addition of work day and peak hours was observed. Results of this evaluation are illustrated in Figure 5.29. The model predicted the southbound traffic of España during the wet season quite well, having a mean RMSE of 0.095 compared to the other. However, this is because of the diversity of the southbound traffic of España during the wet season, having a moderate traffic congestion majority of the time. Given only data of the previous day's traffic, and information on work day and peak hours, the model cannot easily model the sudden peaks and traffic reports on heavy traffic. Additionally, given the percentage of the report on heavy traffic congestion of the data, having only 10.584% during the working days, and 0.301% during the non-working days, the model lacks knowledge on modeling expected heavy traffic.

Disrupted days refer to the period in time wherein the trend of traffic goes out of its normal trend. Traffic that goes out of its normal trend is most expected during days that have heavy rainfall, or periods when typhoons are present. Figure 5.30 illustrates the prediction of TOM for traffic condition intensity for road

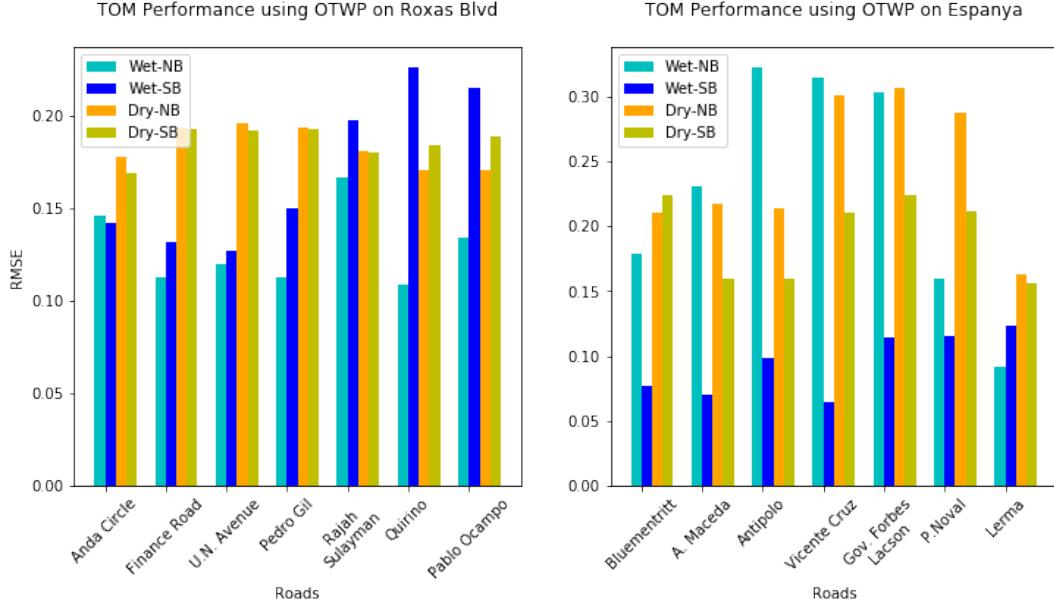


Figure 5.29: Performance of DBN TOM on Roxas Boulevard and España using OTWP traffic feature combination

segments of Pablo Ocampo and Antipolo during the wet season for the month of September. Normal trend includes the week of September 20 to 26, and the disrupted trend includes the week of September 6 to 12, both weeks include weekday and weekend. The period of disruption, specifically September 11 to 12, there are 40 and 56 instances of heavy rainfall, respectively. The actual traffic during the period of disruption transition from heavy traffic to moderate traffic in just a small time interval, unlike normal transitions. The model successfully predicts the abrupt transition of low traffic to high traffic for both normal and disrupted periods. However, the model delays in predicting the abrupt transitions from high traffic to moderate traffic, and moderate traffic to moderately high traffic. These difficulty in prediction can be attributed to the few instances where these abrupt transitions are present. As seen, normal trends do not often include these abrupt transitions.

Figure 5.31 illustrates the comparison of TOM implemented in RNN and DBN in predicting southbound traffic of Pablo Ocampo in the wet season. Results show that RNN performs better in predicting traffic than DBN. RNN could effectively predict traffic with just information on the mean of traffic 6 weeks ago, and traffic a day ago. Rolling and expanding window features that describe immediate past traffic could be removed, as it could add more complexity in predicting traffic, or it could have been a redundant feature, as shown in the small difference between not using these features, and using these features. Moreover, RNN predicts

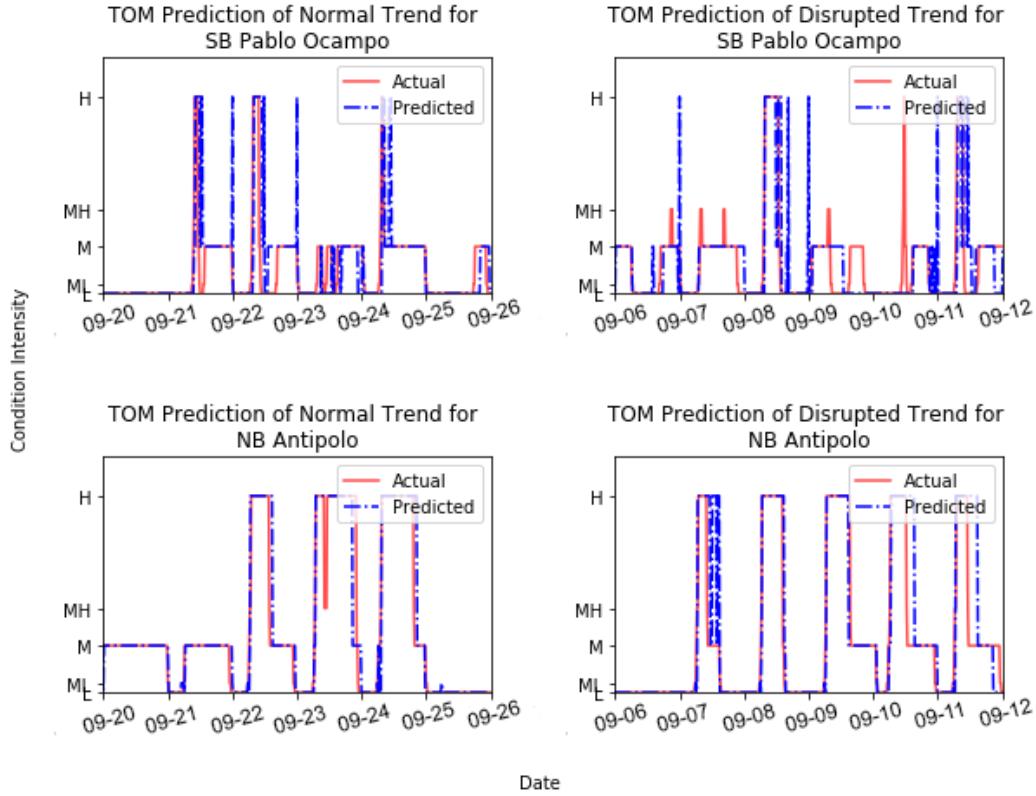


Figure 5.30: DBN TOM Prediction for Normal (left) and Disrupted (right) trends for Pablo Ocampo and Antipolo

disruptions, and sudden traffic changes better than DBN as illustrated in Figure 5.32. The figure clearly illustrates RNN's effective predictions for sudden traffic changes when traffic peaks and heavy traffic condition intensity is most expected, even with the small prior knowledge on heavy traffic unlike DBN.

5.3.2 Weather-Only Model

Given the weak relationship between weather variables with traffic, the model could only predict traffic about 80 to 84% after using weather variables for input as compared to using past traffic that can predict traffic by 90%. Furthermore, the model's performance did not improve significantly with different combinations (see Figure 5.33) of weather variables having changes in error ranging from only 0.001 to 0.003. Weather variables were found to have a low correlation, ranging from 0.01 to 0.3 with respect to the traffic condition intensity. Including and

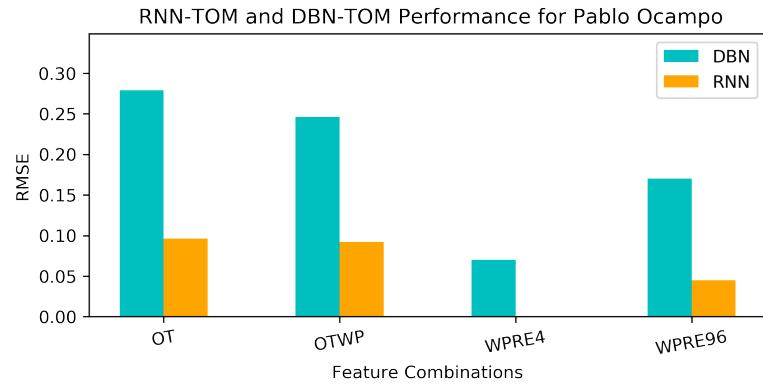


Figure 5.31: Comparison between RNN TOM and DBN TOM

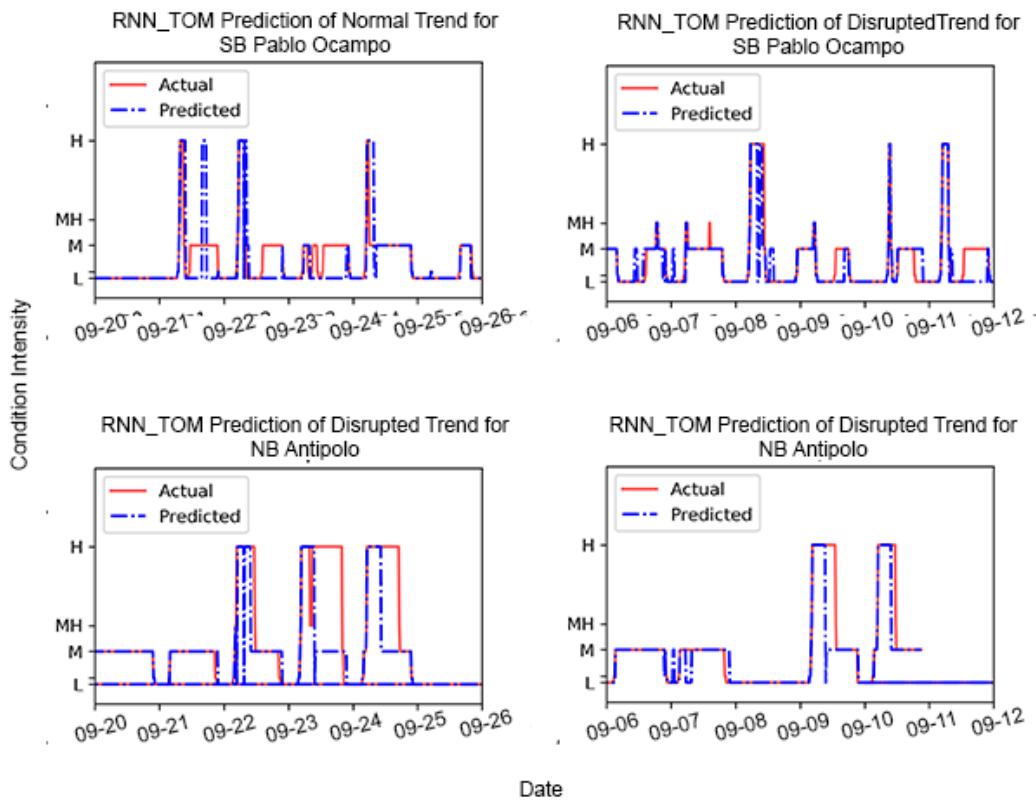


Figure 5.32: RNN TOM Prediction for Normal (left) and Disrupted (right) trends for Pablo Ocampo and Antipolo

removing redundant variables, and other low correlated variables did not have a significant effect on the prediction.

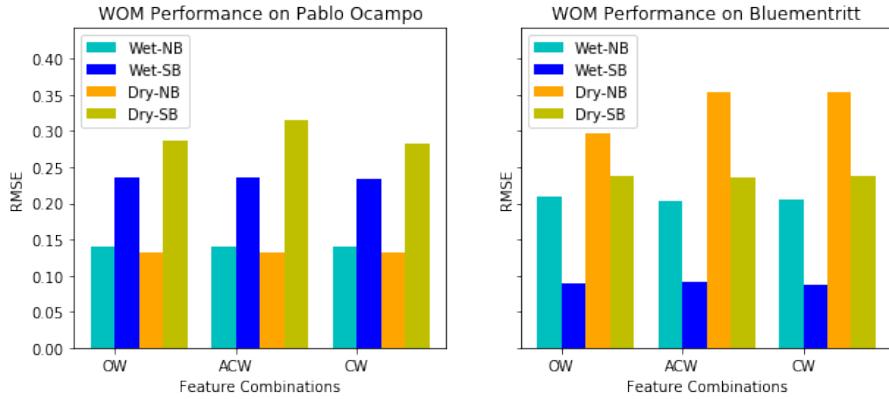


Figure 5.33: Performance of DBN WOM on Pablo Ocampo and Antipolo using weather feature combinations

Figure 5.34 illustrates the performance of WOM following OW feature combination for all road segments of España and Roxas Blvd. For predicting Roxas Blvd road segments using WOM, the model predicts traffic better during the wet season. Additionally, WOM predicts northbound well for most road segments in Roxas Blvd during the wet season. Northbound traffic for these roads is less diverse, meaning that traffic majorly consists of low to moderate traffic, with only a few instances of abrupt transitions from these conditions to heavy traffic. Given these, WOM could not learn the pattern of these transitions given the few instances. In predicting the traffic of Roxas Blvd road segments during the dry season, the WOM could only predict 70% of the traffic for the northbound of all road segments except Pedro Gil having an average RMSE of 0.250.

As for predicting España Road segments using WOM, the model predicts southbound traffic of all roads during the wet season better. The WOM got an average RMSE of 0.329 in predicting northbound traffic for road segments Bluementritt to P. Noval, compared to predicting its southbound counterpart having an average RMSE of 0.116. Like Roxas Boulevard road segments, the southbound traffic of España road segments is less diverse, consisting mostly of low to moderate traffic.

For both roads of Roxas Boulevard and Espana, WOM could better predict the bound of a road segment with less diverse traffic, in which instances where traffic abruptly transitions to another traffic condition is not present. Moreover, WOM cannot predict fully traffic during the dry season, wherein weather, most especially rainfall, is less expected that can affect traffic fully.

Given only temporal information and the weather variables to predict the current traffic condition intensity, and adding the fact that there is a small distri-

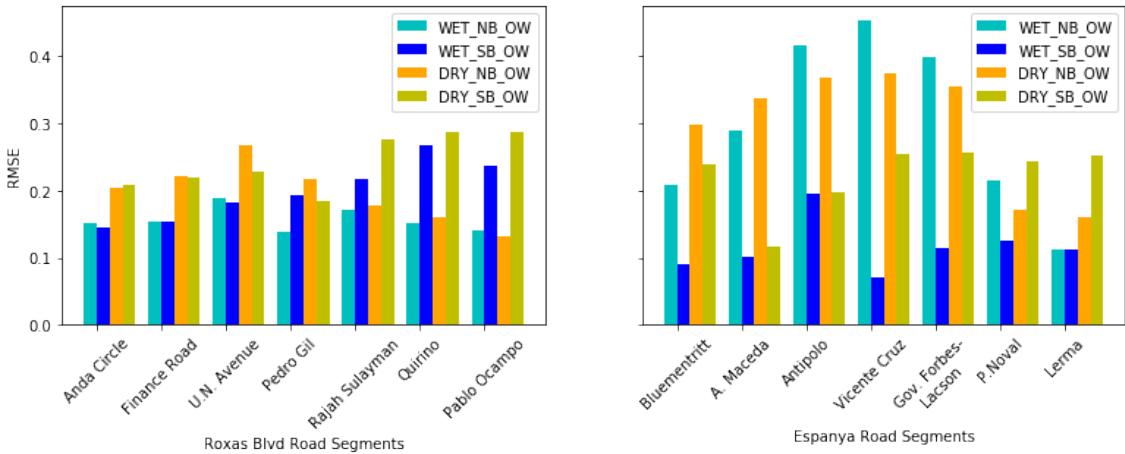


Figure 5.34: Performance of DBN WOM using OW weather feature combination for all road segments

bution of moderately high to high traffic in the data, the model could only predict low to moderate traffic successfully. Figure 5.35 illustrates the prediction of WOM for traffic condition intensity for road segments of Pablo Ocampo and Antipolo during the wet season for the month of September. WOM, however, predicted the transition of traffic from Low Traffic to either moderately low and moderate traffic well. WOM could predict the length of consistent traffic for both normal and disrupted periods.

Figure 5.31 illustrates the comparison of WOM performance implemented in RNN and DBN in predicting southbound traffic of Pablo Ocampo in the wet season. Much like TOM, RNN outperforms DBN and effectively predicted traffic with just information on weather variables. However, much like DBN TOM, the differences in performance between AW, ACW, and CW feature combinations is significantly small. Even with the ability to extract temporal information on a time series, it cannot effectively extract the patterns between weather and traffic. Figure 5.36 illustrates prediction generated by RNN WOM for both normal and disrupted periods. Comparing the performance of DBN WOM, RNN WOM did predict more instances of traffic than the latter. It is important to note that RNN depends on patterns present in time series, such as seasonality, trends, and the like. However, weather does not strongly follow any trend. Using RNN to extract the relationship between traffic and weather may not be effective. Possibly, RNN needs more time-series information.

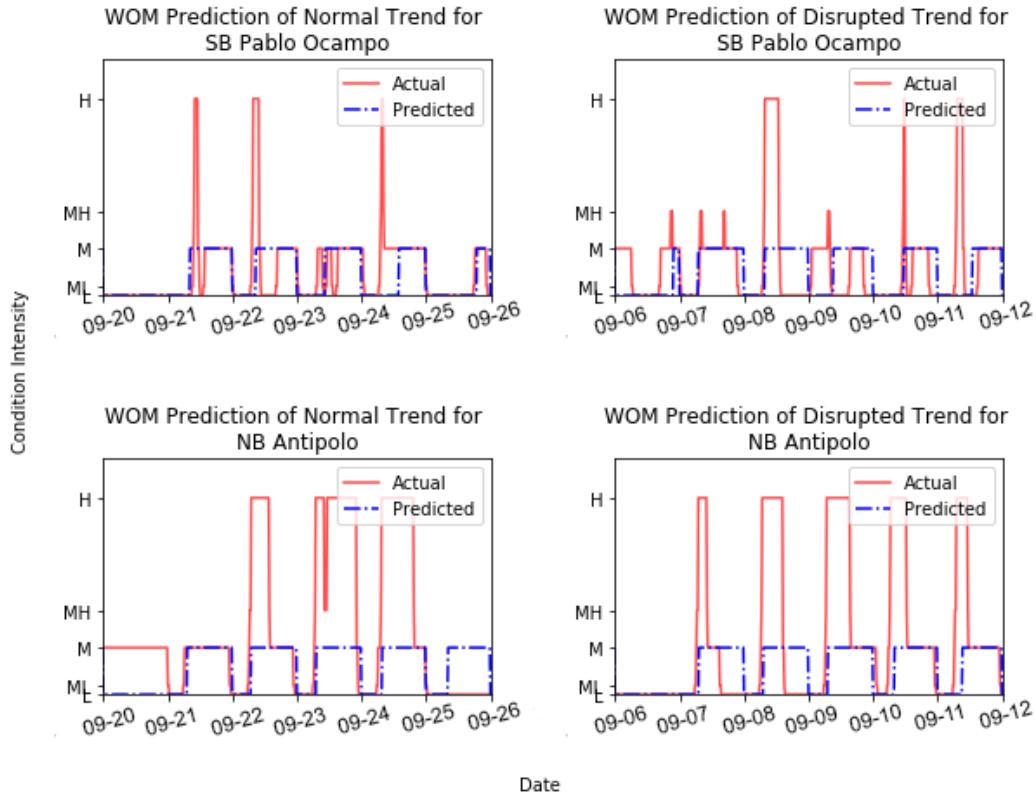


Figure 5.35: DBN WOM Prediction for Normal (left) and Disrupted (right) trends for Pablo Ocampo and Antipolo

5.3.3 Fusion Analysis

In analyzing the effectiveness of including weather as a factor in predicting traffic, the road segments which are strongly correlated with weather variables, and are more dynamic are selected in further analysis. These roads are southbound of Pablo Ocampo and northbound of Antipolo. The final results displayed are the average of the results of these two road segments.

In evaluating the DBN model, fusing traffic and weather at the decision level improved the prediction of TOM from an RMSE of 0.084 to 0.024, improving about 71%. The performance of DBN in fusing data at the feature level was not far from the decision fusion model, only having a difference in RMSE of only 0.019. Predicting traffic considering both traffic and weather at the same time may weigh down the prediction of traffic because of the influence of weather. As discussed in early analysis of the weather data, it was found that weather variables do not have a derivable relationship with traffic. Adding weather features together with

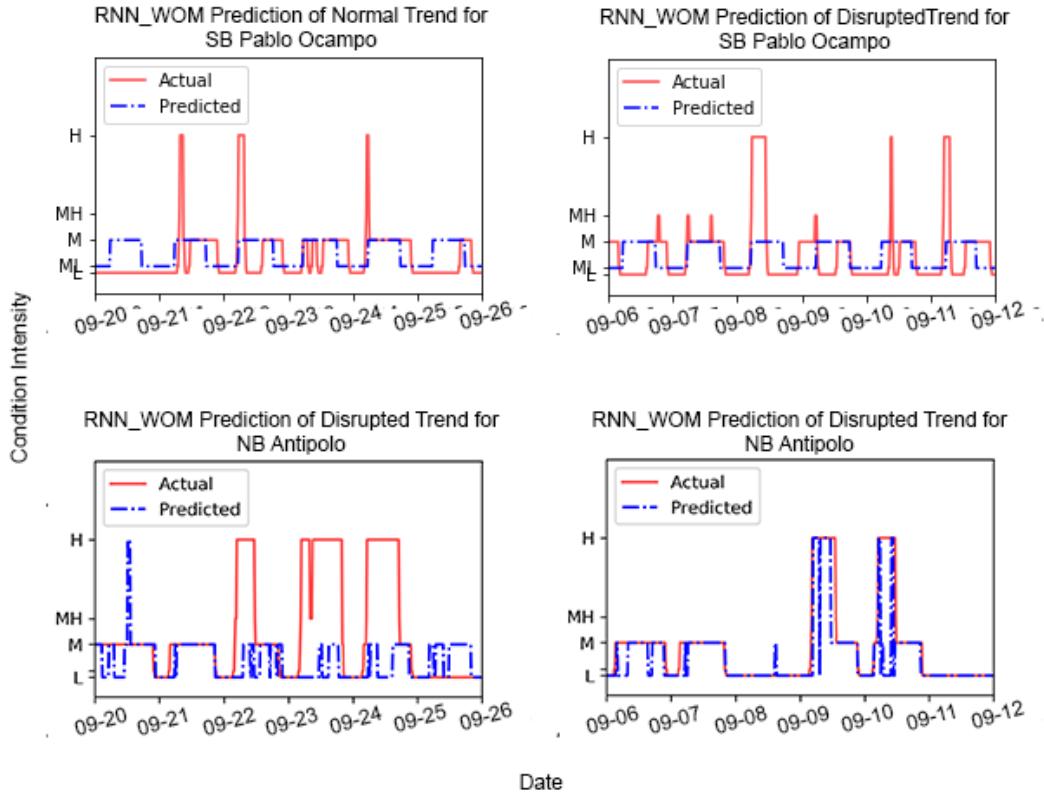


Figure 5.36: RNN WOM Prediction for Normal (left) and Disrupted (right) trends for Pablo Ocampo and Antipolo

Table 5.6: Comparison between Prediction Models and Fusion Models

Fusion Techniques	OTWP + OW		WPRE 4 + OW		WPRE 96 + OW	
	RMSE	MAE	RMSE	MAE	RMSE	MAE
DBN TOM	0.314	0.148	0.084	0.011	0.234	0.090
DBN WOM	0.328	0.149	0.328	0.149	0.328	0.149
RNN TOM	0.092	0.183	0	0	0.045	0.072
RNN WOM	0.147	0.186	0.147	0.186	0.147	0.186
DBN FF	0.322	0.154	0.092	0.017	0.277	0.114
RNN FF	0.078	0.101	0.077	0.119	0.078	0.118
DBN DF	0.312	0.140	0.024	0.003	0.196	0.006
RNN DF	0.072	0.145	0.038	0.086	0.063	0.125
WA DF	0.620	0.618	0.418	0.405	0.510	0.504

traffic adds more complexity to the model, adding more insignificant patterns to the learning, decreases the performance of the model to predict traffic. On the

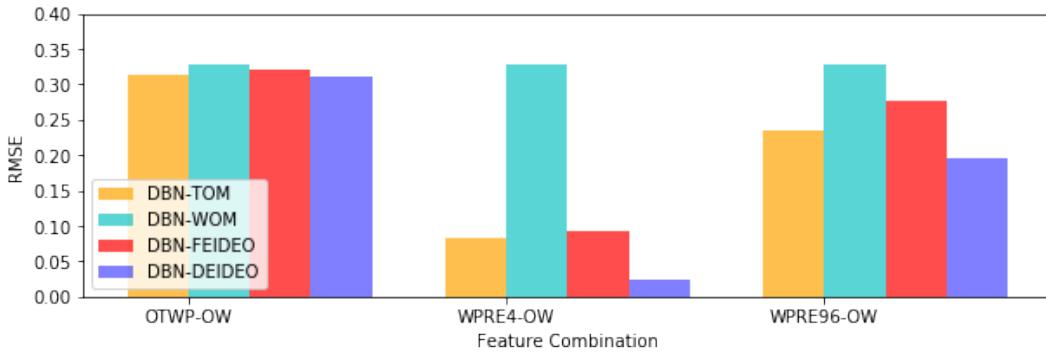


Figure 5.37: Comparison of DBN models in predicting the southbound of Pablo Ocampo for the wet season

other hand, in fusing at the decision level, the traffic predicted by TOM does not have influence with weather, thus, minimizing the weights in predicting traffic.

Figure 5.37 illustrates the differences of performance between DBN models, including decision and feature fusion DBN models that used predictions by the DBN prediction models. Including weather as a factor in predicting traffic improved the final predicting as seen in the results of fusing in the decision level. This improvement is significantly evident in the performance of the model after using predictions of TOM and WOM that used OTWP traffic features, and OW weather features, respectively. The prediction improved by 71%, from having an RMSE of 0.084 to 0.024. As for using predictions of TOM and WOM that used WPRE4 traffic features and OW weather features, the predictions improved by 16%. A reason behind only the small improvement is because of the consideration of rolling and expanding features at window 96, or within the current day. The window may have consisted instances of disruption that may have been generalized by the averaging traffic within 96 windows. Additionally, there is a small number of instances of heavy traffic that assists the rolling and expanding features in generalizing the traffic within said window.

Figure 5.38 illustrates the differences of performance between RNN models, including decision and feature fusion RNN models that used predictions by the RNN prediction models. The difference in performance between the different feature combinations, and models were significantly small, having little to no changes in the performances. As discussed earlier, RNN could efficiently predict traffic with only information on the mean of the past traffic, and instance of traffic a day before. These information already presents sufficient time-series characteristics, that adding more features may not be too significant in improving the performance. Much like DBN, the RNN DEI-DEO fusion model performed better than the RNN DEI-DEO model. However, the difference between the two performances

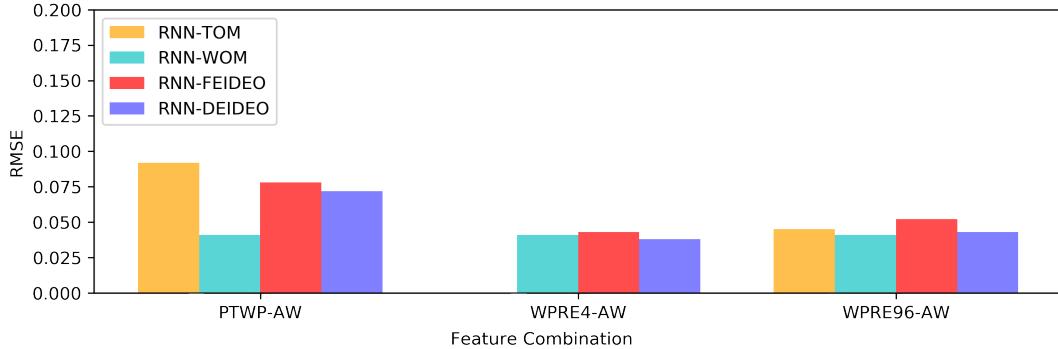


Figure 5.38: Comparison of RNN models in predicting the southbound of Pablo Ocampo for the wet season

are small because of the little significance weather features present in predicting traffic. However, both fusion models mostly improves the traffic prediction that did not consider weather. The prediction only improved by 2%. However, comparing the performances of the RNN models with the DBN models, the RNN models outperformed the latter by 70%. DBN-TOM had an RMSE of 0.314, whereas RNN-TOM had an RMSE of 0.041. DBN-Decision fusion model had an RMSE of 0.312, while RNN-Decision fusion model had an RMSE of 0.072. RNN models significantly outperforms DBN models.

WA performed the worse of all fusion techniques, generating an RMSE of 0.512 to 0.620, as compared to the other techniques. WA, much like the other techniques, significantly improved as rolling and expanding windows were considered. Because the predictions come closer to the truth once rolling and expanding window features are considered, WA comes close as well. However, WA cannot effectively predict traffic that considers weather features. The inclusion of weather features may have added complexity in identifying the weights of the algorithm, and have added more weight in averaging two predictions, rather than improve it. WA considers the outlier and generates an inaccurate prediction. Because of such performance, WA is not considered in further experiments. The farther one prediction is to the other, the farther the outlier is away from the other, the more difficulty WA goes through in fusing decisions.

A noticeable behavior is RNN outperformed the other fusion techniques. RNN has at least 74% less error than DBN and WA. RNN is implemented as an LSTM, or a long short-term memory, compared to DBN which is implemented as a regressor and a classifier. Because of RNN's power of long short-term memory, it can use their internal memory to process a sequence of inputs, successfully extracting ordered patterns. However, as mentioned earlier, RNN could not improve the prediction of the RNN TOM model. However, the fusion model in DBN improved the

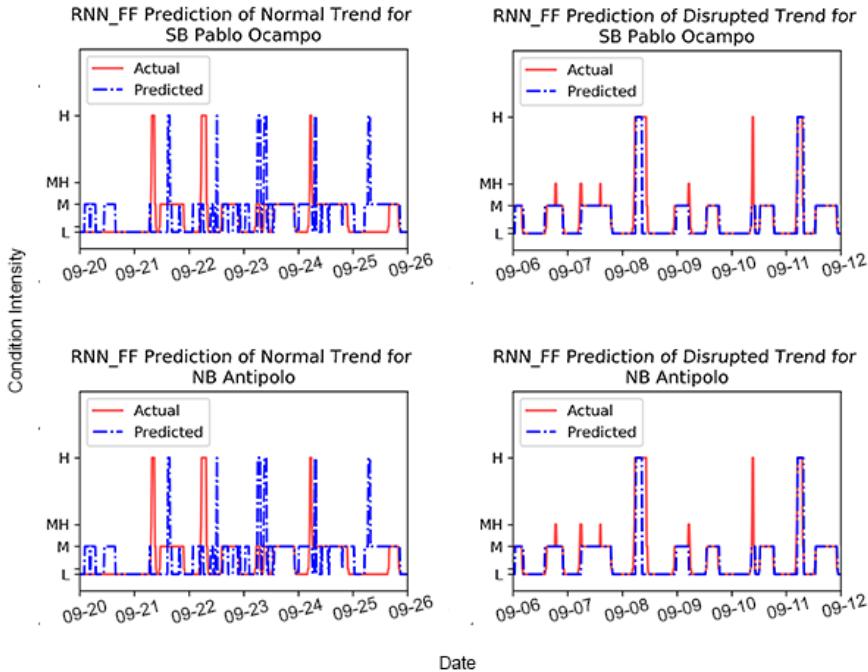


Figure 5.39: Final Prediction generated by RNN Feature Fusion model for Normal (left) and Disrupted (right) trends for Pablo Ocampo and Antipolo using DBN Decision Fusion

TOM and WOM's prediction because of the RBMs implemented into the network that can extract pattern from the data.

The implemented model could predict normal trends of traffic. However, disrupted traffic trends defined in the discussion of the traffic and weather data cannot be accurately predicted. A reason behind the difficulty in prediction is the small number of instances of disruption in the training dataset. There is only a small number of instances of moderately heavy to heavy traffic within the wet season of the training dataset. Another reason may be because of the instances when disruptions in weather were present until the weekends when traffic is least expected. For example, for September 11 to 14 when typhoon Ineng was present, extends from a Friday until Sunday. The model also has a difficulty in predicting traffic using only weather features because of the weak relationship between these variables. For visualization purposes, the final prediction of traffic condition intensity of Pablo Ocampo and Antipolo is illustrated in Figure 5.39.

5.3.4 Sensitivity Analysis

To analyze the effectiveness of including weather as a factor in predicting traffic, the southbound traffic of Pablo Ocampo were selected. The final results displayed are the average of the results of these two road segments.

Traffic-Only Model

Evaluation of the sensitivity of TOM is illustrated in Figure 5.40. It has been discussed in the early sections in evaluating TOM that the inclusion of work day and peak hour variables result in a 22% improvement in performance. In considering the working day and peak hour information, the removal of temporal information decreased the performance from 3.9 to 8.6%. Not one temporal information increased the accuracy. However, the removal of temporal information without considering the working day and peak hour information increased the performance, but only by 0.4 to 3.1%. This change in accuracy can be because of the model being given more complexity as more traffic features that are not exactly strongly connected with each other. An example of this is the variable *Day*. This variable decreased the accuracy the most out of all temporal information, having a decrease in accuracy of 8.6%. Other included traffic features do not depend on the day of the month. Hence, the significant decrease in accuracy. As for other temporal information variables, *Month*, *Hour and Minute*, and *Day of the Week* may describe traffic with the support of other traffic features. However, traffic disruptions and traffic trend changes occur. In the case of *Month*, noticeable traffic in a week in a month does not necessarily mean that it will be traffic the whole month. In the case of *Hour and Minute*, traffic this hour during a Friday does not necessarily mean it will be traffic that particular hour and minute during a Saturday, Sunday or even a Monday. In the case of *Day of Week*, given the number of records of heavy traffic that working day and peak hour information is derived from, day of week which depends on working day and peak hour, cannot effectively describe traffic. Moreover, in considering traffic features that effectively describes its immediate past traffic condition, such as using rolling and expanding window features, adding temporal information adds more complexity to the model such that it contradicts the findings of these traffic features with the patterns extracted by the temporal information variables. This is evident by the significant increase in accuracy by 4% when using rolling and expanding window features at window 96, and small increases and decreases in accuracy from 0.4% to 3.1% at window 4, as compared to having no rolling and expanding window features.

Looking into the effect of the past traffic feature when used with working day

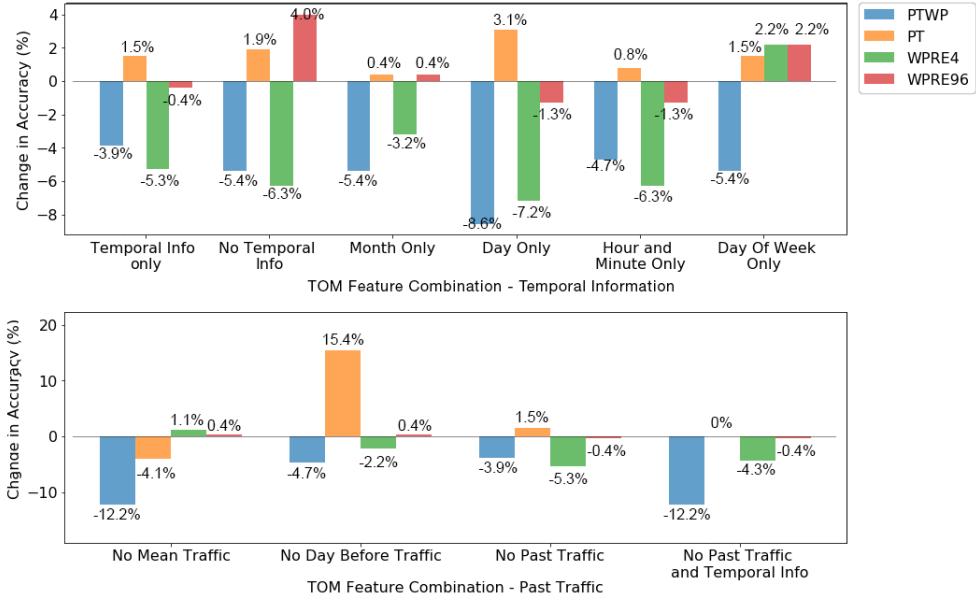


Figure 5.40: Sensitivity of TOM with different feature combinations

and peak hour, removing mean traffic 6 weeks ago significantly decreased the accuracy of the prediction by 12.2%. Moreover, the same decrease of accuracy was observed when past traffic features excluding working day and peak hour, and all temporal information was removed. Using only mean traffic 6 weeks ago as a past traffic feature, without the consideration of working day and peak hour, increased the accuracy by 15.4%. **Meanwhile**, the accuracy decreased by 4.7% to 2.2% after considering working day and peak hour. As discussed, working day and peak hour may have added complexity in predicting traffic using traffic features with patterns that may go against patterns of working day and peak hour. Moreover, given the small records of heavy traffic in the data which working day and peak hour extracts, these traffic features cannot describe traffic as much as the mean traffic 6 weeks ago, and traffic a day ago. Hence the significant increase in accuracy in removing working day and peak hour. Comparing the difference between the changes in accuracy between using mean traffic 6 weeks before, and traffic a day before, the accuracy significantly changed in considering the mean traffic 6 weeks ago. This show that this feature has great importance in predicting traffic. However, with the inclusion of rolling and expanding window features which describes the traffic of the immediate past, using the mean of the traffic 6 weeks before or traffic a day before does not significantly affect the accuracy of the prediction. This can be because of the relationship between the window features with the current traffic, which outperforms the patterns extracted by the mean traffic 6 weeks before and traffic a day before.

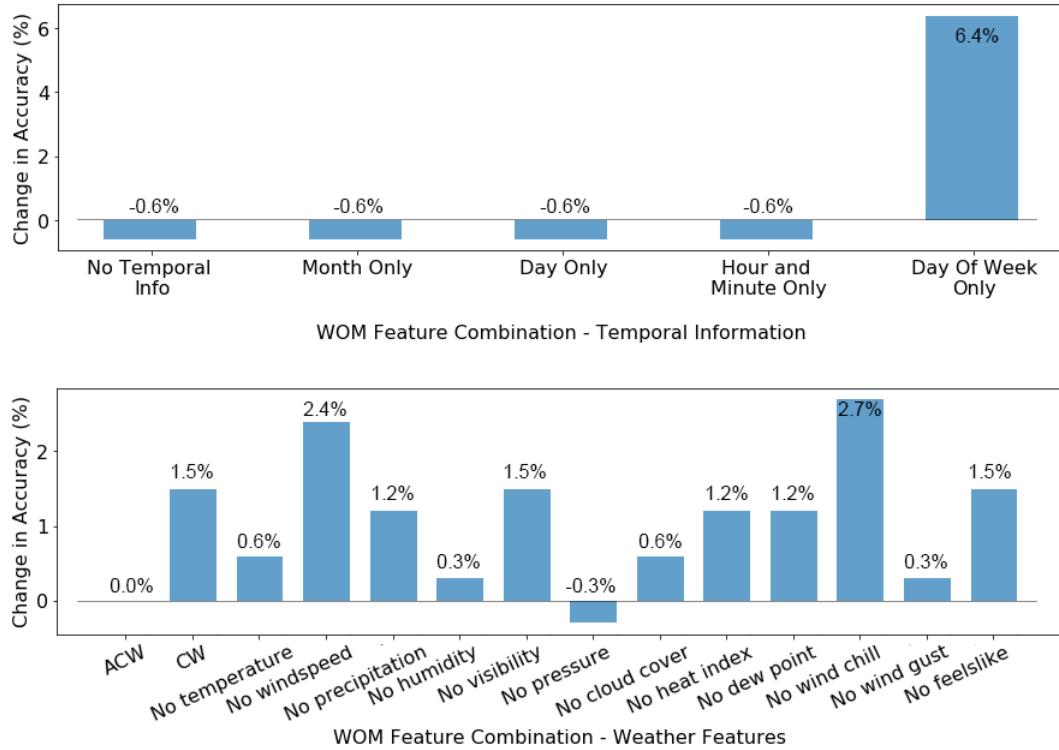


Figure 5.41: Sensitivity of WOM with different feature combinations

Weather-Only Model

Evaluation of the sensitivity of WOM is illustrated in Figure 5.41. As discussed in the evaluation of the WOM with the different combination of the weather features, the varying combinations did not go far from the results of using all weather features, from having a difference in RMSE from 0.001 to 0.003. The strength of the correlation between weather features to traffic were weak that it removing any weather feature did not significantly effect the prediction. Therefore, the change in accuracy ranges from 0 to 2.7%. However, using the weather feature that has the highest correlation with traffic between other weather variables, excluding redundant variables, did improve the prediction but only by 1.5%. This proves that the strength of the relationship between weather and traffic is important to understand to achieve better prediction.

The effect of temporal information to predicting traffic using all weather features was also evaluated, as illustrated in Figure 5.41. WOM uses only weather variables and temporal information to predict traffic. Of all the features, the closest to describe traffic are the temporal information features (e.g. Month, Day, Hour, Minute, Day of the Week). As such, the prediction decreased as temporal

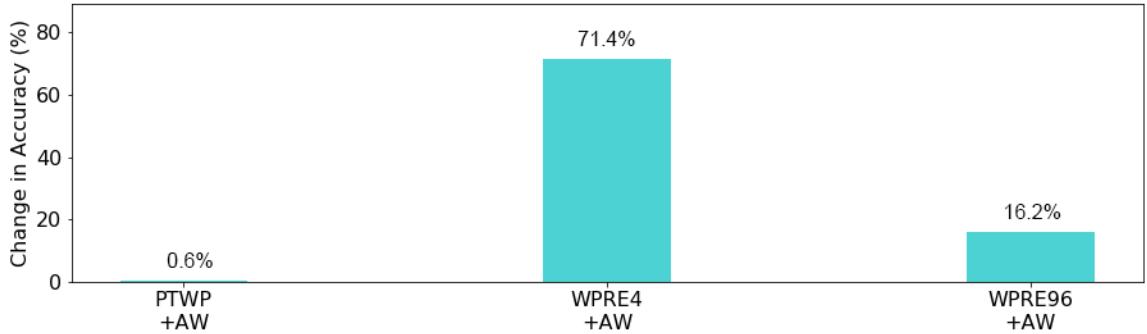


Figure 5.42: Change in performance in different feature combinations

information was removed. However, as mentioned in discussing the sensitivity of the Traffic-Only Model features, temporal information without the support of working day and peak hour flags cannot effectively describe traffic. Hence, the small decrease in accuracy as temporal information was removed. Moreover, using information on the *Day of Week* increased the accuracy by 6.4%. Using information on *Month, Day, Hour and Minute* alone decreased the accuracy, as traffic does not strongly depend on these information, especially in working days and peak hours.

Decision Fusion Model

To evaluate the effectiveness of including weather in predicting traffic, the performance of the fusion model is compared with the performance of the Traffic-Only model for each feature combination. The performances of these models was based from the results illustrated in Table 5.6.

As discussed in the Fusion Analysis, considering the weather prediction in fusing at decision level using WPRE96 feature combination resulted in a 16.2% improvement in performance. However, in evaluating the performance of the weather in predicting traffic, weather only contributed about 23% of the prediction after getting the difference between the performance between TOM and DEI-DEO fusion model, and dividing it by the max of the two. Accuracy significantly improved once window features at window 4 and 96 were considered. Though the difference between TOM and WOM in these feature combinations are far, from an RMSE of 0.084 in TOM to 0.328 in WOM, WOM played as a contributing factor in predicting traffic, achieving the increase in accuracy from 16.2% to 71.4%.

As mentioned in earlier discussions, traffic data mostly comprises of moderate traffic condition intensity reports. Moreover, most road segments experience light

to moderate traffic with few instances of disruptions, most of the day. Additionally, instances where there is a disruption in weather in which traffic is expected lies in weekends when traffic is least expected. Because of the lack of diverse data, it did not completely represent the relationship between weather and traffic, thus resulting in the small weight in prediction.

Chapter 6

Conclusion

Urban centers have long-since been fighting the natural occurrence of traffic congestion in the past decades. To help solve this problem, several traffic models were already developed while also considering weather as an effect. However, these models were not designed and tested in places with substandard drainage systems and poor road management. This research aims to develop a traffic model that considers data on traffic condition and weather variables such as wind speed, wind gust, temperature, humidity, dew point, precipitation, visibility, pressure, cloud cover, heat index, and feels-like.

The relationship between traffic and weather were analyzed through exploratory data analysis. First, the seasonality for weather and traffic was first explored and defined. The weather seasons such as wet and dry seasons are also defined using precipitation analysis. Then, the correlation between traffic and weather were explored through correlating between weather variables, connected road segments, and the immediate past traffic and defined traffic trends. Results show that the current traffic is correlated with its past traffic 1 week ago. Moreover, data shows that majority of the traffic condition during working days and non-working days consist of *light* to *moderate* traffic conditions. It is also observed there is a relationship between roads in terms of traffic condition intensity such that the traffic condition in one road is consistent with its connecting road based on the peak traffic hours, but differs in intensities as the road gets farther from the main road.

As for analyzing the weather, findings show that weather has a weak correlation with traffic. Moreover, among all weather variables, those that have the strongest correlation with traffic, only describes the transition from dawn to morning, or simply the beginning of the morning peak hour, and not its effect on traffic. Findings show that there is no derivable relationship between weather variables

and traffic because of the limited representation of traffic data.

Disruptions in the normal pattern of these variables were also identified. Disruptions are defined as the instances where rain is continuously present for 7 hours from 0:00 to 21:00 during working days. Majority of the found disrupted days are present in the wet season. In analyzing disruptions, it was discovered that traffic that traffic is less evident during wet season where precipitation is present that can base disruptions in the traffic. Disruptions may be disregarded if only traffic a week in the past is considered. Thus, traffic weeks ago is observed, and findings show that current traffic is correlated with the traffic in the past 6 weeks for both normal and disrupted periods.

Afterwards, the study implemented two prediction models, Traffic-Only Model (TOM) and Weather-Only Model (WOM), using Deep Belief Network (DBN) to predict traffic condition intensity based from traffic and weather data, respectively. The findings from the exploratory data analysis were used to select and engineer features, using them in the model to better predict the current traffic condition. The final features selected and engineered are as follows:

1. Temporal Information of the respective traffic record represented as Month, Day, Hour, Minute, Day of Week;
2. Traffic a Day before represented as L, ML, M, MH, H;
3. Traffic 6 weeks ago represented as L, ML, M, MH, H;
4. Current Traffic represented as L, ML, M, MH, H;
5. Rolling and Expanding Traffic Features (mean, max, and minimum) for windows 4, 8, 24, 48, and 96 represented as L, ML, M, MH, H;
6. Flags for Working day and Peak Hour represented as 0 and 1; and,
7. Weather Variables (wind speed, wind gust, temperature, humidity, dew point, precipitation, visibility, pressure, cloud cover, heat index, and feels-like) represented in their respective measurements

Different combinations of these features for their respective prediction models (TOM and WOM) were made to further evaluate which features best represent traffic. Results of the experimentation show that the model best predicts traffic on normal days, and road segments with less diverse traffic. In predicting for disrupted days, TOM cannot accurately predict the abrupt transitions of traffic conditions. Predictions of TOM greatly improves after including information on

immediate past traffic, such as rolling and expanding window features with small windows. On the other hand, WOM could only predict normal traffic trends, and traffic conditions often present in the trend such as traffic conditions of *light* to *moderate*. Using only weather variables as factors in predicting traffic could offer a contributing weight in predicting traffic. However, weather variables alone cannot be used to predict traffic, because of its weak correlation with traffic.

Different fusion approaches, such as feature fusion and decision fusion, were also tested. Moreover, different data fusion algorithms in the decision level were also compared. These data fusion algorithms were DBN, Recurrent Neural Network (RNN), and Weighted Average (WA) using Least Square Estimate. Predictions were evaluated with the different fusion approaches and algorithms. Results show that fusing traffic and weather at the decision level generates a better prediction than fusing at the feature level. Moreover, fusing at the decision level using RNN outperforms fusing with WA and DBN. The capability of LSTM of RNN contributes to the high performance of the model, thus outperforming the other algorithms.

The sensitivity of the models TOM and the fusion model implemented in DBN were evaluated. Analysis shows that the flags for working day and peak hours were connected with the temporal information of the data. Moreover, information on past immediate traffic such as the mean traffic of a 6 weeks ago, traffic a day ago, rolling and expanding features an hour and a day ago, highly affects the prediction of the model. Additionally, in analyzing the fusion model, the inclusion of weather as a factor in predicting traffic only contributed 27% in the prediction.

Chapter 7

Future Works

Using historical data is a good and common entry for data-driven researches. However, in the case of traffic, it is better to consider real-time information to predict future traffic conditions. In the event that something unexpected happens, such as road accidents or just-closed lanes, the historical traffic data may not be as useful as it is. Sudden events may also include typhoon warnings, which has no annual pattern and cannot be easily predicted. With historical traffic and weather data combined with real-time information, future traffic predictions may become more accurate.

Considering traffic reports in social media may also be an additional feature in the model. Social media platforms such as Twitter and Facebook allows people to let out their frustrations including everyday problems such as road traffic. One study (Gu et al., 2016) retrieves real-time traffic information by crawling, processing, and filtering public tweets to detect road traffic incidents using natural processing language techniques. Using this as an added feature in the model may boost its accuracy.

Unpredicted road catastrophes also contribute to traffic congestion, including road accidents, road constructions, and recently-closed lanes. Car accidents block the roads, which then hinder other vehicles to efficiently pass through, causing heavy traffic jam (Wang et al., 2009). Road constructions such as building of bridges, expanding the roads, fixing the water pipes underneath the roads, among others, also tend to increase traffic congestion, especially if there is no notice beforehand. The sudden closing of a road may also contribute to traffic jams, since it disrupts the normal flow of traffic. Studying these kinds of road catastrophes may be helpful in achieving a better traffic prediction. Data may be collected as historical data or using real-time information.

In urban places where drainage systems are not properly managed or road infrastructures are not properly built and maintained, the amount of rain accumulating on the roads may increase traffic congestion as vehicles have difficulty moving forward. It is worse on places where adverse weather conditions such as typhoons bring heavy rains, which then causes immense flooding if the rain is not properly drained. Although the existing application Waze allows drivers and passengers to report flooding incidents in the roads, Waze does not use these reports in learning and predicting future traffic conditions. In future works, considering the height of flood as a contributing factor may help the model in predicting future traffic condition.

Appendix A

Research Ethics Documents

This appendix contains all documents related to research ethics.

DE LA SALLE UNIVERSITY
General Research Ethics Checklist

This checklist is to ensure that the research conducted by the faculty members and students of De La Salle University is carried out according to the guiding principles outlined in the Code of Research Ethics of the University. The investigator is advised to refer to the [De La Salle University Code of Research Ethics and Guide to Responsible Conduct of Research](#) before completing this checklist. Statements pertinent to ethical issues in research should be addressed below. The checklist will help the researchers and evaluators determine whether procedures should be undertaken during the course of the research to maintain ethical standards. The University's [Guide to the Responsible Conduct of Research](#) provides details on these appropriate procedures.

Details of the Research	
Students	MAGPALE, Nicolle G. NIEVA, Dyan Raisa L. REAMON, David Angelo H. RECCION, Maria Victoria B.
Thesis Adviser	CABREDO, Rafael A., Ph.D.
Department	Software Technology Department
Title of the Research	TrafficBaTo: Towards a Weather-Aware Traffic Model
Term(s) and Academic year in which research is to be conducted	Terms 1 to 3 AY 2017-2018

This checklist must be completed AFTER the De La Salle University Code of Ethics has been read and BEFORE gathering data.

Questions	Yes	No
1. Does your research involve human participants (this includes new data gathered or using pre-existing data)? If your answer is yes , please answer Checklist A (Human Participants) .		✓
2. Does your research involve animals (non-human subjects)? If your answer is yes , please answer Checklist B (Animal Subjects) .		✓
3. Does your research involve Wildlife? If your answer is yes , please answer Checklist C (Wildlife) .		✓
4. Does your research involve microorganisms that are infectious, disease causing or harmful to health? If your answer is yes , please answer Checklist D (Infectious Agents) .		✓
5. Does your research involve toxic/chemicals/ substances/materials? If your answer is yes , please answer Checklist E (Toxic Agents) .		✓

Research with Ethical Issues to address:

If you have a YES answer to any of the above categories, you will be required to complete a detailed checklist for that particular category. A YES answer does not mean the disapproval of your research proposal. By providing you with a more detailed checklist, we ensure that the ethical concerns are identified so these can be addressed in adherence to the University Code of Ethics.

Declaration of Conflict of Interest

I do not have a conflict of interest in any form (personal, financial, proprietary, or professional) with the sponsor/grant-giving organization, the study, the co-investigators/personnel, or the site.

[] I have a personal/family or professional interest in the results of the study (family members who are co-proponents or personnel in the study, membership in relevant professional associations/organizations).

Please describe the personal/family or professional interest: _____

[] I have propriety interest vested in this proposal (with the intent to apply for a patent, trademark, copyright, or license)

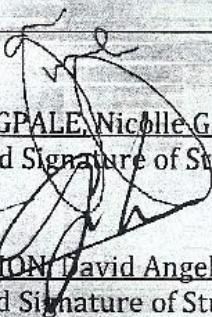
Please describe propriety interest: _____

[] I have significant financial interest vested in this proposal (remuneration that exceeds P250,000.00 each year or equity interest in the form of stock, stock options or other ownership interests).

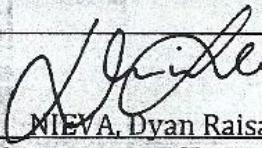
Please describe financial interest: _____

Declaration

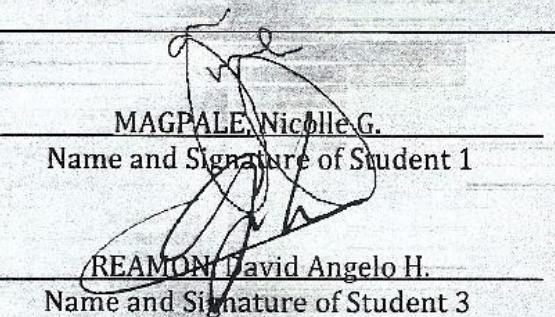
We certify that we have read and understand the De La Salle University Code for the Responsible Conduct of Research and will abide by the ethical principles in this document. We will submit a final report of the proposed study to the DLSU-Research Ethics Office. We will not commence with data collection until we receive an ethics review approval from the College Research Ethics Committee.


MAGPALE, Nicholle G.

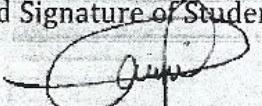
Name and Signature of Student 1


NIEVA, Dyan Raisa L.

Name and Signature of Student 2

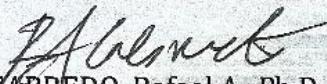

REAMON, David Angelo H.

Name and Signature of Student 3


RECCION, Maria Victoria B.

Name and Signature of Student 4

Endorsement from thesis adviser to the thesis panel for proposal defense...


CABREDO, Rafael A., Ph.D.

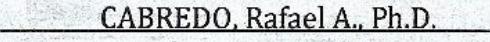
Name and Signature of Adviser

Nov. 3, 2017

Date

Endorsement from thesis adviser to the thesis panel for final defense...

This is to certify that the research was conducted in a manner that adheres to ethical research standard I am thus endorsing the group for final defense.


CABREDO, Rafael A., Ph.D.

Name and Signature of Adviser

Date

RESEARCH ETHICS CLEARANCE FORM

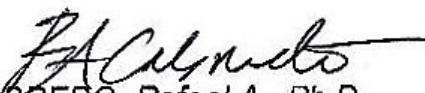
For Thesis Proposals¹

Names of student researcher/s :	MAGPALE, Nicolle G. NIEVA, Dyan Raisa L. REAMON, David Angelo H. RECCION, Maria Victoria B.
College:	College of Computer Studies
Department:	Software Technology Department
Course:	BS Computer Science with specialization in Software Technology
Expected duration of project:	from: T1 AY '17-'18 to: T3 AY '17-'18

Ethical considerations

The data to be used is publicly available data.

To the best of our knowledge, the ethical issues listed above have been addressed in the research.


CABREDO, Rafael A., Ph.D.

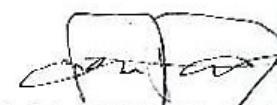
Name and signature of adviser/mentor

Date: 12/13/2017


LAO, Angelyn R., Ph.D.

Name and signature of panelist

Date: 12/12/2017


DELOS SANTOS, Duke Danielle T.

Name and signature of panelist

Date: 12/12/17

Appendix B

Turnitin Similarity Report

This appendix contains the similarity report from Turnitin.

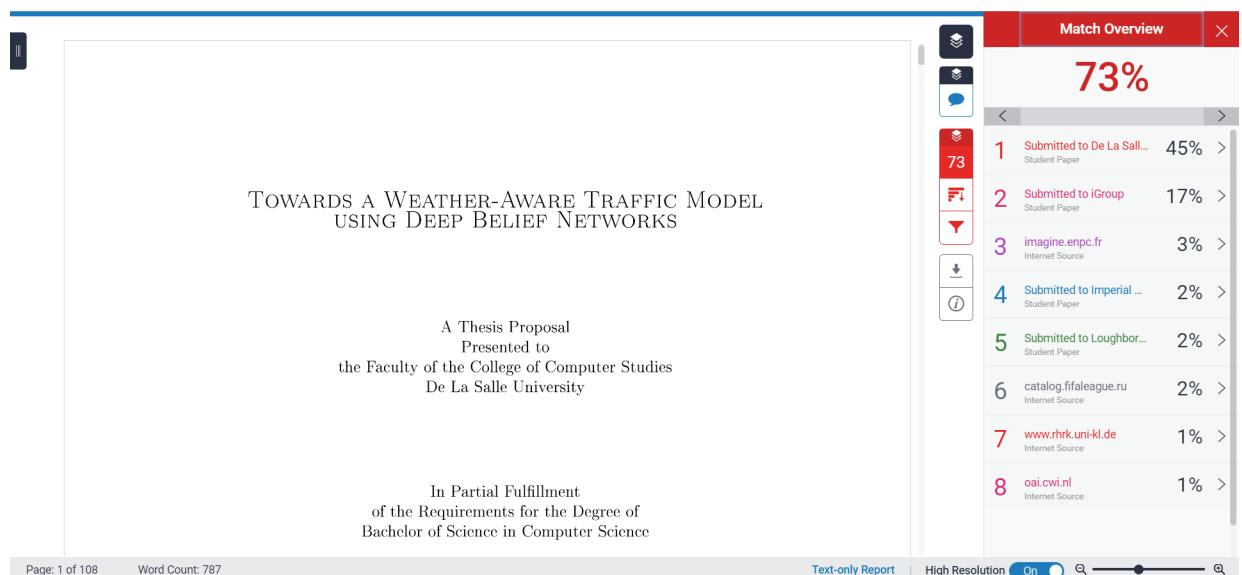


Figure B.1: Turnitin Similarity Report

Appendix C

Research Project Timeline

This appendix contains the time line of the research project.

Figure C.1: Research Project Timeline

Appendix D

Preliminary Results

In this section, an implementation of feature fusion, using the collected traffic and weather dataset, will be discussed through a feedforward ANN. To evaluate the performance of feature fusion, two experiments will be performed: predicting the traffic condition using weather variables only and predicting the traffic condition by applying feature fusion to both the traffic condition and weather variables.

D.1 Data Pre-processing

Before feeding the data to the ANN model, the data must be cleaned and processed. Recall that the collected dataset for both the weather and traffic are sampled at a 15-minute interval and an hourly interval respectively and that the traffic dataset contains missing records (see Section 4.1). Given these anomalies, interpolation must be done for the traffic dataset to supply the missing records and intervals, whereas resampling and interpolation must be performed for the weather dataset to match the traffic dataset's interval.

D.1.1 Traffic Dataset

For the traffic dataset, we must first separate the records based on their respective road segments. For instance, we must have a separate dataset only containing the records from Taft Avenue, Quirino, Buendia and the other road segments. This is to ensure that our interpolation later on will not be influenced by other road segments rather than itself.

Before cleaning the data, we must consider that interpolation requires numerical values so that the missing values can be estimated. Therefore, we must convert the traffic conditions for both the northbound and southbound to their numerical equivalents. Since they are classified as light, moderate and heavy, we could rank them based on their intensities. As a result, light, moderate and heavy are classified into 0.0, 0.5 and 1.0 respectively. These values are chosen so that the min-max scaling normalization is no longer needed to perform later on.

Next, to clean the traffic dataset, we have to consider the two cases of missing data that it has: having *none*(N) conditions and having a particular interval not recorded at all. To resolve the first case, first, we must remove all *none*(N) condition from both the northbound and southbound traffic condition features. Next, we perform linear interpolation to fill in these filtered records. For the second case, we must fill in the unrecorded intervals. Hence, although the traffic dataset is already in our target series interval, we need to resample the dataset at a 15-minute interval so that all the intervals, including the missing ones, will be added. Next, we perform linear interpolation again to fill in these missing records.

D.1.2 Weather Dataset

Before processing our dataset, recall that our weather dataset contains 20 weather variables, having the temperature, heat index, dew point, wind chill and feels like on both their Celcius and Fahrenheit form, and wind speed and wind gust on both their miles per hour and kilometers per hour form. In our case, we opted to use their Celcius form and kilometers per hour form. Thus, scoping down our weather variables to 13.

For the weather dataset, since, fortunately, our data is complete per interval, we could directly start resampling our records. But, before this, we must ensure that our weather variables are in their numerical equivalents as a preparation for interpolation. With that, the data is ready for interpolation and is already normalized.

After processing our dataset, we could now match our weather dataset to the intervals of our traffic dataset. To do this, we must first resample our dataset at a 15-minute interval. Next, we perform linear interpolation to fill in the missing intervals, similar to how we filled the missing records from our traffic data.

D.2 Input Dataset

To scale down our experiment, we sampled three consecutive months of 2015 as our dataset (from September 2015 to November 2015) for both traffic and weather. Furthermore, we only used the traffic records of Taft Avenue with the weather of Manila as our input dataset. For the features, we only considered the southbound traffic condition for the traffic. On the other hand, we considered 13 features for the weather. These include temperature (in Celsius), wind speed (in kilometers per hour), weather condition, precipitation (in millimeters), humidity, visibility, pressure, cloud cover, heat index (in Celsius), dew point (in Celsius), wind chill (in Celsius), wind gust (in kilometers per hour), and feels-like (in Celsius). It must be noted, however, that the correlation of these features has not been considered in this experiment.

D.3 Developing the Model

Developing our feedforward ANN consists of 5 steps: preparing the data, defining the training and test data, building the ANN model itself, training the model and finally evaluating the model. Our model will be implemented using Python, utilizing the Keras library with Tensorflow. For our experiment, we would be performing two cases: predicting the traffic condition using weather variables only and predicting the traffic condition by applying feature fusion to both the traffic condition and weather variables.

D.3.1 Preparing the Data

Aside from the pre-processing that was performed earlier, we also have to perform some additional pre-processing targeted for our model. First, we have to merge both our traffic dataset and weather dataset. Since they already have matching intervals and the traffic dataset is already separated based on its road segments, we could simply merge it without any additional processing involved. It is important to note that only one road segment dataset will only be used per model, especially in our case where the weather dataset is the generalized weather for all road segments, since the generalized weather may be biased on a particular road segment.

Next, we remove the unnecessary features from our merged dataset. These include the road, road segment and the date and time, leaving us with the numerical

Figure D.1: Predict Southbound Traffic without Feature Fusion

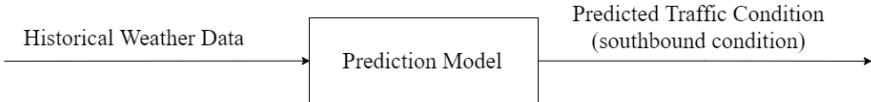
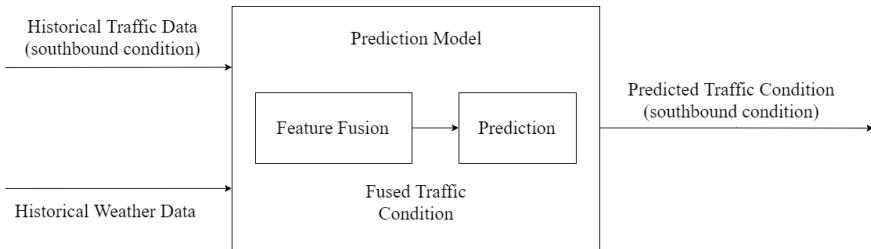


Figure D.2: Predict Southbound Traffic with Feature Fusion



traffic features and weather variable features. Finally, we must perform normalization to standardize the values. In our case, we performed min-max scaling normalization to scale our data from 0.0 to 1.0.

D.3.2 Defining the Training and Testing Dataset

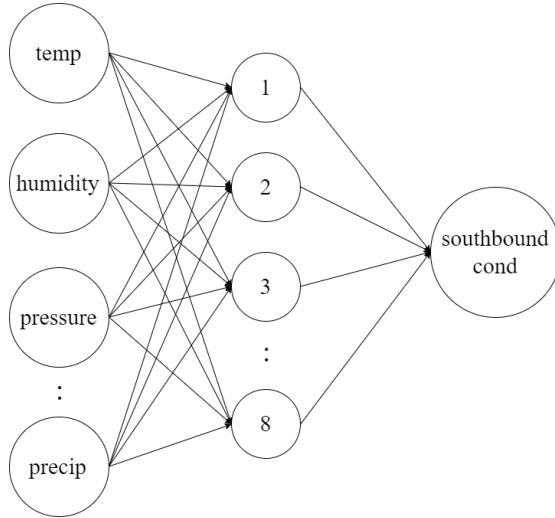
The dataset is split into two sub-datasets: the training dataset which includes September 2015 to October 2015 and the testing dataset which includes November 2015. From this, the target label, the feature that we want to predict, and the training features, the features from which the prediction will be based on, are defined. To further minimize the scope of the experiment, we would only predict the traffic condition of the southbound lane. Thus, for the experiment, our target label would be the traffic condition of the southbound lane.

In order to illustrate the benefits of feature fusion, two experiments will be performed. First, the training features will be solely based on weather variable features. Second, the training features will include the traffic condition from the southbound lane and the weather variable features thus, performing feature fusion on the traffic and weather variables features. To further illustrate these experiments, Figures D.1 and D.2 show the diagram of these scenarios.

D.3.3 Building the Model

In building our feedforward ANN model, we used three densely-connected neural network layer: one for the input, one for the hidden layer and one for the out-

Figure D.3: ANN Model for Predicting Southbound Traffic without Feature Fusion

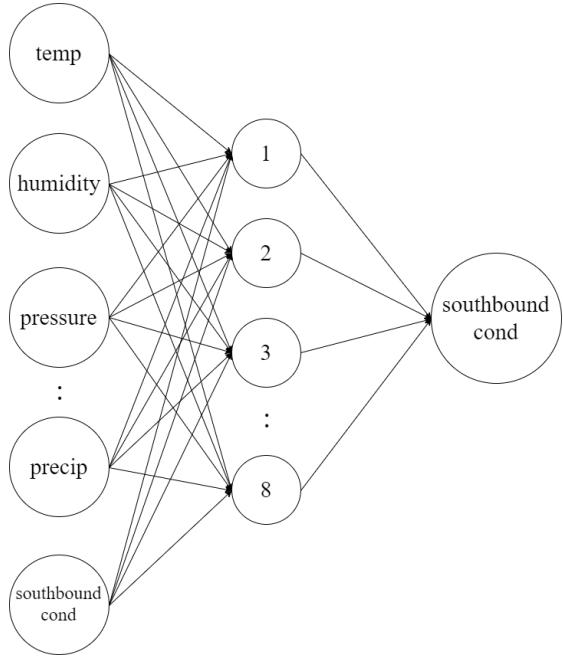


put. For each of our experiments, both uses rectified linear unit (ReLU) as the activation function, and each has 13 input dimensions and 14 input dimensions respectively. The dimensions correspond to the number of training features that we will use for the model. The model has 13 weather variable features for our first experiment scenario, whereas we have 13 weather variable features and 1 traffic feature for our second scenario. For both experiments, it uses one hidden layer that similarly uses ReLU as its activation function, and has 8 input dimensions. It also has one output layer with only one output dimension for our southbound traffic condition. Figure D.3 and D.4 illustrate the diagram of these models.

D.3.4 Training the Model

In preparation for training the model, we configured the model's optimizer, loss function, and evaluation metrics. For its optimizer, we set it to use the Adam optimizer, having a learning rate of 0.001 and a decay factor of 0.0. Meanwhile, for its loss function, we used mean squared error (MSE). Finally, for its evaluation metrics, we used mean absolute percentage error (MAPE). Using the training dataset, for both experiments, we trained the model using 1000 epochs and a batch size of 5.

Figure D.4: ANN Model for Predicting Southbound Traffic with Feature Fusion



D.3.5 Evaluation of the Model

For the first experiment, where the model only uses weather variable features as its training features, the model generated a root-mean-square error (RMSE) of 6.57% and a MAPE of 57,787,420%. On the other hand, the second experiment, where the model uses feature fusion for the southbound traffic condition and weather variables as its training features, generated an RMSE of 0.0001% and a MAPE of 8,396%. Although the MAPE is quite high due to the lack of epochs, we could observe how massive the difference is between the first model and the second model. Given that, we can conclude that using feature fusion can significantly increase the accuracy of the model.

References

- Aguado, E., Burt, J. E., Rohli, R. V., & Schmidlin, T. W. (2007). *Understanding weather and climate*. Pearson Prentice Hall Upper Saddle River, NJ, USA.
- Ahlgren, P., Jarneving, B., & Rousseau, R. (2003). Requirements for a cocitation similarity measure, with special reference to Pearson's correlation coefficient. *Journal of the American Society for Information Science and Technology*, 54(6), 550–560.
- Armstrong, J. S., & Collopy, F. (1992). Error measures for generalizing about forecasting methods: Empirical comparisons. *International journal of forecasting*, 8(1), 69–80.
- Bando, M., Hasebe, K., Nakayama, A., Shibata, A., & Sugiyama, Y. (1995). Dynamical model of traffic congestion and numerical simulation. *Physical Review E*, 51(2), 1035–1042.
- Biham, O., Middleton, A. A., & Levine, D. (1992). Self-organization and a dynamical transition in traffic-flow models. *Physical Review E*, 46(10), 46–50.
- Bossé, É., Valin, P., Boury-Brisset, A.-C., & Grenier, D. (2006). Exploitation of a priori knowledge for information fusion. *Information Fusion*, 7(2), 161–175.
- Bovy, P. H., Salomon, I., et al. (2002). Congestion in europe: Measurements, patterns and policies. *Chapters*.
- Castanedo, F. (2013). A review of data fusion techniques. *The Scientific World Journal*, 2013.
- Chai, T., & Daxler, R. R. (2014). Root mean square error (RMSE) or mean absolute error (MAE)? – Arguments against avoiding RMSE in the literature. *Geoscientific Model Development*, 7(3), 1247–1250.
- Climate of the philippines*. (n.d.). Retrieved from <https://kidlat.pagasa.dost.gov.ph/index.php/climate-of-the-philippines>
- Constantinidis, A., Fairhurst, M. C., & Rahman, A. F. R. (2001). A new multi-expert decision combination algorithm and its application to the detection of circumscribed masses in digital mammograms. *Pattern Recognition*, 34(8), 1527–1537.
- Dai, X., & Khorram, S. (1999). Data fusion using artificial neural networks: a

- case study on multitemporal change analysis. *Computers, Environment and Urban Systems*, 23(1), 19–31.
- Dasarathy, B. V. (1997). Sensor fusion potential exploitation-innovative architectures and illustrative applications. *Proceedings of the IEEE*, 85(1), 24–38. doi: 10.1109/5.554206
- Datla, S., & Sharma, S. (2008). Impact of cold and snow on temporal and spatial variations of highway traffic volumes. *Journal of Transport Geography*, 16(5), 358–372.
- De Fabritiis, C., Ragona, R., & Valenti, G. (2008). Traffic estimation and prediction based on real time floating car data. In *Intelligent transportation systems, 2008. itsc 2008. 11th international ieee conference on* (pp. 197–203).
- D'Mello, S. K., & Graesser, A. (2010, Apr). Multimodal semi-automated affect detection from conversational cues, gross body language, and facial features. *User Modeling and User-Adapted Interaction*, 20(2), 147–187. doi: 10.1007/s11257-010-9074-4
- Downs, A. (1962). The law of peak-hour expressway congestion. *Traffic Quarterly*, 16(3).
- Downs, A. (2005). *Still stuck in traffic: coping with peak-hour traffic congestion*. Brookings Institution Press.
- Dunne, S., & Ghosh, B. (2013, March). Weather adaptive traffic prediction using neurowavelet models. *IEEE Transactions on Intelligent Transportation Systems*, 14(1), 370-379. doi: 10.1109/TITS.2012.2225049
- Fincher, D. W., & Mix, D. F. (1990). Multi-sensor data fusion using neural networks. In *Systems, man and cybernetics, 1990. conference proceedings., ieee international conference on* (pp. 835–838).
- Fischer, A., & Igel, C. (2014). Training restricted Boltzmann machines: An introduction. *Pattern Recognition*. doi: 10.1016/j.patcog.2013.05.025
- Gaul, L. E., & Underwood, G. (1952). Relation of dew point and barometric pressure to chapping of normal skin. *Journal of Investigative Dermatology*, 19(1), 9–19.
- Gauthier, T. D. (2001). Detecting trends using spearman's rank correlation coefficient. *Environmental Forensics*, 2(4), 359–362.
- Geetha, K., & Radhakrishnan, V. (2013, May). Multimodal biometric system: A feature level fusion approach. *International Journal of Computer Applications*, 71(4), 25–29. doi: 10.5120/12347-8635
- Gu, Y., Qian, Z. S., & Chen, F. (2016). From twitter to detector: Real-time traffic incident detection using social media data. *Transportation research part C: emerging technologies*, 67, 321–342.
- Hall, D., & Llinas, J. (2001). *Multisensor data fusion*. CRC press.
- Hamad, K., Ali Khalil, M., & Shanableh, A. (2017). Modeling roadway traffic noise in a hot climate using artificial neural networks. *Transportation Research*

Part D: Transport and Environment. doi: 10.1016/j.trd.2017.04.014

- Hauke, J., & Kossowski, T. (2011). Comparison of Values of Pearson's and Spearman's Correlation Coefficients on the Same Sets of Data. *Quaestiones Geographicae*, 30(2). Retrieved from <http://www.degruyter.com/view/j/quageo.2011.30.issue-2/v10117-011-0021-1/v10117-011-0021-1.xml> doi: 10.2478/v10117-011-0021-1
- Hu, W., Yan, L., Wang, H., Du, B., & Tao, D. (2016). Real-time traffic jams prediction inspired by Biham, Middleton and Levine (BML) model. *Information Sciences*, 381, 209–228.
- Hueper, J., Dervisoglu, G., Muralidharan, A., Gomes, G., Horowitz, R., & Varaiya, P. (2009). Macroscopic modeling and simulation of freeway traffic flow. *IFAC Proceedings Volumes*, 42(15), 112 - 116. Retrieved from <http://www.sciencedirect.com/science/article/pii/S1474667016317839> (12th IFAC Symposium on Control in Transportation Systems) doi: <https://doi.org/10.3182/20090902-3-US-2007.0078>
- Hunter, A., Kennedy, L., Henry, J., & Ferguson, I. (2000). Application of neural networks and sensitivity analysis to improved prediction of trauma survival. *Computer Methods and Programs in Biomedicine*, 62(1), 11–19. doi: 10.1016/s0169-2607(99)00046-2
- Jain, V., Sharma, A., & Subramanian, L. (2012). Road traffic congestion in the developing world. In *Proceedings of the 2nd acm symposium on computing for development* (pp. 11:1–11:10). New York, NY, USA: ACM. Retrieved from <http://doi.acm.org/10.1145/2160601.2160616> doi: 10.1145/2160601.2160616
- Jimenez, L. O., Morales-Morell, A., & Creus, A. (1999). Classification of hyperdimensional data based on feature and decision fusion approaches using projection pursuit, majority voting, and neural networks. *IEEE Transactions on Geoscience and Remote Sensing*, 37(3), 1360–1366.
- King, R. C., Villeneuve, E., White, R. J., Sherratt, R. S., Holderbaum, W., & Harwin, W. S. (2017). Application of data fusion techniques and technologies for wearable health monitoring. *Medical Engineering & Physics*, 42, 1–12. doi: 10.1016/j.medengphy.2016.12.011
- Koesdwiyadi, A., Soua, R., & Karray, F. (2016, Dec). Improving traffic flow prediction with weather information in connected cars: A deep learning approach. *IEEE Transactions on Vehicular Technology*, 65(12), 9508-9517. doi: 10.1109/TVT.2016.2585575
- Kumar, S. V., & Vanajakshi, L. (2015). Short-term traffic flow prediction using seasonal arima model with limited input data. *European Transport Research Review*, 7(3), 21.
- Lee, J., Hong, B., Kyungmin, L., & Yang-Ja, J. (2015). A prediction mode of traffic congestion using weather data. *IEEE Computer Society*, 81–88.
- Lee, W.-H., Tseng, S.-S., & Tsai, S.-H. (2009). A knowledge based real-time

- travel time prediction system for urban network. *Expert Systems with Applications*, 36(3), 4239 - 4247. Retrieved from <http://www.sciencedirect.com/science/article/pii/S0957417408001875> doi: <http://dx.doi.org/10.1016/j.eswa.2008.03.018>
- Liu, D., Cho, S. Y., Sun, D. M., & Qiu, Z. D. (2010). A Spearman correlation coefficient ranking for matching-score fusion on speaker recognition. *IEEE Region 10 Annual International Conference, Proceedings/TENCON*, 736–741.
- Liu, J., Zhou, C., & Chen, J. (2008). Wdcm: a workday calendar model for workflows in service grid environments. *Concurrency and Computation: Practice and Experience*, 20(4), 377–392.
- Liu, Z., Li, Z., Li, M., Xing, W., & Lu, D. (2016). Mining road network correlation for traffic estimation via compressive sensing. *IEEE Transactions on Intelligent Transportation Systems*, 17(7), 1880–1893.
- Mahmud, K., Gope1, K., & Chowdhury, S. M. R. (2012). Possible causes & solutions of traffic jam and their impact on the economy of Dhaka city. *Journal of Management and Sustainability*, 2(2), 112–135. doi: 10.5539/jms.v2n2p112
- Mahmud, K., & Town, G. E. (2016). A review of computer tools for modeling electric vehicle energy requirements and their impact on power distribution networks. *Applied Energy*, 172, 337–359.
- Mangai, U. G., Samanta, S., Das, S., & Chowdhury, P. R. (2010). A survey of decision fusion and feature fusion strategies for pattern classification. *IETE Technical review*, 27(4), 293–307.
- May, A. D. (1990). *Traffic flow fundamentals*.
- Meurant, G., & Meurant, G. (1992). Multisensor fusion. In *Data fusion in robotics & machine intelligence* (p. 41). Academic Press.
- More, R., Mugal, A., Rajgure, S., Adhao, R. B., & Pachghare, V. K. (2016). Road traffic prediction and congestion control using artificial neural networks. In *2016 international conference on computing, analytics and security trends (cast)* (pp. 52–57).
- Pan, B., Demiryurek, U., & Shahabi, C. (2012). Utilizing real-world transportation data for accurate traffic prediction. In *Data mining (icdm), 2012 ieee 12th international conference on* (pp. 595–604).
- Paull, R. (1999). Effect of temperature and relative humidity on fresh commodity quality. *Postharvest biology and technology*, 15(3), 263–277.
- Rakha, H., & Van Aerde, M. (1995). Statistical analysis of day-to-day variations in real-time traffic flow data. *Transportation research record*, 26–34.
- Refenes, A. N., Zapranis, A., & Francis, G. (1994). Stock performance modeling using neural networks: a comparative study with regression models. *Neural networks*, 7(2), 375–388.
- Regidor, J. R. F. (2013). Traffic congestion in metro manila: Is the uvvrp still

- effective? *Philippine Engineering Journal*, 34(1), 66–75.
- Saltelli, A., Chan, K., & Scott, E. M. (2000). *Sensitivity analysis*. New York: Wiley.
- Saputri, T. R. D., & Lee, S.-W. (2013). Using artificial neural networks for predicting traffic conditions: A learning algorithm fro long-term time series forecasting. *Journal of Convergence Information Technology (JCIT)*, 8(14).
- Sohn, S. Y., & Lee, S. H. (2003). Data fusion, ensemble and clustering to improve the classification accuracy for the severity of road traffic accidents in korea. *Safety Science*, 41(1), 1–14.
- Sommer, M., Tomforde, S., & Hahner, J. (2013). Using a neural network for forecasting in an organic traffic control management system. In *ESOS*.
- Tanner, J. (1952). Effect of weather on traffic flow. *Nature*, 169(4290), 107.
- Varangis, P., Skees, J., & Barnett, B. (2003). Weather indexes for developing countries. *Forest*, 4, 3–754.
- Vuchic, V. R., Bruun, E. C., Krstanoski, N. B., Shin, Y. E., Kikuchi, S., Chakroborty, P., & Perincherry, V. (1994). The bus transit system: Its underutilized potential.
- Wang, C., Quddus, M. A., & Ison, S. G. (2009). Impact of traffic congestion on road accidents: A spatial analysis of the m25 motorway in england. *Accident Analysis & Prevention*, 41(4), 798–808.
- Wang, C., Quddus, M. A., & Ison, S. G. (2013). The effect of traffic and road characteristics on road safety: A review and future research direction. *Safety Science*, 57, 264–275.
- Yan, Z.-Z., Yan, X.-P., Xie, L., & Wang, Z. (2011). The research of weighted-average fusion method in inland traffic flow detection. *Information Computing and Applications Lecture Notes in Computer Science*, 89–96. doi: 10.1007/978-3-642-25255-6_12
- Y. Jia, M. X., J. Wu. (2017, Aug). Traffic flow prediction with rainfall impact using a deep learning method. *Hindawi: Journal of Advanced Transportation*, 2017.
- Zar, J. (1972). Significance Testing of the Spearman Rank Correlation Coefficient. *Journal of the American Statistical Association*, 67(339), 578–580.
- Zhang, N., Ding, S., Zhang, J., & Xue, Y. (2017). An overview on restricted boltzmann machines. *Neurocomputing*. Retrieved from <http://www.sciencedirect.com/science/article/pii/S0925231217315849> doi: <https://doi.org/10.1016/j.neucom.2017.09.065>
- Zhao, L., Lai, Y.-C., Park, K., & Ye, N. (2005). Onset of traffic congestion in complex networks on. *Physical Review E*, 71(2), 026125.